COMPARATIVE ANALYSIS OF CONTROL STRATEGIES FOR AC to DC CONVERTERS

A DISSERTATION

Submitted in partial fulfillment of the requirements for the award of the degree of

MASTER OF TECHNOLOGY

in

ELECTRICAL ENGINEERING

(With Specialization in Power Apparatus and Electric Drives)

By

SWATHI YERRAGUNTLA

IP

DEPARTMENT OF ELECTRICAL ENGINEERING
INDIAN INSTITUTE OF TECHNOLOGY ROORKEE
ROORKEE-247 667 (INDIA)

JUNE, 2006

ID NO. MT-318|2006-13|SY-PA

CANDIDATE'S DECLARATION

I here by declare that the work which is being presented in the Dissertation Thesis entitled **"Comparative Analysis of Control Strategies for AC-to-DC Converters"** in partial fulfillment of the requirements for the award of the degree **Master of Technology** in **Electrical Engineering** with specialization in **Power Apparatus and Electric Drives,** submitted in the **Department of Electrical Engineering, Indian Institute of Technology, Roorkee, INDIA – 247667**. This is an authentic record of my own work carried out in the period of last two semesters from Aug 2005 to June 2006, under the supervision of **Dr. Pramod Agarwal,** Professor, Department of Electrical Engineering, Indian Institute of Technology, Roorkee, INDIA – 247667.

The matter embodied in this Dissertation Thesis has not been submitted by me for the award of any other degree or diploma.

Date: 15/06/06
Place: ROORKEE

Y. Swathi
(Swathi Yerraguntla)

CERTIFICATE

This is to certify that the above statements made by the candidate are correct to the best of my knowledge.

(Dr. Pramod Agarwal)
Professor,
Electrical Engineering Dept,
Indian Institute of Technology, Roorkee'
Roorkee-247667

Acknowledgements

I wish to express my deep sense of gratitude and indebtedness to my guide, **Dr. Pramod Agarwal, Professor, Electrical engineering Department, Indian Institute of Technology Roorkee, Roorkee** for his whole heartedness and high dedication with which they involved in this work. I am grateful for his patience to discuss and explain even the minute details of the work in spite of his hectic schedule of work in the department. He listened patiently and authoritatively as he guided me and made his valuable suggestions.

I am grateful to all my teachers of the PAED group for their suggestions and constant encouragement. I am also grateful to all the Research Scholars of the PAED group for their suggestions and motivation.

Grateful acknowledgements to my parents who have always encouraged and supported me. I am thankful to my class mates and other well wishers whose timely help has gone a long way in this work.

Y. Swathi

(Swathi Yerraguntla)

M. Tech (Elect) PAED

Date: 15/06/06

Place: ROORKEE

Abstract

AC-to-DC converters have been dominated by uncontrolled rectifiers or line commutated phase controlled rectifiers followed by a bulk capacitor. These rectifiers are inexpensive, highly reliable. Passive filters are often used to filter the low order harmonics as they have a simple circuit configuration. Pulse width modulated (PWM) AC-to-DC voltage source converters or current controlled rectifiers (CCR's) have the merits of nearly sinusoidal input current, good power factor and regeneration ability. A significant improvement in converter behavior has been achieved by means of closed loop control techniques.

This thesis aims at the comparative analysis of various PWM control strategies for AC-to DC converters some of which include Hysteresis Current Control, Sinusoidal Pulse Width Modulation, Space Vector modulation, Indirect Current Control, Average Predictive Current Control for four wire rectifiers etc.

Simulation models are developed in MATLAB for different control strategies to compare the results and obtain a performance evaluation. The performance of an AC-to-DC converter controlled by each control strategy has been evaluated under various conditions by varying the load, switching frequency, changing the operating mode from generative to regenerative. The performance parameters are calculated for all the converters and then compared with each other. A tabulation of all the performance measures is made.

List of Figures

Figure No	Figure Description	Page No
Fig 2.1	Single-switch three-phase DCM boost rectifier	8
Fig 2.2	Control Circuit of a three phase boost rectifier	9
Fig 2.3	Six Pulse Bridge Converter	10
Fig 2.4	SPWM Controlled converter	11
Fig 2.5	Principle of SPWM	11
Fig 2.6	Control block diagram for instantaneous control SPWM	13
Fig 2.7	Hysteresis Current Controlled Converter	15
Fig 2.8	Principle of operation of HCC controlled converter	15
Fig 2.9	Control block diagram for Hysteresis band PWM	16
Fig 2.10	Variation of load with switching frequency under HCC	17
Fig 2.11	Voltage phasor diagram of ac circuit	19
Fig 2.12	(a) A-phase supply voltage(b) Fundamental component of A-phase voltage at rectifier terminal (c) Switched voltage(d) Carrier and modulating waveform	20
Fig 2.13	Block diagram implementing indirect current control	22
Fig 2.14	Three Phase Four Wire Rectifier	24
Fig 2.15	Control Circuit of the four wire PFCR	25
Fig 3.1	Representation of Rotating Vector in Complex Plane	29
Fig 3.2	Voltage Space Vector and its components in d-q	29
Fig 3.3	Reference vector as a combination of adjacent vectors at sector1	31
Fig 3.4	Switching pulse pattern for the three phase in the 6 different sectors	33
Fig 4.1	SIMULINK model of the single switch high power factor rectifier	35
Fig 4.2	Output Voltage of the rectifier for fs = 1 KHz	36
Fig 4.3	Phase A current for fs = 1 KHz for boost rectifier	36
Fig 4.4	FFT analysis of Source Current	37
Fig 4.5	Output Power Vs THD for Single switch high power factor rectifier	37
Fig 4.6	Output Power Vs Input Current for Single switch high power factor rectifier	38
Fig 4.7	Output Power Vs Input Power Factor for Single switch high power factor rectifier	38

Fig 4.8	Output Power Vs Input Harmonic factor for Single switch high power factor rectifier	38
Fig 4.9	SIMULINK model of the converter under SPWM	39
Fig 4.10	DC Output voltage for a switching frequency of 1 KHz	40
Fig 4.11	Phase A current for fs = 1KHz	40
Fig 4.12	FFT Analysis of source current for fs = 1KHz	41
Fig 4.13	Phase A current for fs = 10 KHz	41
Fig 4.14	FFT Analysis of source current for fs = 10 KHz	42
Fig 4.15	Output Power Vs THD for SPWM	42
Fig 4.16	Output power Vs Input current for SPWM	43
Fig 4.17	Output power Vs Input power factor for SPWM	43
Fig 4.18	Output power Vs Input harmonic factor for SPWM	44
Fig 4.19	SIMULINK model of HCC controlled converter	44
Fig 4.20	DC output voltage of HCC converter where HB=$\pm$5Amps	45
Fig 4.21	A Phase Current of the converter where HB=$\pm$5Amps	45
Fig 4.22	FFT Analysis of Source current where HB=$\pm$5Amps	46
Fig 4.23	Phase A Current where HB=$\pm$0.5 Amps	47
Fig 4.24	FFT Analysis of Source current	47
Fig 4.25	Output power Vs Total Harmonic Distortion for HCC	48
Fig 4.26	Output power Vs Input current for HCC	48
Fig 4.27	Output power Vs input power factor for HCC	49
Fig 4.28	Output power Vs input harmonic factor for HCC	49
Fig 4.29	SIMULINK model of the converter under IDC	50
Fig 4.30	Output Voltage for fs = 1 KHz under IDC	50
Fig 4.31	Phase A current for fs = 1KHz	51
Fig 4.32	FFT analysis of source current for fs = 1KHz	51
Fig 4.33	Phase A Current for fs = 10KHz	52
Fig 4.34	FFT analysis of source current for fs = 10 KHz	52
Fig 4.35	Output Power Vs THD for IDC	53
Fig 4.36	Output Power Vs Input Current for IDC	53
Fig 4.37	Output Power Vs Input Power Factor for IDC	54
Fig 4.38	Output Power Vs Input Harmonic Factor for IDC	54
Fig 4.39	SIMULINK Model of the converter under SVM	55
Fig 4.40	Output Voltage for fs = 1KHz for SVM	55
Fig 4.41	Phase A Voltage for fs = 1KHz under SVM	56
Fig 4.42	FFT Analysis of the source current for fs = 1KHz under SVM	56
Fig 4.43	Phase A Current for fs = 10 KHz under SVM	57
Fig 4.44	FFT Analysis of the source current for fs = 10KHz under SVM	57

Fig 4.45	Output Power Vs Total Harmonic Distortion for SVM	58
Fig 4.46	Output Power Vs Input Current for SVM	58
Fig 4.47	Output Power Vs Input power factor for SVM	59
Fig 4.48	SIMULINK model of the converter under APCC	59
Fig 4.49	Output Voltage of the converter for fs = 10 KHz	60
Fig 4.50	Phase A current for fs = 10 KHz	60
Fig 4.51	FFT Analysis of source current for fs = 10 KHz	61
Fig 4.52	Output Power Vs THD for 4wire APCC	61
Fig 4.53	Output Power Vs Input Current for 4wire APCC	62
Fig 4.54	Output Power Vs Input Power Factor for 4wire APCC	62
Fig 4.55	Output Power Vs Input Harmonic factor for 4wire APCC	63
Fig 4.56	SIMULINK model of the 4 wire rectifier under HCC	63
Fig 4.57	Output Voltage for fs = 10 KHz for 4wire rectifier under HCC	64
Fig 4.58	Phase A Current for fs = 10KHz for 4 wire rectifier under HCC	64
Fig 4.59	FFT Analysis of Source Current for fs = 10 KHz	65
Fig 4.60	Output Power Vs THD for 4 wire rectifier under HCC	65
Fig 4.61	Output Power Vs Input Current for 4 wire rectifier under HCC	66
Fig 4.62	Output Power Vs Input Power Factor for 4 wire rectifier under HCC	66
Fig 4.63	Output Power Vs Input Harmonic Factor for 4 wire rectifier under HCC	67
Fig 5.1	Output power Vs THD	74
Fig 5.2	Output power Vs Input current	75
Fig 5.3	Output Power Vs Input power factor	75
Fig 5.4	Output power Vs Input harmonic factor	76

List of Tables

Table No	Table Description	Page No
Table 3.1	Switching sequence table	34
Table 5.1	Various Parameters of the converters for load resistance=40ohms, load inductance=2mH and switching frequency of 1 KHz	70
Table 5.2	Various Parameters of the converters for load resistance=40ohms, load inductance=2mH and switching frequency of 10 KHz	71
Table 5.3	Various Parameters of the converters for load resistance=40ohms and switching frequency of 1 KHz	72
Table 5.4	Various Parameters of the converters for load resistance=40ohms and switching frequency of 5 KHz	73

Glossary

AC	Alternating Current
APCC	Average Predictive Current Control
DC	Direct Current
DCM	Discontinuous Current Mode
Fc	Carrier Frequency
FFT	Fast Fourier Transform
Fs	Switching Frequency
HB	Hysteresis Band
HCC	Hysteresis Current Control
HPF	High Power Factor
ICC	Instantaneous Current Control
IDC	Indirect Current Control
IEEE	Institute of Electrical and Electronics Engineers
IGBT	Insulated Gate Bi-polar Transistor
KHz	Kilo-Hertz
PCC	Point of Common Coupling
PF	Power Factor
PFCR	Power Factor Corrected Rectifier
PI	Proportional Integral
PWM	Pulse Width Modulation
RMS	Root Mean Square
SPWM	Sinusoidal Pulse Width Modulation
SVM	Space Vector Modulation
THD	Total Harmonic Distortion
UPS	Uninterruptible Power Supply

Contents

Candidate's Declaration
Acknowledgement
Abstract
List of Figures *i*
List of Tables *iv*
Glossary *v*

Chapter 1
Introduction and Literature Survey

1.1 Introduction 1
1.2 Harmonic Standards 2
1.3 Literature Survey 3

Chapter 2
High Power Factor Rectifiers

2.1 Introduction 6
2.2 Single Switch High Power Factor Rectifiers 6
2.2.1 Control Strategy 8
2.3 Six Switch Rectifiers 9
2.3.1 Amplitude and Phase Control 9
2.3.2 Sinusoidal Pulse Width Modulation 10
2.3.3 Hysteresis Current Control 13
2.3.3.1 Fixed Band Control 14
2.3.3.2 Sinusoidal Band Control 14
2.3.4 Indirect Current Control 18
2.3.4.1 Principle of Indirect Current Control 18
2.3.4.2 Sinusoidal PWM Control 20
2.3.4.3 Modulating Signal 21
2.3.5 Four Wire PWM Rectifiers 22
2.3.5.1 PFCR Control in Stationary Reference Frame 24

Chapter 3
Space Vector Modulation

3.1 Introduction 27
3.2 Features of Space Vector PWM 27
3.3 Space Vector Concept 28

3.4 Space Vector Representation of three phase quantity 30
3.5 Principle of Space Vector PWM 30
3.6 Realization of Space Vector PWM 31
3.6.1 Determine Vd, Vq, Vref, angle α 31
3.6.2 Determine time duration 31
3.6.3 Determine the switching time for each thyristor 33
3.6.4 Switching time table at each sector 34

Chapter 4
Simulation Study

4.1 Introduction 35
4.2 Single Switch High Power Factor Rectifier 35
4.3 Sinusoidal Pulse Width Modulation 39
4.4 Hysteresis Current Control 44
4.5 Indirect Current Control 50
4.6 Space Vector Modulation 55
4.7 Four Wire Rectifiers 59
4.7.1 Average Predictive Current Control 59
4.7.2 Hysteresis Current Control 63

Chapter 5
Comparative Analysis of Control Strategies Studied

5.1 Introduction 68
5.2 External Performance Measures 69

Chapter 6
Conclusion and Future Scope 77

References 79
Bibliography 82
Appendix A 87

CHAPTER 1

Introduction and Literature Survey

1.1 Introduction

AC/DC power converters are extensively used in various applications like power supplies, dc motor drives, front-end converters in adjustable-speed ac drives, slip power recovery control of induction motors, HVDC transmission, SMPSs, UPSs, utility interface with non-conventional energy sources such as solar PVs, wind, etc., in process technology like welding, power supplies for telecommunications systems, aerospace, military environment and so on.

Up to now AC-to-DC converters have been dominated by uncontrolled rectifiers or line commutated phase controlled rectifiers followed by a bulk capacitor. These rectifiers are inexpensive, highly reliable. The problems related to these uncontrolled rectifiers can be summarized as follows:

(i) Large reactive power drawn by the rectifiers from the power system which requires that the distribution equipment handle large power, thus increasing its volt-ampere ratings.

(ii) Voltage drops at the buses.

(iii) Higher input current harmonics resulting in the distorted line current which tends to distort the line voltage waveform. This often creates problems in the reliable operation of sensitive equipment operating on the same bus.

(iv)Increased losses in the equipments (due to harmonics) such as transformers and motors connected to the utility.

(v) Deteriorated performance of induction motors in terms of poor efficiency and torque pulsations.

(vi) Electromagnetic interference with the nearby communications circuits.

(vii) Blown-fuses on power factor correction capacitors due to high voltages and currents from resonance with line-impedance and capacitor bank failures.

(viii) Nuisance operation of protective devices including false tripping of relays.

(ix) Damaging dielectric heating in cables.

(x) Lower rectifier efficiency due to large rms values of input current.

Passive filters are often used to filter the low order harmonics as they have a simple circuit configuration. The main drawbacks of passive filters are bulk passive elements, fixed compensation characteristics and series and parallel resonance with the system impedance. Nowadays more and more applications require that the front AC-to-DC converters have both rectifying and regenerating abilities with fast response to improve the dynamic performance of the whole system. To fulfill this bidirectional requirement a dual converter (12 thyristor) structure with circulating current control may be used. This results in both complicated power circuit and control. A better solution is to use pulse width modulated (PWM) AC-to-DC voltage source converters or current controlled rectifiers (CCR's) which have the merits of nearly sinusoidal input current, good power factor and regeneration ability. A significant improvement in converter behavior has been achieved by means of closed loop control techniques. A number of control strategies have been applied to three phase AC-to-DC converters some of which include sinusoidal pulse width modulation (SPWM), hysteresis current control (HCC), indirect current control (IDC), SPWM with instantaneous current control, space vector modulation (SVM). All these control strategies achieve the same steady-state characteristics, but with different implementations, dynamic response, PWM patterns and harmonic contents. This new breed of converters has been made possible mainly because of the use of modern solid-state, self-commutating power semi-conducting devices such as Power MOSFETs, IGBTs, GTOs, etc.

1.2 Harmonic Standards

Different standards that are followed are listed below

- IEEE 519: Harmonic control Electrical power systems.
- IEEE Harmonic's working group.
- IEC Norm 555-3, prepared by the International Electrical Commission.
- IEC Power quality standards.
- US Military Power Quality Standards
- EN 50 006, "The limitation of disturbances in electricity supply networks caused by domestic and similar appliances equipped with electronic devices", European standard prepared by CENELEC.
- West German Standards VDE 0838 for household appliances, VDE 0160 for converters, and VDE 0712 for fluorescent lamp ballasts.

In the thesis IEEE-519 standards is taken for comparison with the obtained simulation results.

This is common standard which is used, briefly the total harmonic distortion of current drawn must be below 5% and individual harmonic components shouldn't be greater than 3%.

1.3 Literature Survey:

PSPICE has been the most popular tool for the simulation of electronic circuits. However some of the aspects like controller design, system linearization pose a problem with this software package. To handle such problems, the MATLAB/SIMULINK tool has been reported as the best choice. By Tarasantisuk and Tunyasrirut [16]. The authors suggest that many of the converters like buck, boost, buck-boost, fly back and cuk converters can be simulated in SIMULINK and the control system design also becomes simpler.

Hysteresis Current Control is one of the best control strategies for AC-to-DC converters. It can be applied to either single phase rectifiers [2] or three phase rectifiers. Green and Boys [3] have clearly explained the principle of HCC for a three phase AC-to-DC converter. The converter has been modeled to derive the switching states of the six power devices. This three phase converter controlled can be used as a DC voltage source for a voltage source inverter fed variable speed AC drive whose load is regularly overhauling.

In HCC, the switching frequency does not remain constant. Therefore, to restrict the maximum available converter frequency, Gatlan C. and Gatlan L. [1] have proposed the concept of lock out circuits which restrict the frequency. An alternative solution to maintaining constant switching frequency in HCC has been suggested by Dewan and Slemon [4]. They proposed a new control strategy called the "Predictive Current Control with fixed switching frequency (PCFF)" which is a modification of the HCC scheme. By modeling and simulating a three phase AC-to-DC converter under this control, it has been found that the switching frequency remains constant while retaining all the advantages of HCC.

The implementation of HCC in three phase AC-to-DC converters requires three current sensors. This causes an increase in the cost of the converter. As an alternative to this, Dixon and Ooi [5] have introduced the "Indirect Current Control (IDC)" scheme which eliminates the need for current sensors. The contro law of IDC can be derived using Space Vector Modulation [6]. The modeling and implementation are easier as compared to the conventional method.

Space Vector Modulation (SVM) is an advanced and computational intensive technique for control of AC drives. It is the best among all the PWM techniques. SVM can be implemented by the representation of voltages in the α-β plane [8]. The authors have given a step by step procedure of generating the PWM pulse pattern for a voltage source inverter in detail. The SIMCOUPLER module that provides an interface between PSIM software package and MATLAB/SIMULINK tool is used for simulation.

The SVM control algorithm can be simplified by eliminating the need for calculating the angle α which decides the sector [9]. Instead timings are used to decide the sector through the use of counters. Mao, Yunping and Huiming have used the PE-PRO VC33 experimental platform for experimentation.

Single switch DCM boost rectifier has the problem of large number of harmonics in the input current. Jang and Jovanovic [11] have designed a fifth harmonic trap filter for this rectifier as this is the major order harmonic. A comparative analysis of the performance of a single switch three phase DCM boost rectifier, a multi resonant switching buck rectifier and three phase DCM boost rectifier is detailed.

In a single switch DCM boost rectifier, power factor correction is achieved by operating the switch at constant frequency [10]. The authors explain the design procedure for all the parameters of the rectifier circuit.

Four wire rectifiers are mainly used in UPS systems and AC-DC-AC converters. The control strategy of four wire rectifiers can be designed either in the stationary reference frame or rotating reference frame. Fraser and Manning [12, 13] have described the control strategy of four wire rectifier in stationary and rotating reference frames. In [13] the authors explain the design of a predictive average current controller that controls a four wire rectifier digitally. This is definitely an improvement over the analogue controller as it reduces the component count and improves the reliability. DSP's can be used for implementation.

Three-level PWM rectifiers are [14,19] an advantage over two-level rectifiers as they generate high voltage pattern with low voltage rating power switches, reduces dv/dt stresses and decreases the voltage harmonic content on the AC side.

The other control schemes reported in literature are Slope Generated Hysteresis (SGH) current control [15] and Power balance control [17].

In [20], author M.H.Rashid has briefly presented different ideas about control strategies. The control method of boost regulators is clearly explained. In [21], B.K.Bose has explained the principle of HCC, Sinusoidal PWM with instantaneous current control and SVM in detail. This greatly helps in the design of closed loop control system.

The aim of this thesis is to make a comparative analysis of some of the control strategies of AC-to-DC converters discussed in literature. The converter is modeled and simulated in the MATLAB/SIMULINK program. The performance of the converter controlled by these schemes has been evaluated under varying conditions of load, switching frequency and change of the operating mode. Finally all the schemes are compared by means of some external performance measures and graphs.

CHAPTER 2

High Power Factor Rectifiers

2.1 Introduction

AC to DC converters controlled by PWM methods have the merits of nearly sinusoidal input current, high power factor and regeneration capability. However non PWM methods have also been used for the control of these converters. These converters can be classified in a number of ways based on the number of switches used, the control scheme adopted etc. Based on the number of switches used in the converter, the three phase converter can be classified as:

1. Single switch high power factor rectifier
2. Six switch rectifier

The single switch rectifier consists of a three phase diode bridge followed by a single switch whereas the six switch rectifier consists of six power switches that have to be controlled. The control schemes that are available for the control of the three phase converter are enlisted below:

- Amplitude and Phase Control
- Sinusoidal Pulse Width Modulation
- Hysteresis Current Control
- Indirect Current Control
- Space Vector Modulation
- Predictive Current Control
- Average Current Control

This chapter discusses the basic principle of each of the above schemes and gives a detailed description of the method of implementation for a three phase AC-to-DC converter. The method of generation of gate pulses for the power devices is explained.

2.2 Single Switch High power factor rectifiers:

HPF rectifiers can be classified as multi- or single-switch rectifiers. Generally, the rectification performance of the multi-switch rectifiers is superior to that of the single-switch rectifiers since the multiple-switch rectifiers can achieve higher power factors and lower harmonic distortions of the line currents. Specifically, six-switch rectifiers have been extensively used in a variety of HPF applications While the use of multi-switch rectifiers is quite justified in high-power, high-performance applications, the increased number of switches and the complexity of their control make multi-switch rectifiers too

expensive in lower power, cost sensitive applications. For example, today's HPF telecommunication rectifiers, which only need to reduce the total harmonic distortion (THD) of the line current to below 10-15%, are exclusively implemented either with passive LC filters or active, single-switch rectifiers. Three phase rectifiers employed have a single active switch and perform HPF rectification naturally without a need for a complex control circuitry; they are very suitable for the low-cost, low-power three phase ac-dc applications [11]

The circuit diagram of the power stage of the single-switch, three-phase, PWM, DCM boost rectifier is shown in Fig 2.1. Since the boost rectifier in Fig 2.1 (a) is operated in DCM with a constant frequency and constant duty cycle, all three-phase input currents, ia, ib, and ic, are zero at the end of a switching period, immediately before boost switch S is turned on. After switch S is turned on, ia, ib, and ic, increase linearly to the peak values, which are proportional to the line to- neutral voltages as shown in Fig 2.1(b). Therefore, during the switch-on period, each line current forms a triangular pulse with the peak value proportional to the associated line to-neutral voltage. As a result, during the switch-on period, the average line currents are proportional to the line-to neutral voltages. When the switch is turned off, the input currents start decreasing because output voltage Vo is higher than the peak of the input voltage. In DCM, the input currents reach zero before the end of the switching period. Since the rate of the input-current decrease is proportional to the difference between output voltage Vo and line-to-neutral voltage, the average line currents during the off period of the switch are not proportional to the line voltages, i.e., even if the line voltages are perfectly balanced and sinusoidal, the line currents are distorted. The normalized harmonic content of the rectifier input current is a function of the voltage-conversion ratio M, which is defined as

$$M = Vo/\sqrt{3}\ Vm$$

where Vo is the rectifier output voltage and Vm, is the peak line-to-neutral voltage. The rectifier input-current spectrum, which contains only odd harmonics, is dominated by the 5th-order harmonic, i.e., the lowest order harmonic.[11]

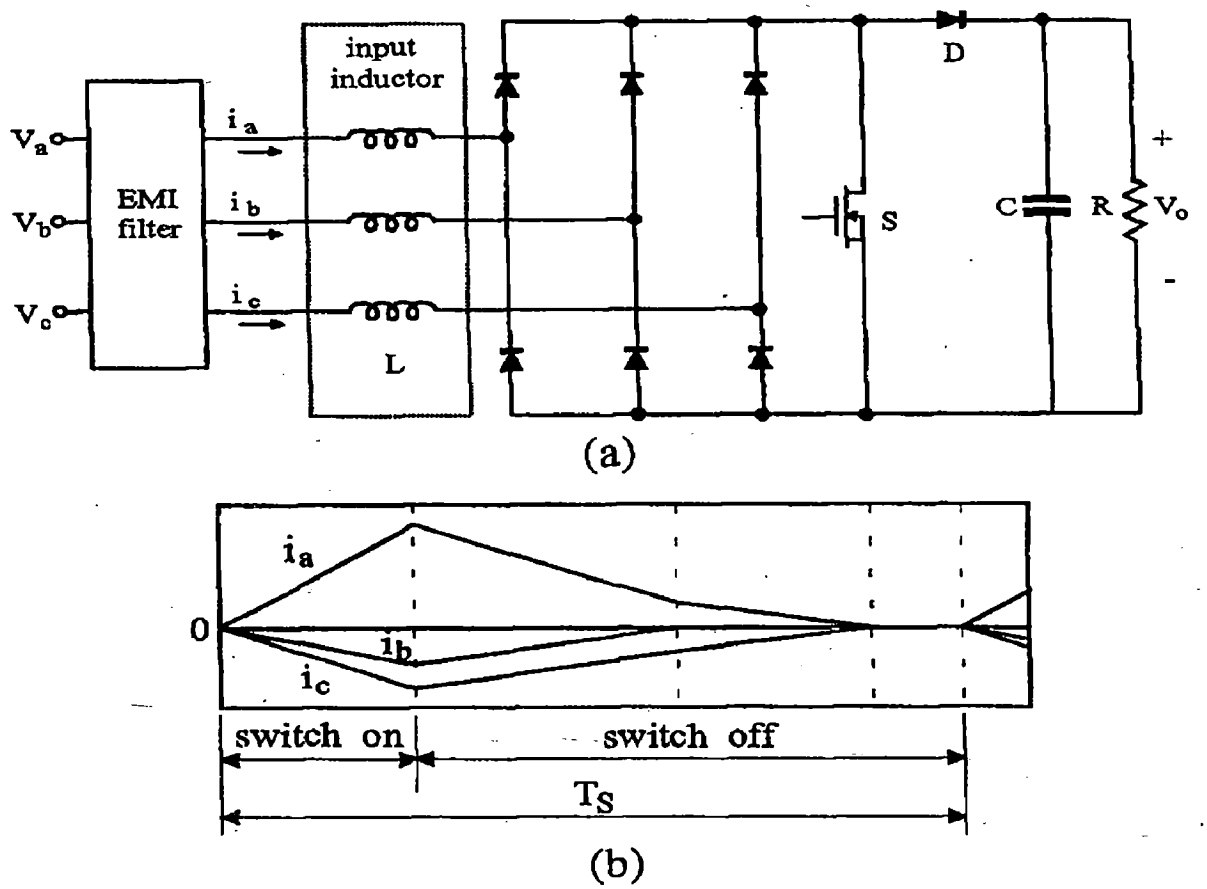

Fig 2.1 Single-switch three-phase DCM boost rectifier (a) circuit diagram (b) input current waveforms during switching cycle [11]

2.2.1 Control Strategy: [20]

The control signals for the single device in three phase boost rectifier are generated by comparing a control voltage with a saw tooth waveform of fixed frequency i.e. the device is switched at constant frequency. The control voltage can be obtained by comparing the output voltage with its desired value. The control and power circuit of the three phase boost rectifier are as shown in the figure 2.2:

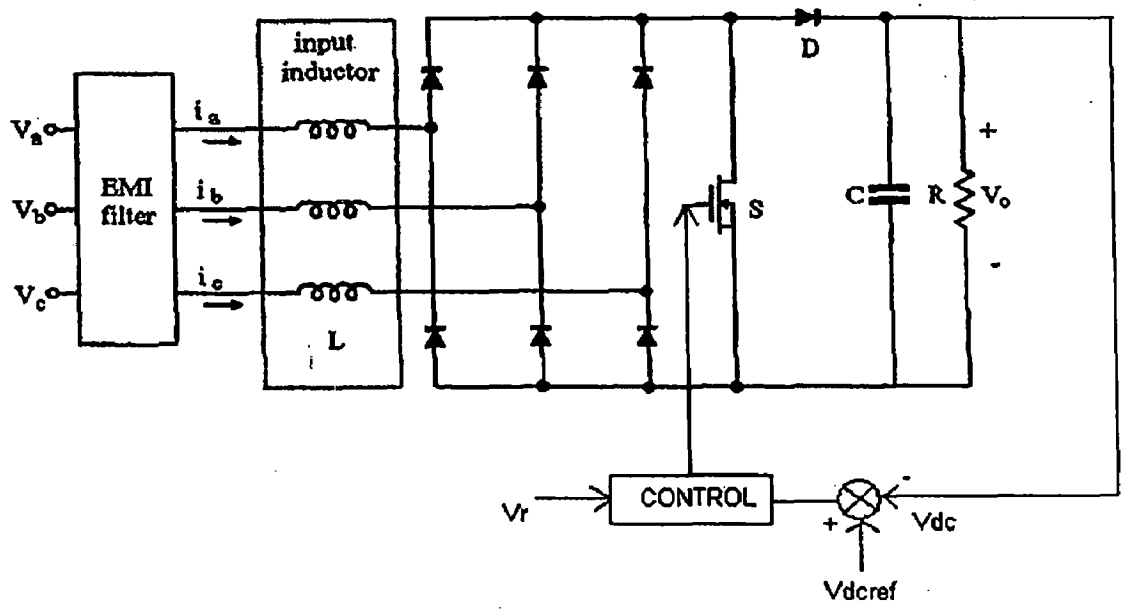

Fig 2.2 Control Circuit of a three phase boost rectifier

2.3 Six Switch Rectifiers

The six switch rectifiers can be controlled by any of the methods listed earlier. However the phase and amplitude control strategy is a non PWM method and is the oldest control scheme.

2.3.1Amplitude and Phase Control [22]

The circuit of a six pulse bridge converter is as shown in the figure 2.3. It consists of six thyristors. The thyristors T1, T3, T5 are called the positive group since they are turned on when the supply voltages are positive. Similarly the thyristors T4, T6, T2 which conduct when the supply voltages are negative form the negative group. . The firing angle for positive group of thyristors (T1, T3, T5) is measured from 30° with reference to the positive half cycle of the phase voltage. The negative group of thyristors are turned on 180° after the positive group thyristors. In each input cycle there are six pulses in the output voltage. The thyristors conduct for a period of 120° each and each phase conducts the positive current for 120° and negative current for 120°. The output voltage is obtained by conduction of two phases at any time. Because of the higher pulse number, the distortion factor of the supply current improves significantly and the output voltage ripple is considerably reduced.

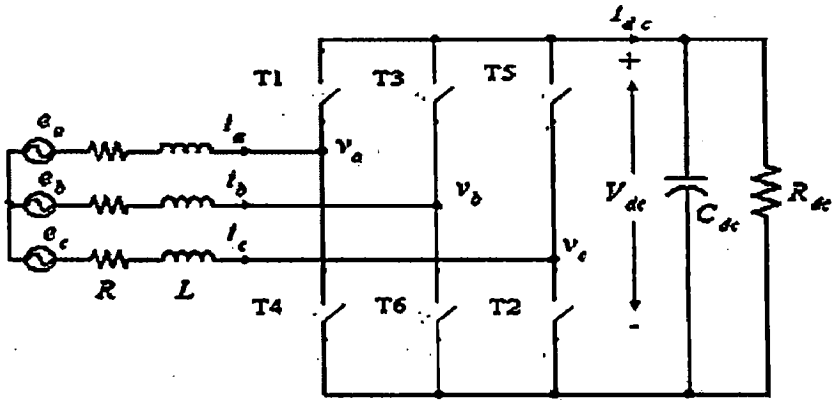

Fig 2.3 Six Pulse Bridge Converter

The six thyristors need to be triggered in a sequence so as to make the supply currents balanced. If the output current is assumed to be constant, the output voltage at any instant is equal to one of the six line voltages. This requires that two thyristors two in the positive group and one in the negative group be gated together simultaneously. In order to vary the average value of output voltage, the gate pulses to the thyristor pairs are to be controlled. The earliest instant at which each thyristor can be turned on is taken as the datum for measuring the firing angle of each thyristor i.e. the instants at which the phase voltages crossover are the reference points for the measurement of firing angles. Thus by proper generation of the firing pulses for the six thyristors the output voltage of the converter can be controlled.

2.3.2 Sinusoidal Pulse Width Modulation with instantaneous Current Control: [21]

The sinusoidal PWM technique is very popular for industrial converters. . In this, isosceles triangle carrier wave of frequency fc is compared with the fundamental frequency f sinusoidal modulating wave, and the points of intersection determine the

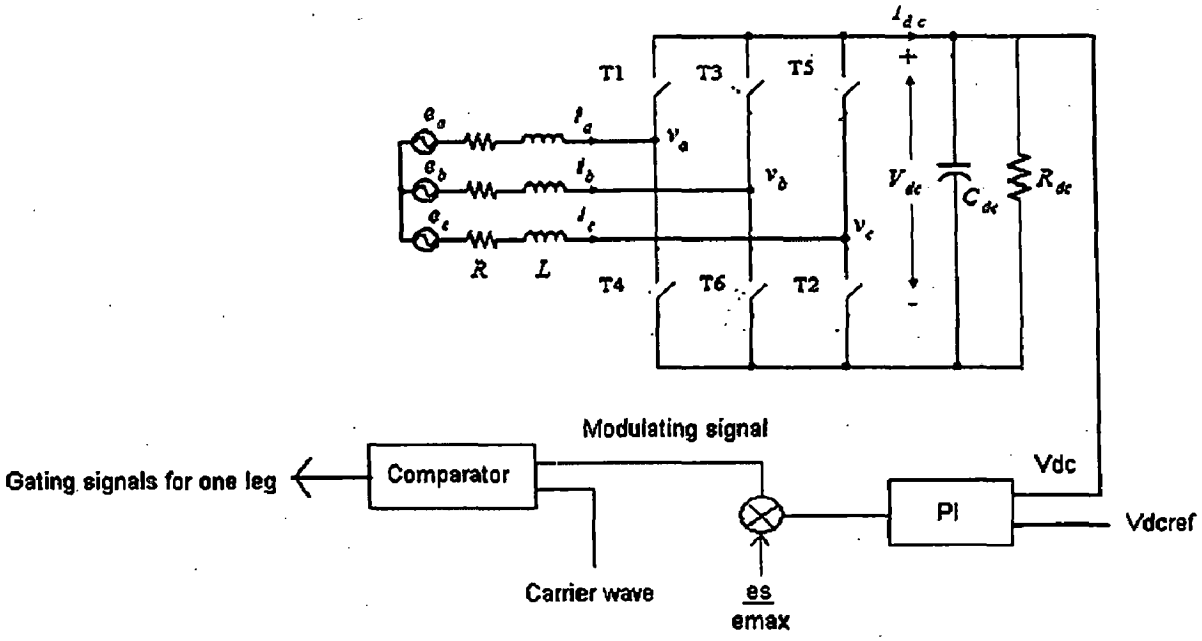

Fig 2.4 SPWM Controlled converter

switching points of power devices. The notch and pulse widths vary in sinusoidal manner so that average or fundamental component frequency is same as f and its amplitude is proportional to the command modulating voltage. The same carrier wave can be used for all 3 phases. Fig 2.5 illustrates the SPWM method based on using the intersection points of the modulation signal and the triangle carrier signal as the time instants for turning the switches in a given phase, complementarily ON and OFF This method of encoding the modulating signal through the pulse width is accurate when the frequency of the carrier is sufficiently high. The modulation signal is amplified with a constant gain, without delay.

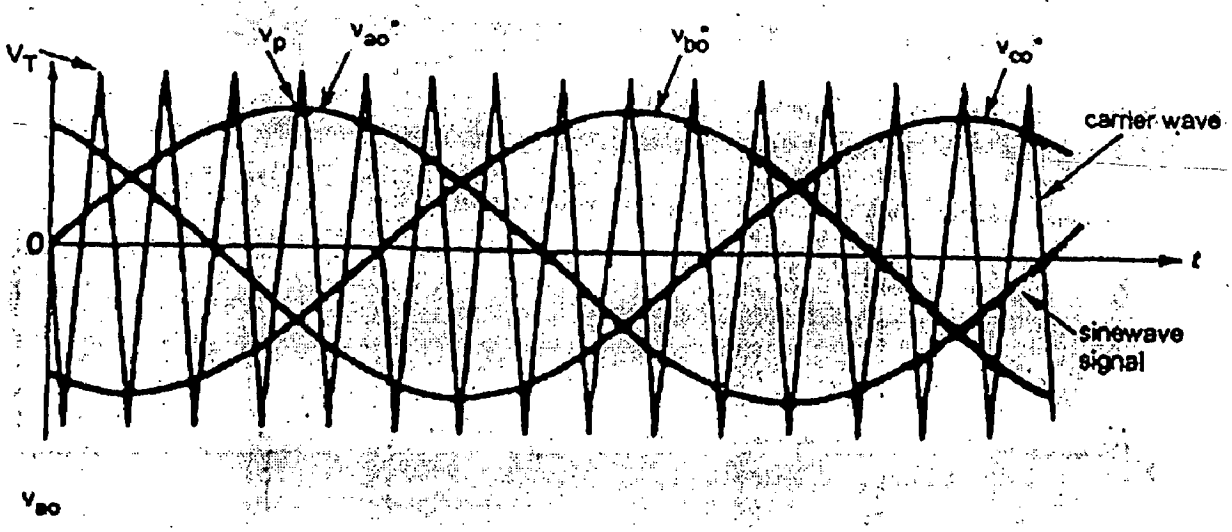

Fig 2.5 Principle of SPWM [21]

Modulation Index (M.I): [20]

$$M.I = \frac{Amplitude\_of\_modulating\_wave}{Amplitude\_of\_carrier\_wave}$$

- M.I. determines the fundamental component output voltage
- If 0<M.I<1 , V_1 = M.I (V_{in}) where V_1,V_{in} are the fundamental of the output voltage and input DC voltage respectively

Modulation Ratio (Freq Ratio), M_R: [20]

$$M_R = \frac{Frequency\_of\_carrier\_wave}{Frequency\_of\_modulating\_wave}$$

- Modulation ration determines the incident of harmonics in the spectra
- f=K.M_R (f_m), where f_m is the frequency of modulating signal and k is integer (1, 2, 3....)

Total Harmonic Distortion (THD) : [20]

If V_n is voltage of n^{th} harmonic voltage;

$$THDv = \frac{\sqrt{\sum_{n=2}^{\infty}(V_{n,RMS})^2}}{V_{1,RMS}}$$

$$= \frac{\sqrt{V_{2,RMS}{}^2 + V_{3,RMS}{}^2 + ... + V_{2,RMS}{}^2}}{V_{1,RMS}}$$

The selection of a carrier frequency depends on the trade-off between converter loss and the system loss. Higher carrier frequency increases converter switching loss but decreases the system harmonic loss. An optimal carrier frequency should be selected such that the total system loss is minimal. An important effect of PWM switching frequency is the generation of acoustic noise (known as magnetic noise) by the magnetostriction effect when the converter supplies power to a machine. The effect can be alleviated by randomly varying the switching frequency, or it can be completely eliminated by increasing the switching frequency above the audio range. Modern high-speed IGBT's easily permit such acoustically noise-free variable-frequency drives. Low-pass line filters can also eliminate this problem.

If SPWM is applied in open loop, the results are not satisfactory. In order to control the input current, a feedback current loop is applied. In such cases the converter operates as a programmable current source. Fig 2.6 shows an instantaneous current control scheme with

sinusoidal voltage PWM in the inner loop. The error in the sinusoidal current loop is converted to sinusoidal voltage command through a proportional-integral (P-I) controller. This voltage is the compared with the carrier wave to generate the gating pulses. For a

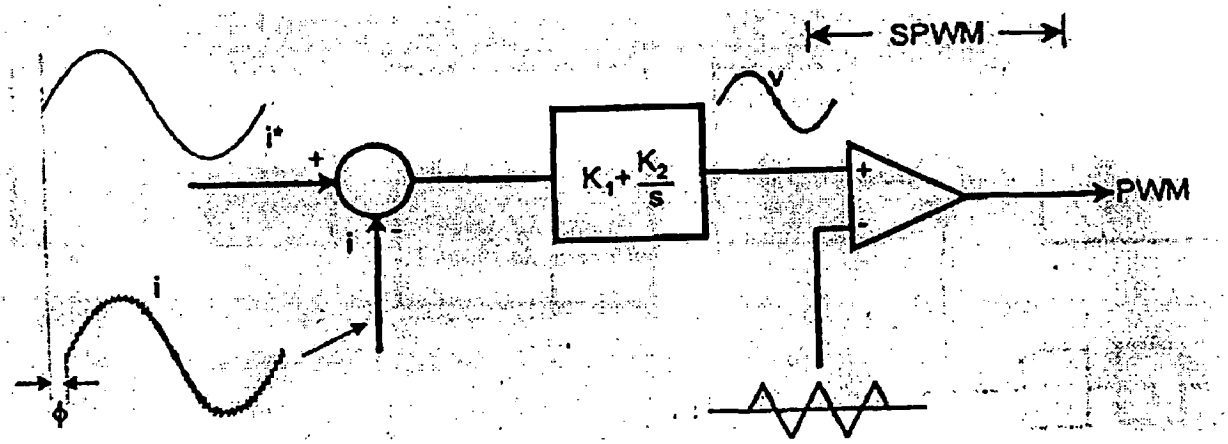

Fig 2.6 Control block diagram for instantaneous control SPWM [21]

three phase converter, three similar controllers are used. The control is simple but there are a few problems. Due to limited band-width of the control system, the actual current will have a phase lag and magnitude error which will increase with frequency. Such phase deviation is very harmful in high-performance drive systems. The sinusoidal voltage command generated by the current control loop may contain ripple, which may create a multiple zero crossing problem in the SPWM comparator.

2.3.3 Hysteresis Current Control

Hysteresis-band PWM is basically an instantaneous feedback current control method of PWM where the actual current continually tracks the command current within a hysteresis band. This is a simple current control method where hysteresis comparators are used to impose a dead band or hysteresis around the reference current. This control scheme provides excellent dynamic performance because it acts quickly. Also, an inherent peak current limiting capability is provided. This technique does not need any information on system parameters. [21]

The hysteresis current control generates an asymmetrical pulse pattern. The hysteresis band can be fixed or variable over a fundamental period.

2.3.3.1 Fixed band control: [1]

In this scheme the hysteresis bands are fixed over the fundamental period.
The algorithm for this scheme is:

$i_{ref} = i_{max} \sin wt$

upper band $i_u = i_{ref} + H/2$

lower band $i_l = i_{ref} - H/2$

where H= hysteresis band limits

2.3.3.2 Variable or sinusoidal band control: [1]

In this scheme the hysteresis band varies sinusoidally over a fundamental period. The upper and lower bands are given as:

$i_{ref} = i_{max} \sin wt$

upper band $i_u = (i_{max} + H/2) \sin wt$

lower band $i_l = (i_{max} - H/2) \sin wt$

The hysteresis current controlled converter is as shown below (Fig 2.7):

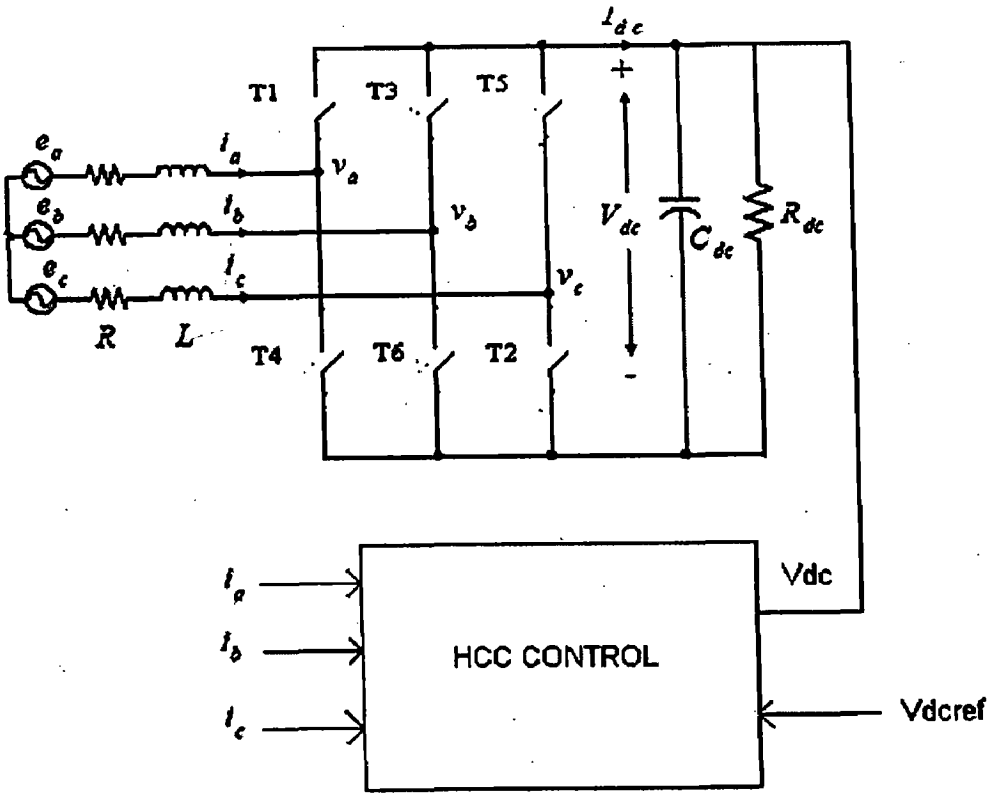

Fig 2.7 Hysteresis Current Controlled Converter

Fig 2.8 explains the operation principle of hysteresis-band PWM for one leg of the three phase converter.

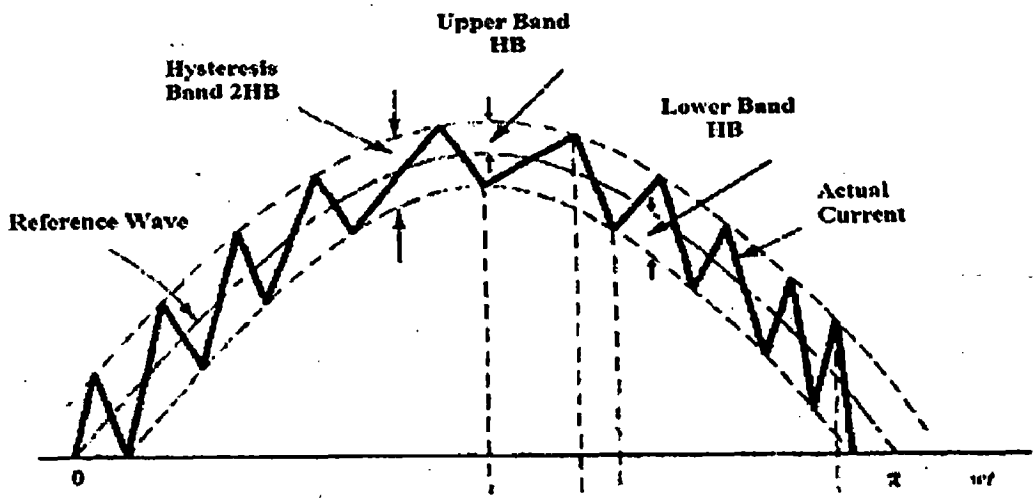

Fig 2.8 Principle of operation of HCC controlled converter [21]

The control circuit generates the sine reference current wave of desired magnitude and frequency, and it is compared with the actual phase current wave. As the current exceeds a prescribed hysteresis band, the upper switch of the leg is turned of and lower switch is turned on. As the current crosses the lower band limit, the lower switch is turned off and the upper switch is turned on. The actual current wave is thus forced to track the sine reference wave within the hysteresis band by back-and-forth (or bang-bang) switching of the upper and lower switches. The peak-to-peak current ripple and switching frequency are related to the width of the hysteresis band. A smaller band will increase the switching frequency and lower the ripple. So, an optimum band that maintains a balance between the harmonic ripple and switching loss should be chosen. [21]

The control block diagram for implementation of hysteresis band PWM is shown in the figure 2.9. The error in the current control loop is impressed at the input of a comparator with a hysteresis band as shown. The bandwidth of hysteresis band is given as

$$HB = V * R2 / (R1+R2)$$

Where V= Comparator supply voltage.

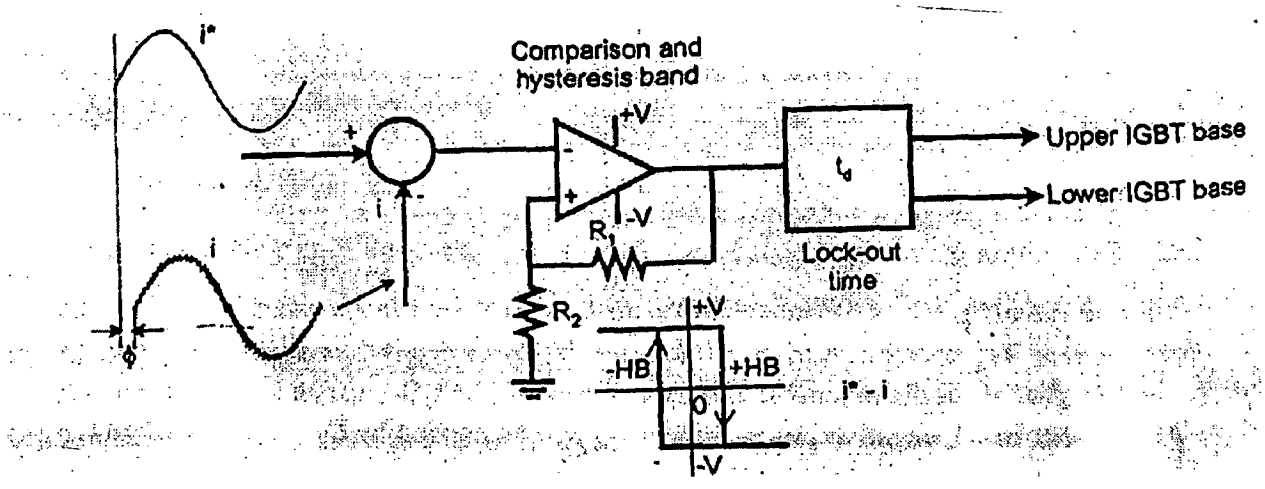

Fig 2.9 Control block diagram for Hysteresis band PWM [21]

The conditions for switching devices are:

Upper switch on:

$$(i^*-i)>HB$$

Lower switch on:

$$(i^*-i)<HB$$

For the three phase converter, a similar control circuit is used in all the phases.
The advantages of the hysteresis current control scheme can be enlisted as below:

1. The scheme generates nearly sinusoidal current waveform with unity power factor.
2. Implementation is simple.
3. Fast transient response.
4. Direct limiting of device peak current.
5. Practical insensitivity of Dc link voltage ripple that permits a lower filter capacitor.

However this scheme suffers from some disadvantages. The fundamental current suffers a phase lag that increases at higher frequency. The major problem of HCC is that its average frequency Fs varies with the DC load current [4]. At heavy loads, frequency increases substantially. The switching pattern is uneven and random and the instantaneous switching frequency is higher than the average value as shown in the figure 2.10 below causing excessive stress on switching devices.

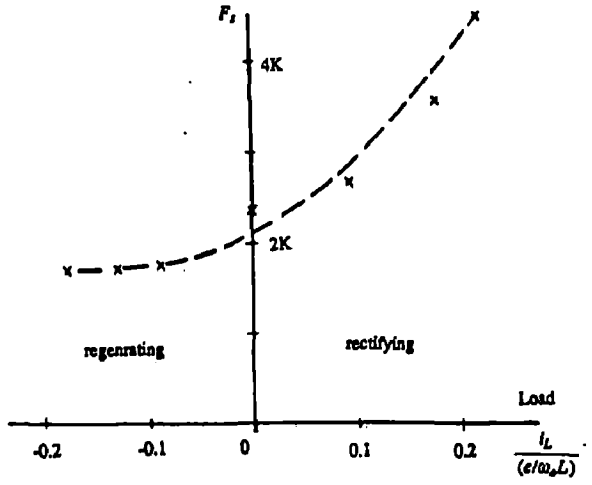

Fig 2.10 Variation of load with switching frequency under HCC [4]

2.3.4 Indirect Current Control:

Many PWM control schemes for voltage source converters usually employ two or three current sensors to implement the instantaneous current control and to limit the line currents for the protection of the switching devices. But these current sensors bring some additional hardware such as A/D converters in case of digital implementation in its train and cause the system complexity, cost-up and reduction of system reliability. In the indirect control as the name implies, the function of the inner hysteresis current control feedback loop is mimicked and implemented by hardware representing transfer function blocks. The ac currents are indirectly controlled by standard sinusoidal PWM, which essentially modulates the fundamental harmonic component of voltage. In eliminating the inner hysteresis current feedback loop, one dispenses with the need for at least two high-quality broad band-width current measuring transducers. This method falls back on the well-known sinusoidal PWM control in which the switching instants are determined by the intersections of the triangular wave carrier and the modulating sine wave. [6]

2.3.4.1 Principle of Indirect Current control: [5]

The objective is to be able to operate the rectifier so that the fundamental harmonic component of the phase current, which is represented by the phasor I in Fig, makes a constant power angle ϕ . As the rectifier becomes more heavily loaded, it is the current magnitude I that increases. For inverter operation I takes a negative value (180° phase reversal). Considering the fundamental harmonic of the supply frequency only, if the phase circuit impedance is

$$Z = R + jwL = R + jX,$$

one can indirectly control the current by the fundamental component of the voltage V*ph* at the terminals of the rectifier. Based on Kirchhoff s Voltage Law, the required voltage V*ph* is obtained from the equation

$$V_{ph} = V - IZ \qquad (1)$$

The above equation is represented in the phasor diagram of Fig. In the time-domain, one sees that if

$$Va(t) = \sqrt{2}\, V \sin wt \qquad (2)$$

then the requisite control voltage has to be

$$V_{pha}(t) = \sqrt{2}\, V_{ph} [\cos \xi \sin wt - \sin \xi \cos wt] \qquad (3)$$

where the in-phase component is

$$V_{ph} \cos \xi = V + (X \sin \varphi - R \cos \varphi).\, I \qquad (4)$$

and the in-quadrature component is

$$V_{ph} \sin \xi = (X \cos \varphi + R \sin \varphi).\, I \qquad (5)$$

From (4) and (5) one sees that since V, R, and X can be measured beforehand from the ac circuit, one can operate at any power angle φ for any demand of the current magnitude I provided the in-phase and the quadrature components of V_{ph} are made to satisfy (4) and (5).

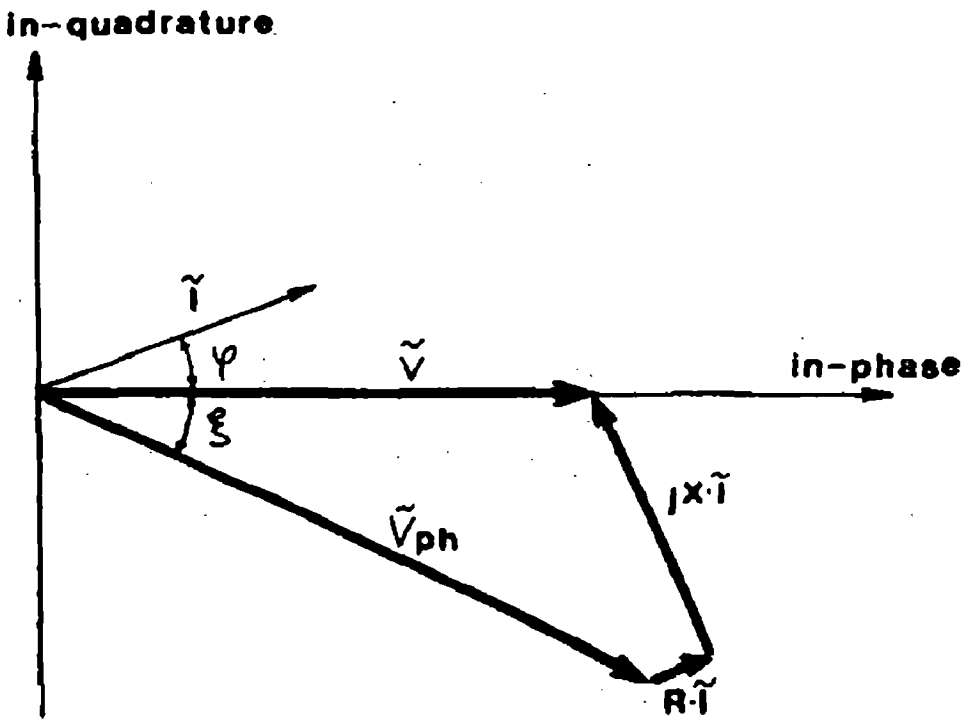

Fig 2.11 Voltage phasor diagram of ac circuit [5]

2.3.4.2 Sinusoidal PWM Control [5]

Fig. 2.12 (a) and (b) illustrates the waveforms of Va(t) and $V_{ph}(t)$ The voltage $V_{ph}(t)$ is the fundamental component of the voltage at the rectifier terminals, the rectifier being under sinusoidal PWM control. If one imagines the capacitor C to have a center-tap, then the waveform of the voltage between the A-phase rectifier terminal and the center-tap consists of the square wave shown in Fig. 2.12 (c). This modulating waveform switches from +0.5Vc to -0.5Vc, and it is desired that the switching pattern is such that it yields as fundamental component the waveform of V_{ph} (t). Fig. 2.12 (d) illustrates how the switching pattern is generated in the conventional sinusoidal PWM strategy. The switching instants are based on the intersections of the triangular waveform Vt and the modulating sinusoidal waveform Vm (t).

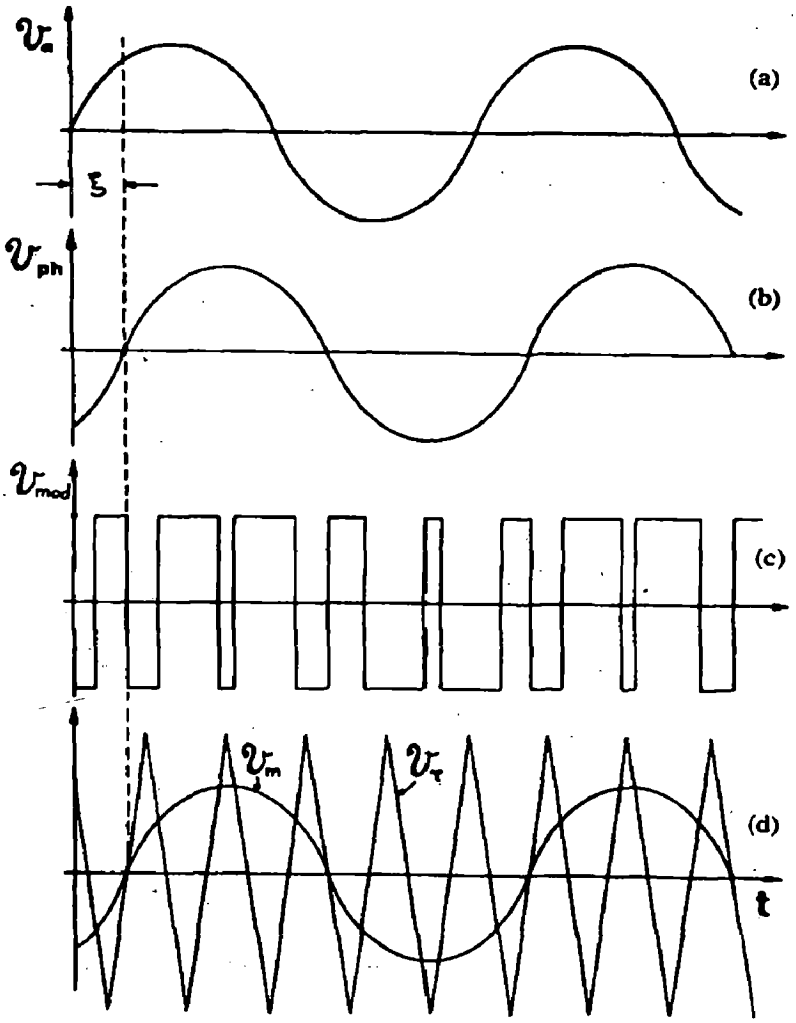

Fig 2.12 (a) A-phase supply voltage (b) Fundamental component of A-phase voltage at rectifier terminal (c) Switched voltage (d) Carrier and modulating waveform [5]

2.3.4.3 Modulating Signal Vm [5]

The generation of the modulating signal of the A-phase is illustrated in the block diagram of Fig.2.13. The input comes from the current magnitude demand I, which is based on the voltage error of the dc link voltage Vc, with respect to the voltage reference Vref . This signal is combined with proportional amplifiers of gains K_1, K_2, and K_3, multipliers, and the generators of the in-phase and the in-quadrature waveforms. The in-phase waveform generator is taken from the voltage transformer across the line-to-neutral of the A-phase. After filtering its output is

$$Vx = \sqrt{2}\, Vs \sin wt \qquad (6)$$

The in-quadrature waveform generator is obtained from subtracting the B-phase from the C-phase voltage, and multiplied by $1/\sqrt{3}$ factor so that its output is

$$Vy = \sqrt{2}\, Vs \cos wt \qquad (7)$$

For the Vm (t) prescribed by the functional blocks of Fig. 2.13, the output voltage at the rectifier terminal is

$$V_{mod}(t) = Vs.Vc\,[(K_1+K_2I)\sin wt - K_3I\cos wt]/\sqrt{2}.V_{tpeak} + \text{Bessel function harmonic terms.} \qquad (8)$$

The objective is to make the fundamental component in (8) identical to (3)-(5). This is done by choosing the values of the constants K_1, K_2, and K_3.

Choosing Constants K_1, K_2, K_3:

By comparing (8) with (3)-(5), the amplifier gains K_1, K_2, K_3 are determined as,

$$K_1 = 2K_4 Va/Vs$$

Where $K_4 = V_{tpeak}/Vc$

$$K_2 = 2K_4(X \sin \varphi - R \cos \varphi) / Vs$$

$$K_3 = 2K_4 (X \cos \varphi + R \sin \varphi)/ Vs$$

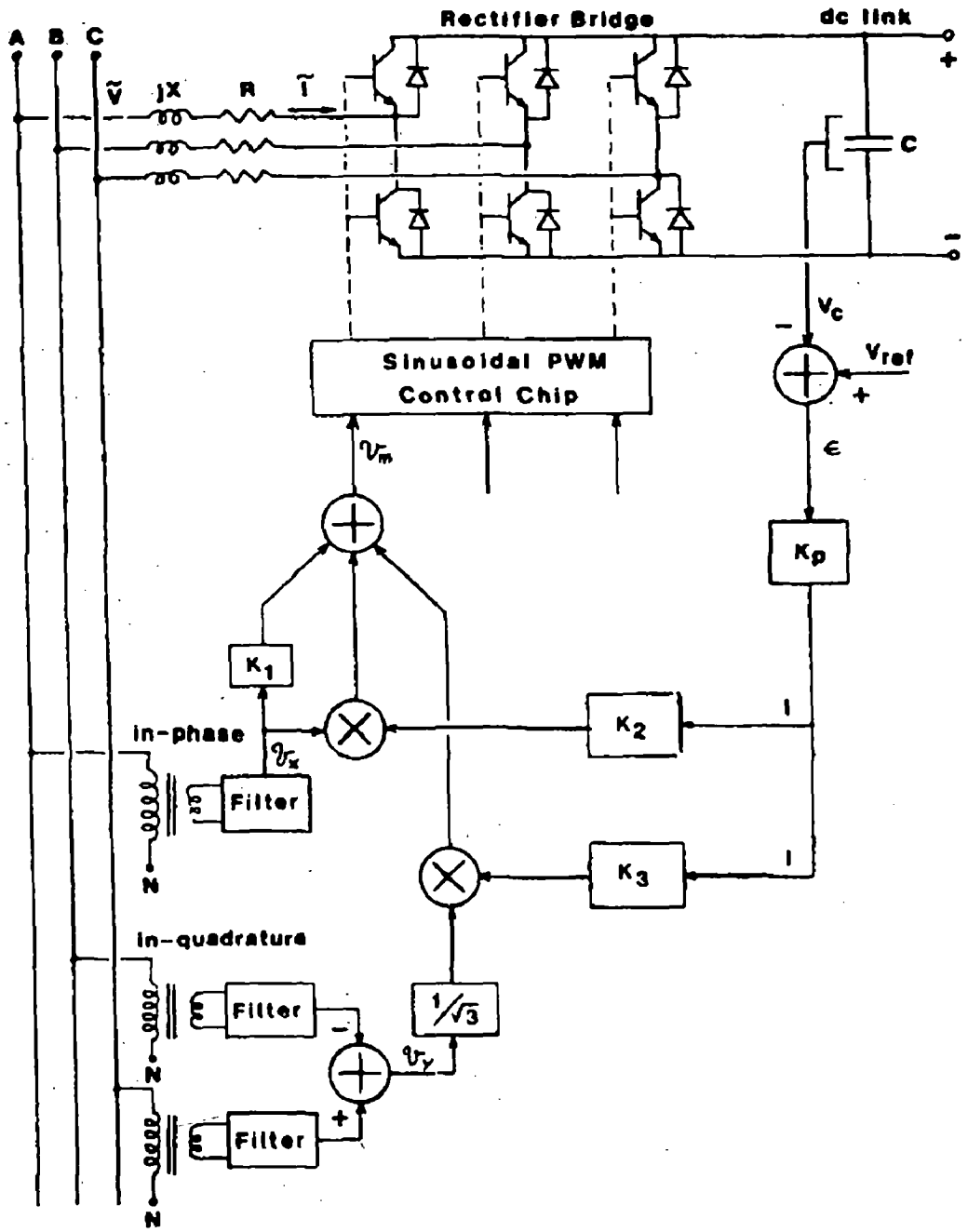

Fig 2.13 Block diagram implementing indirect current control [5]

2.3.5 Four wire PWM rectifiers:

In the last twenty years the voltage quality concept has become essential both for industrial applications and for daily life. Nowadays, electrical systems have become less and less tolerant as regards to power supply disturbances as harmonics, outages, fluctuation and transients. Moreover, solving the VAR compensation problem is essential in transmission and distribution systems design. The impact of non-linear loads on line harmonic voltages and neutral wire sizing is serious for distribution LV networks. [24]

A three-wire AC-boost rectifier has been utilized but its drawback is that the converter line currents cannot be regulated independently the one from the other because their sum must be zero. As a consequence:

- Any voltage disturbance, that is present on all the three supply lines with the same phase (i.e. a third harmonic voltage), cannot be eliminated by the converter.
- HCR control loop ensures that only two of three boost AC currents are within the hysteresis band.
- Voltages on phase to neutral loads cannot be regulated.
- Harmonic and inter-harmonic effects due to single-phase non-linear loads cannot be compensated.

.The advantage of using a four wire rectifier is that the sum of line AC-currents is free, so they can be controlled independently the one from the other. As a consequence all kind of PCC (Point of Common Coupling) voltage disturbance can be compensated and harmonic and inter harmonic effect can be neutralized. However the price to pay using the rectifier as a multi functional converter is an oversizing of the device. One of the main applications of the four-wire rectifier is in the use of transformer less AC-DC-AC converters for uninterruptible power supplies (UPS). This allows the supply neutral and load neutral of the AC-DC-AC converter to be connected together without the requirement of a transformer where galvanic isolation is not required, without any supply neutral current flowing regardless of the load.
The four-wire power factor corrected boost rectifier (PFCR) is shown in Fig. 2.14. This is similar to the three wire PFCR, but provides a neutral connection from the star point of the supply to the centre point of the DC bus using a centre-tapped capacitor. The topology is similar to a four-wire inverter using centre-tapped capacitors for the load neutral connection. Connecting the DC centre-point to the supply neutral can allow harmonic currents to flow in the supply neutral mainly third harmonic owing to the diodes in the bridge. This can be overcome for the four-wire PFCR if

$$V_{dc} > \sqrt{8}\sqrt{V_{ph}^2 + I_{ph}^2 L_{boost}^2 \omega^2}$$

To prevent any low-order harmonic currents flowing in the neutral it is now up to the switch controllers to shape the line currents accordingly. If the three sinusoidal line currents are controlled to keep the amplitudes equal and each with a phase of 120° apart, the neutral current will always be zero.

$$i_{ns} = i_a + i_b + i_c$$
$$= I(t)[\sin(\omega t) + \sin(\omega t - 120°) + \sin(\omega t - 240°)]$$
$$= 0$$

The only neutral current flowing will be a switching frequency ripple current from the summation of the three phases set by the size of the boost inductance in the lines.
This system requires current controllers with a 'good' steady-state and dynamic response to maintain three equally balanced sinusoidal currents during both steady-state and dynamic operation. [12]

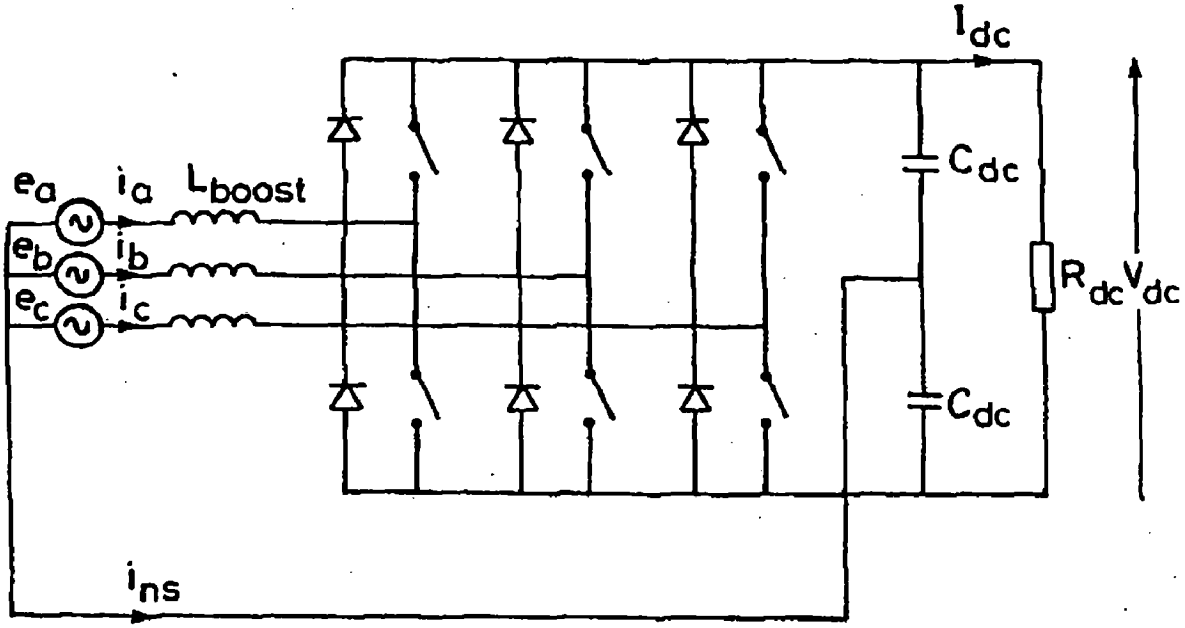

Fig 2.14 Three Phase Four Wire Rectifier

2.3.5.1 PFCR control in stationary reference frame [12]

A current-mode control scheme is required for the line currents. There are different forms of current-mode control including peak current-mode control, hysteresis control and average current-mode control. Average current-mode control has significant advantages over hysteresis and peak current-control including constant switching frequency, improved noise immunity and true average current-mode control afforded by sensing and controlling the average inductor current; thus average current-mode control of the line boost inductor current is used here.

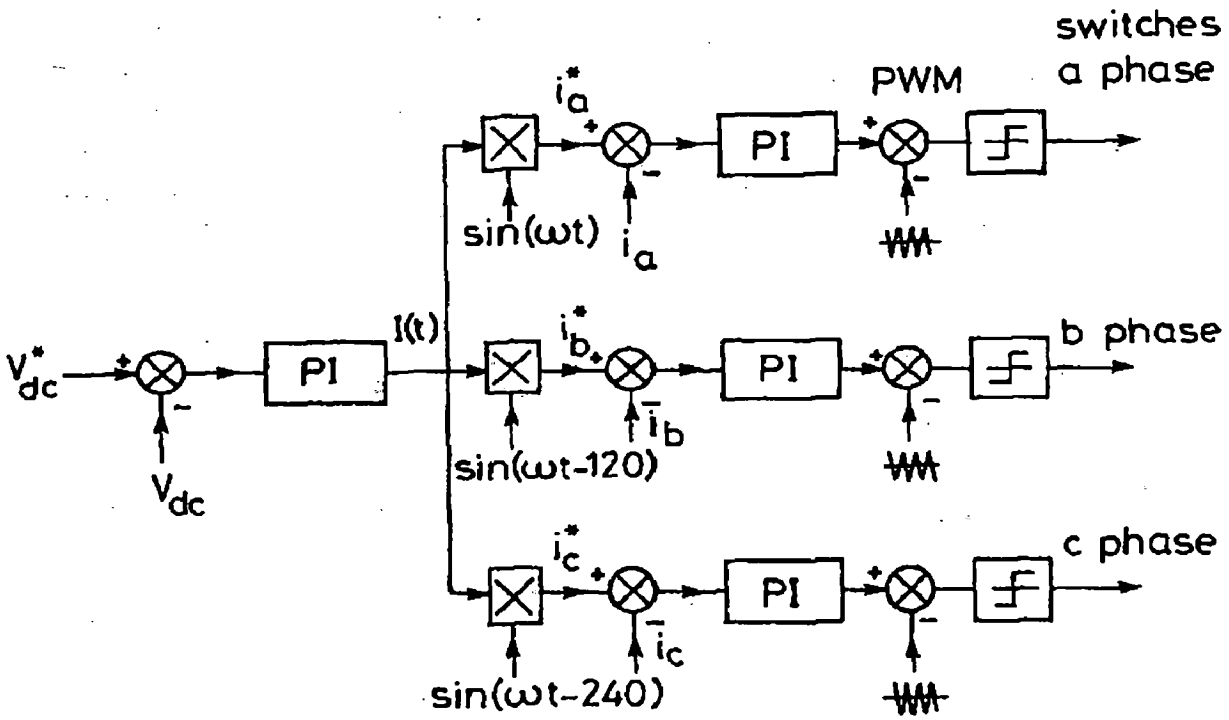

Fig 2.15 Control Circuit of the four wire PFCR [12]

The neutral connection in the four-wire PFCR decouples the three phases and allows individual control of each phase. Fig. 2.15 shows the average current mode control system. The inductor current is measured and compared to a reference. The current error is passed through a proportional and integral (PI) controller providing high gain at low frequencies, but having a filtering effect on the high-frequency ripple current. This signal is compared to a triangular carrier wave to generate the required pulse width modulated (PWM) signal to control the switches. The average current-mode controllers form the inner current loops. The DC bus voltage is controlled by measuring the DC bus voltage and comparing it to a reference. This error signal is passed through a PI controller which then forms the current amplitude reference required for all three inner current loops. The current amplitude reference is multiplied by three sinusoidal templates each with a phase 120° apart to form the true current references. As a unity power factor system is required each sinusoidal reference is in phase with the respective supply phase voltage. The constants of the PI controllers are set to produce a stable system with good steady-state and dynamic response.

Boost inductance

The switching action of the PWM rectifier gives a ripple current in the boost inductors. For an average current mode control scheme the ripple current varies over the cycle of the mains,

the worse case being when the supply voltage e = 0. By approximating the boost inductor current ripple to a triangular wave it can be shown that the worse case ripple is

$$\Delta i = \frac{V_{dc}}{4 f_s L_{boost}} \quad \text{(pk-pk)} \qquad (1)$$

The ripple current is set by the value of the boost inductance and the switching frequency, but independent of load. The required boost inductance is obtained from eqn1.

DC bus capacitance

The DC bus is inherently free from low-order harmonics during steady-state resistive loading apart from the high-frequency ripple voltage. The ripple voltage requires only a relatively small amount of DC capacitance for smoothing. A larger DC capacitance is used though to hold up the DC bus during transient loading and to absorb cyclic power ripple from, say, an inverter load. [12]

The control schemes for three phase single switch rectifier, three phase multi switch rectifier, three phase four wire rectifier have been discussed. The basic principle, control circuit and implementation of the scheme for a three phase AC-to-DC converter are described. The advantages and disadvantages of each strategy are stated and the area of application is given.

CHAPTER 3

Space Vector Modulation

3.1 Introduction

This chapter describes the basic principle of space vector modulation and gives the methodology of generating gate pulses for the power devices of a three phase AC to DC converter.

Space Vector modulation (SVM) technique was originally developed as a vector approach to pulse-width modulation (PWM) for three-phase inverters. It is a more sophisticated technique for generating sine wave that provides a higher voltage to the motor with lower total harmonic distortion. It confines space vectors to be applied according to the region where the output voltage vector is located. A different approach to PWM modulation is based on the space vector representation of voltage in the α-β plane. The α-β components are found by transformations. The determination of switching instant may be achieved using space vector modulation technique based on the representation of switching vectors in α-β plane. The Space vector modulation technique is an advanced, computation intensive PWM technique and is possibly the best among all the PWM techniques for drives applications. Because of its superior performance characteristics, it is been finding wide spread application in recent years. [9]

3.2 Features of Space Vector PWM [8]

The main aim of any modulation technique is to obtain variable output having a maximum fundamental component with minimum harmonics. During the past years many PWM techniques have been developed for letting the inverters to posses various desired output characteristics to achieve the following aim:

- wide linear modulation range
- Less switching loss.
- Lower total harmonic distortion.

The space vector modulation (SVM) technique is more popular than conventional technique because of the following excellent features:

- It achieves the wide linear modulation range associated with PWM third-harmonic injection automatically.

- ❖ It has lower base band harmonics than regular PWM or other sine based modulation methods, or otherwise optimizes harmonics.
- ❖ 15% more output voltage then conventional modulation, i.e. better DC-link utilization.
- ❖ More efficient use of DC supply voltage.
- ❖ SVM increases the output capability of SPWM without distorting line-line output voltage waveform.
- ❖ Advanced and computation intensive PWM technique.
- ❖ Higher efficiency.
- ❖ Prevent un-necessary switching hence less commutation losses.
- ❖ A different approach to PWM modulation based on space vector representation of the voltages in the α-β plane.

3.3 Space Vector concept

The concept of space vector is derived from the rotating field of AC machine which is used for modulating the inverter output voltage. In this modulation technique the three phase quantities can be transformed to their equivalent 2-phase quantity either in synchronously rotating frame (or) stationary frame. From this 2-phase component the reference vector magnitude can be found and used for modulating the inverter output. The process of obtaining the rotating space vector is explained as below, considering the stationary reference frame.

Let the three phase sinusoidal voltage component be,

$V_a = V_m \sin \omega t$

$V_b = V_m \sin (\omega t - 2\pi/3)$

$V_c = V_m \sin(\omega t - 4\pi/3)$ (1)

When this 3-phase voltage is applied to the AC machine it produces a rotating flux in the air gap of the AC machine. This rotating flux component can be represented as single rotating voltage vector. The magnitude and angle of the rotating vector can be found by mean of Clark's Transformation as explained below in the stationary reference frame. The representation of rotating vector in complex plane is shown in Figure 3.1.

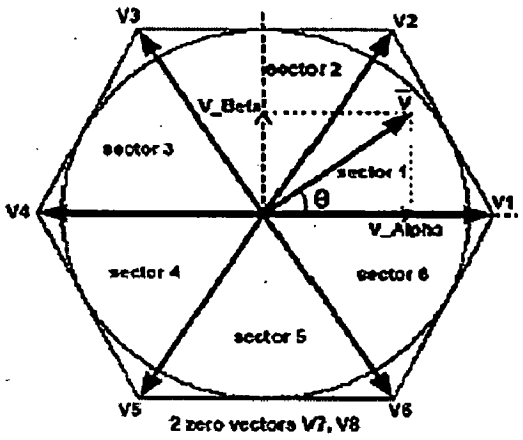

Fig 3.1 Representation of Rotating Vector in Complex Plane [8]

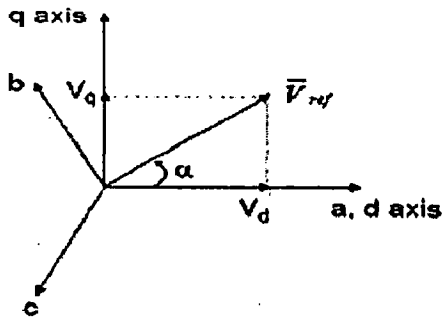

Fig 3.2 Voltage Space Vector and its components in d-q [8]

3.4 Space vector representation of the three phase quantity

$$V^* = V\alpha + jV\beta = 2(Va+aVb+a^2Vc)/3 \quad (2)$$

Where,

$$a = e^{j2\pi/3}$$

$$|V| = \sqrt{V\alpha^2 + V\beta^2},\ \tan\alpha = V\beta/V\alpha \quad (3)$$

$$V\alpha + jV\beta = 2/3\{ Va + e^{j2\pi/3}Vb + e^{-j2\pi/3}Vc\} \quad (4)$$

$$V\alpha + jV\beta = 2/3\{ Va + \cos 2\pi/3Vb + \cos 2\pi/3Vc\} + j2/3\{\sin 2\pi/3Vb - \sin 2\pi/3Vc\}$$

Equating real and imaginary parts:

$$V\alpha = 2/3\{ Va + \cos 2\pi/3Vb + \cos 2\pi/3Vc\} \quad (5)$$

$$V\beta = 2/3\{0.Va + \sin 2\pi/3Vb - \sin 2\pi/3Vc\} \quad (6)$$

$$\begin{bmatrix} V\alpha \\ V\beta \end{bmatrix} = 2/3 \begin{bmatrix} 1 & \cos 2\pi/3 & \cos 2\pi/3 \\ 0 & \sin 2\pi/3 & -\sin 2\pi/3 \end{bmatrix} \begin{bmatrix} Va \\ Vb \\ Vc \end{bmatrix} \quad (7)$$

$$\begin{bmatrix} V\alpha \\ V\beta \end{bmatrix} = 2/3 \begin{bmatrix} 1 & -0.5 & -0.5 \\ 0 & \sqrt{3}/2 & -\sqrt{3}/2 \end{bmatrix} \begin{bmatrix} Va \\ Vb \\ Vc \end{bmatrix} \quad (8)$$

3.5 Principle of Space Vector PWM

- Treats the sinusoidal voltage as a constant amplitude vector rotating at constant frequency.
- This PWM technique approximates the reference voltage V_{ref} by a combination of the eight switching patterns (V0 to V7).
- Coordinate Transformation (abc reference frame to the stationary d-q frame): A three-phase voltage vector is transformed into a vector in the stationary d-q coordinate frame which represents the spatial vector sum of the three-phase voltage.

3.6 Realization of Space Vector PWM

The space vector PWM is realized based on the following steps:

Step1. Determine Vd, Vq, Vref, and angle (α).

Step2. Determine time duration T1, T2, T0.

Step3. Determine the switching time of each transistor (S1 to S6).

3.6.1 Determine Vd, Vq, Vref, and Angle (α):

Coordinate transformation: abc to dq

The Voltage Space vector and its components in dq plane is shown in Figure 3.2

$Vd = Van - Vbn \cos 60° - Vcn \cos 60°$

$= Van - ½\, Vbn - ½\, Vcn$

$Vq = 0 + Vbn \cos 30° - Vcn \cos 30°$

$= Van + \sqrt{3}/2\, Vbn - \sqrt{3}/2\, Vcn$ (9)

$$\begin{bmatrix} Vd \\ Vq \end{bmatrix} = 2/3 \begin{bmatrix} 1 & -1/2 & -1/2 \\ 0 & \sqrt{3}/2 & -\sqrt{3}/2 \end{bmatrix} \begin{bmatrix} Van \\ Vbn \\ Vcn \end{bmatrix} \quad (10)$$

$|Vref| = \sqrt{Vd^2 + Vq^2}$

$\tan \alpha = Vq/Vd = \omega st = 2\pi fst$

(where, fs = fundamental frequency)

The voltage Vd, Vq, Vref, and angle α are calculated using the above equation.

3.6.2 Determine Time Duration T1, T2, T0:

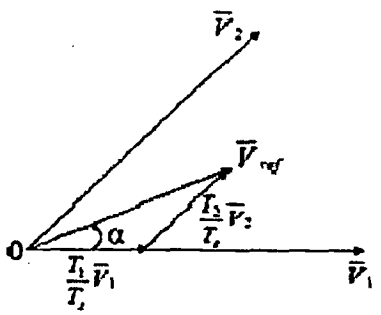

Fig 3.3 Reference vector as a combination of adjacent vectors at sector1 [8]

$$\int_0^{T2} Vref = \int_0^{T1} V1\,dt + \int_{T1}^{T1+T2} V2\,dt + \int_{T1+T2}^{T2} V0$$

therefore, Tz..Vref = (T1.V1+T2.V2)

$$Tz\,|Vref| \begin{bmatrix} \cos\alpha \\ \sin\alpha \end{bmatrix} = T1.2/3.Vdc \begin{bmatrix} 1 \\ 0 \end{bmatrix} + T2.2/3.Vdc \begin{bmatrix} \cos\pi/3 \\ \sin\pi/3 \end{bmatrix}$$

Where $0 \le \alpha \le 60^\circ$

$T1 = Tz.a.\sin(\pi/3-\alpha)/\sin(\pi/3)$

$T2 = Tz.a.\sin\alpha/\sin(\pi/3)$

$T0 = Tz-(T1+T2)$, (where Tz 1/fs and $a = |Vref|/(2/3).Vdc$)

WhereT1,T2,T0 represent the time widths for vectors V1,V2,V0.T0 is the period in a sampling period for null vectors should be filled. As each switching period (half of sampling period) Tz starts and ends with zero vectors i.e. there will be two zero vectors per Tz or four null vectors per Ts, duration of each null vector is to/4. Figure 3.4 gives switching pattern for all sectors.

Switching time duration at any Sector:

$$T1 = \sqrt{3}.Tz.|Vref|/Vdc\left[\sin\left[\pi/3 - \alpha + (n-1).\pi/3\right]\right]$$

$$= \sqrt{3}.Tz.|Vref|/Vdc\left[\sin n\pi/3 - \alpha\right]$$

$$= \sqrt{3}.Tz.|Vref|/Vdc\left[\sin n\pi/3\cos\alpha - \cos n\pi/3\sin\alpha\right]$$

$$T2 = \sqrt{3}.Tz.|Vref|/Vdc[\sin[\alpha - (n-1)\pi/3]]$$

$$= \sqrt{3}.Tz.|Vref|/Vdc\left[-\cos\alpha\sin(n-1)\pi/3 + \sin\alpha\cos(n-1)\pi/3\right]$$

$T0 = Tz-T1-T2$, (where n= 1 through 6 i.e. sector 1 to 6, $0 \le \alpha \le 60^\circ$)

3.6.3 Determine the Switching time for each thyristor [8]

(a) Sector 1

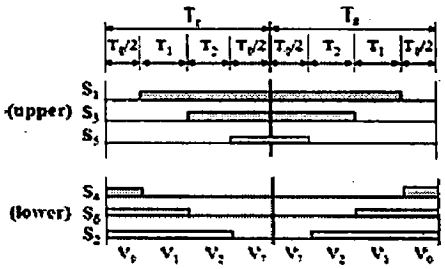

(b) Sector 2

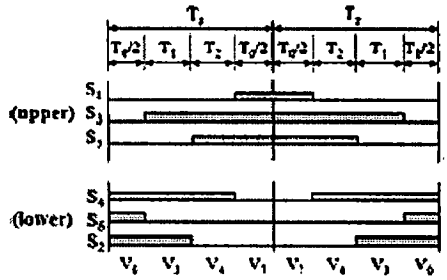

(c) Sector 3

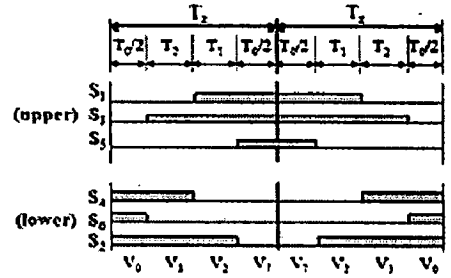

(d) Sector 4

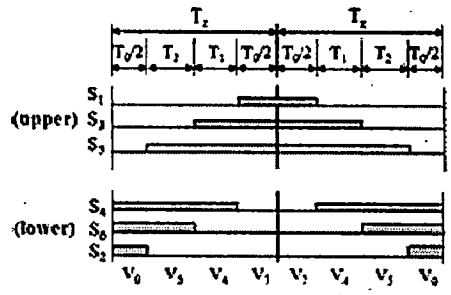

(e) Sector 5

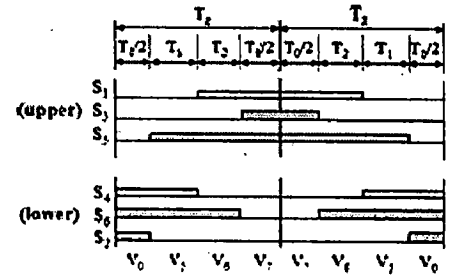

(f) Sector 6

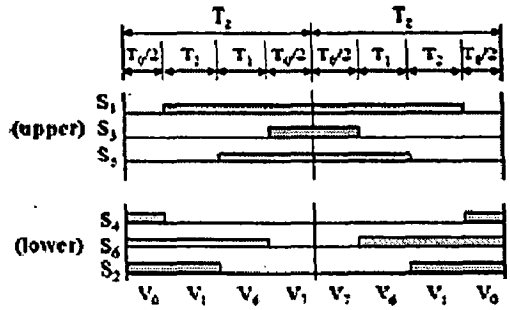

Fig 3.4 Switching pulse pattern for the three phase in the 6 different sectors

3.6.4 Switching time table at each sector:

Sector	Upper Switches (S_1, S_3, S_5)	Lower Switches (S_4, S_6, S_2)
1	$S_1 = T_1 + T_2 + T_0/2$ $S_3 = T_2 + T_0/2$ $S_5 = T_0/2$	$S_4 = T_0/2$ $S_6 = T_1 + T_0/2$ $S_2 = T_1 + T_2 + T_0/2$
2	$S_1 = T_1 + T_0/2$ $S_3 = T_1 + T_2 + T_0/2$ $S_5 = T_0/2$	$S_4 = T_2 + T_0/2$ $S_6 = T_0/2$ $S_2 = T_1 + T_2 + T_0/2$
3	$S_1 = T_0/2$ $S_3 = T_1 + T_2 + T_0/2$ $S_5 = T_2 + T_0/2$	$S_4 = T_1 + T_2 + T_0/2$ $S_6 = T_0/2$ $S_2 = T_1 + T_0/2$
4	$S_1 = T_0/2$ $S_3 = T_1 + T_0/2$ $S_5 = T_1 + T_2 + T_0/2$	$S_4 = T_1 + T_2 + T_0/2$ $S_6 = T_2 + T_0/2$ $S_2 = T_0/2$
5	$S_1 = T_2 + T_0/2$ $S_3 = T_0/2$ $S_5 = T_1 + T_2 + T_0/2$	$S_4 = T_1 + T_0/2$ $S_6 = T_1 + T_2 + T_0/2$ $S_2 = T_0/2$
6	$S_1 = T_1 + T_2 + T_0/2$ $S_3 = T_0/2$ $S_5 = T_1 + T_0/2$	$S_4 = T_0/2$ $S_6 = T_1 + T_2 + T_0/2$ $S_2 = T_2 + T_0/2$

Table 3.1 Switching sequence table [8]

The Switching pulse pattern for the three phases in the 6 different sectors are shown in the Figure 3.4.The Switching sequence table for the lower and upper thyristors are shown in the table 3.1.

The above construction of the symmetrical pulse pattern for two consecutive Tz intervals are shown and Ts = 2Tz = 1 / fs (fs = Switching frequency) is the sampling time. Note that the null time has been conveniently distributed between the V0 and V7 vectors to describe the symmetrical pulse width. Studies have shown that a symmetrical pulse pattern gives minimal output harmonics

A new approach to the implementation of SVM by representation of the three phase voltages in the α-β plane is described clearly and the gate pulse generation methodology is detailed. This procedure of generation of the pulses can be applied to a converter and inverter.

Simulation Study

4.1 Introduction

Extensive simulation is carried out to investigate the performance of the converter under each control strategy. A simulation model is developed for each of these schemes using **MATLAB** and its **POWER SYSTEM BLOCKSET** in **SIMULINK**. Simulation results are obtained under varying conditions of load, switching frequency and change of the mode of operation of the converter. The universal bridge block of the power system block has been used as a common three phase converter for all the models.

The different components that are used to develop the models are listed as follows: Power Supply, Three Phase universal Bridge, Three Phase Diode Bridge, Current Measurement, Voltage Measurement, Capacitor, Inductor, Multiplexers/De-Multiplexers, Scopes etc. Scopes are used to obtain the nature of currents and voltages at any point in the system. The THD of the voltages and currents can also be determined by the POWERGUI block of SIMULINK.

4.2 Single Switch High Power Factor Rectifier:

The SIMULINK model of the single switch high power factor rectifier is as shown below:

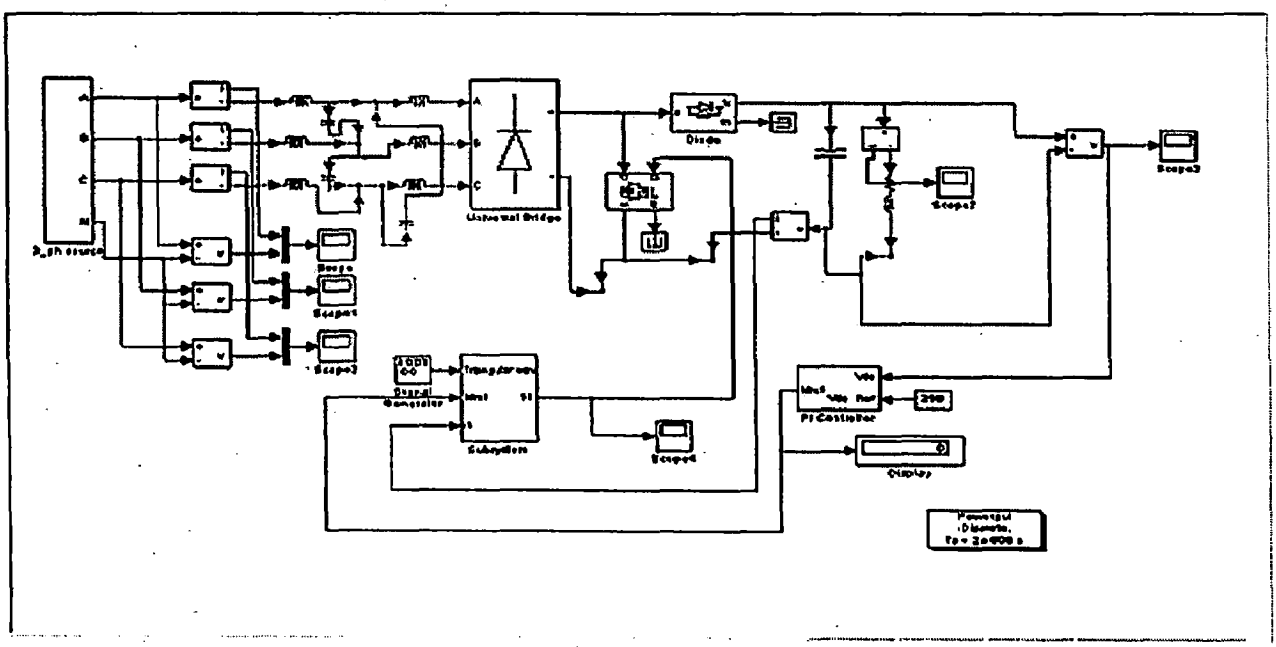

Fig 4.1 SIMULINK model of the single switch high power factor rectifier

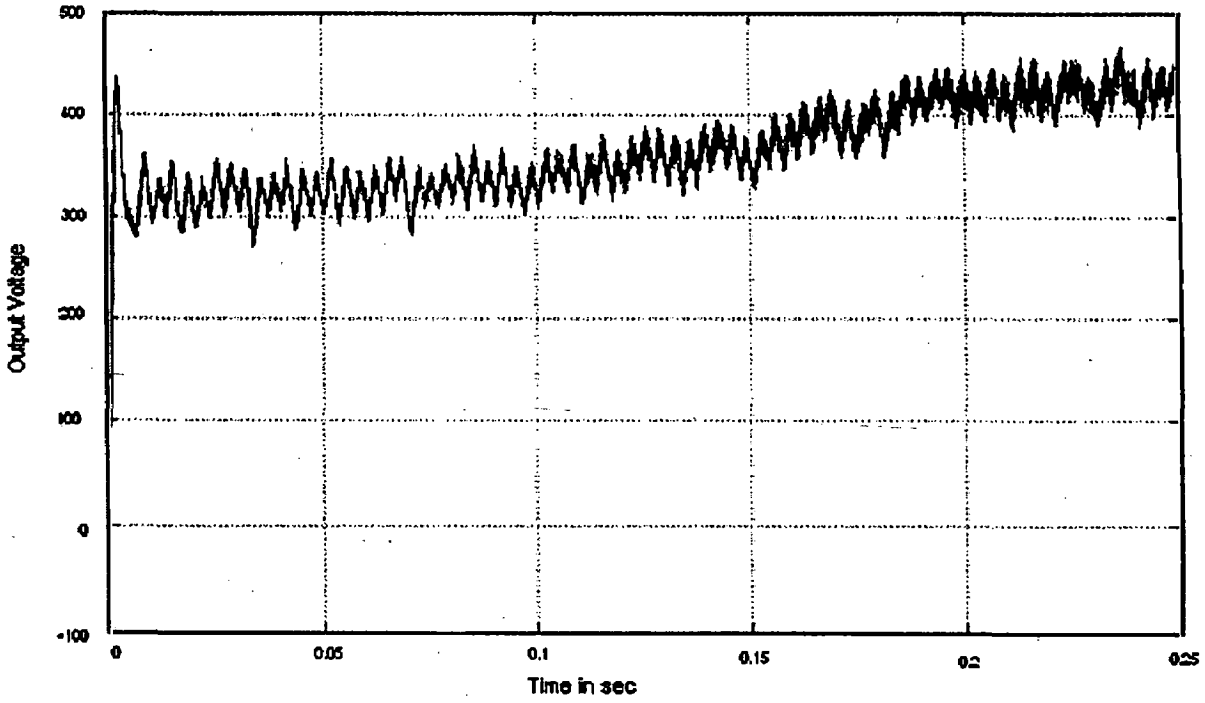

Fig 4.2 Output Voltage of the rectifier for fs = 1 KHz

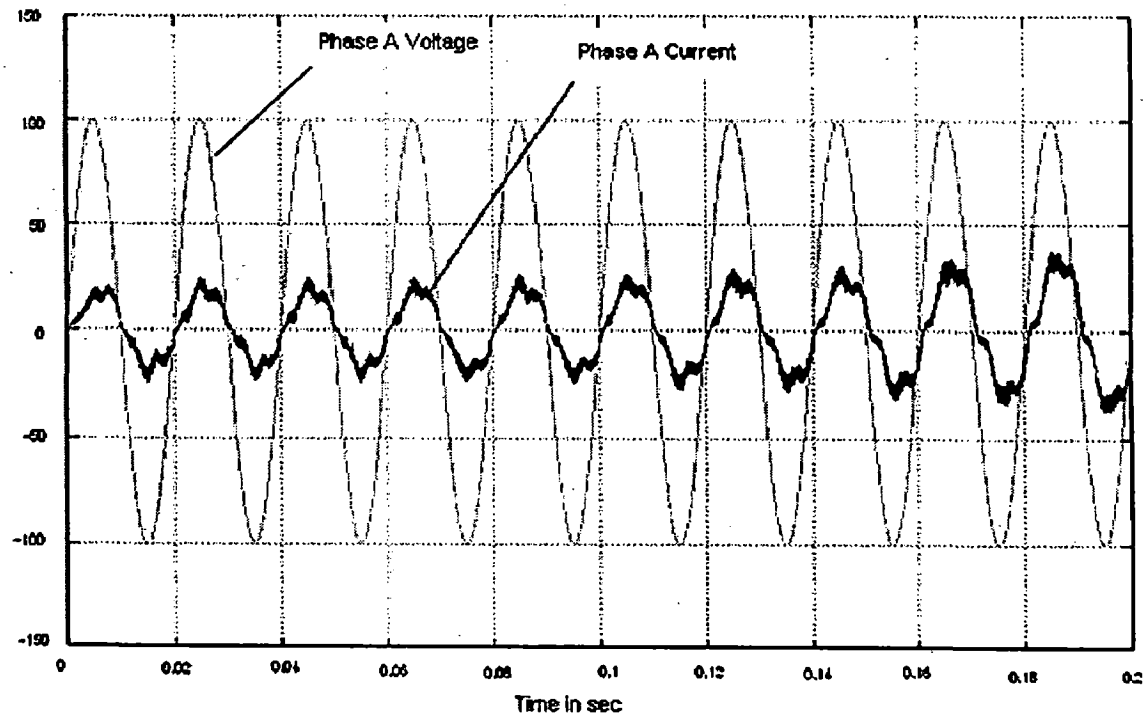

Fig 4.3 Phase A current for fs = 1 KHz for boost rectifier

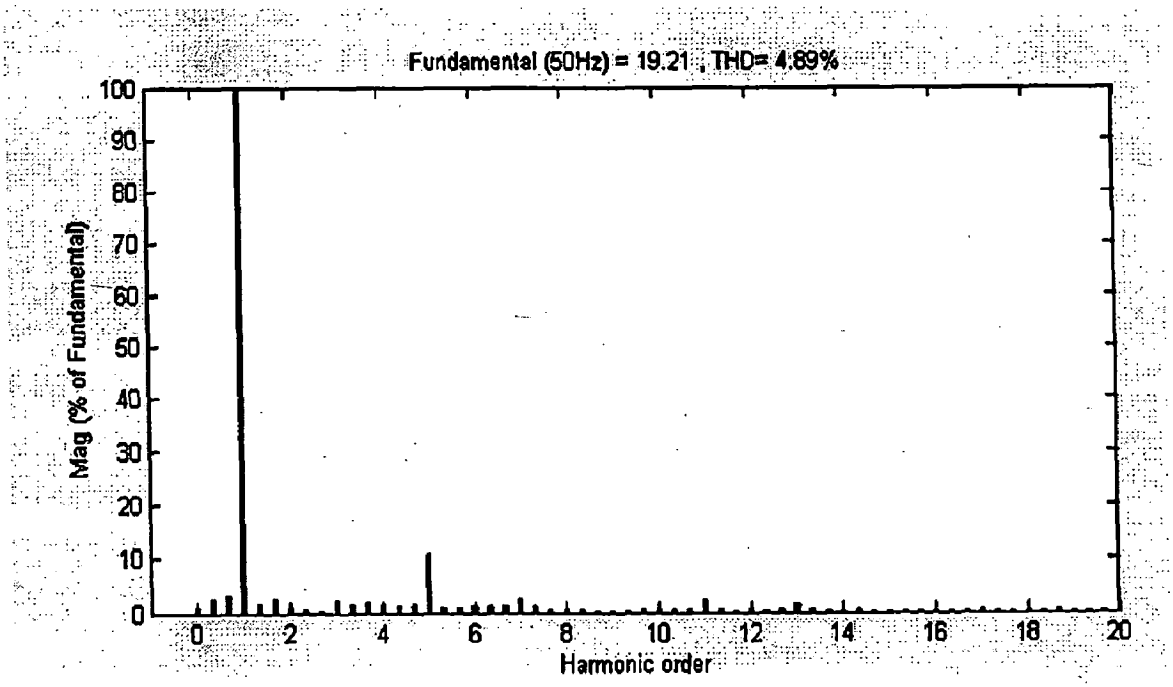

Fig 4.4 FFT analysis of Source Current

The output voltage of the single switch high power factor rectifier for a switching frequency of 10 KHz is shown in fig 4.2. The output voltage of this converter is very high as compared to other converters. However the ripples in the output voltage are also very high. The source current waveform is shown in fig 4.3. It can be clearly observed that the source current is sinusoidal and in phase with the source voltage. The FFT analysis reveals that the total harmonic distortion of the source current is 4.89% which satisfies the IEEE_519 standards. The major harmonics in the input current are the DC component and the fifth harmonic. The plots are shown below.

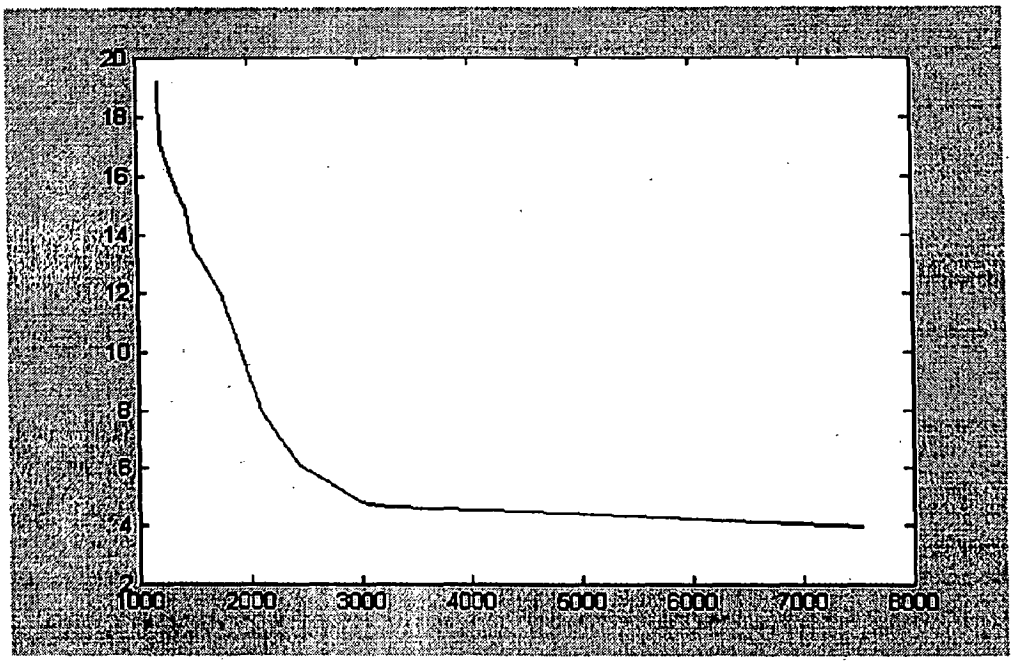

Fig 4.5 Output Power Vs THD for Single switch high power factor rectifier

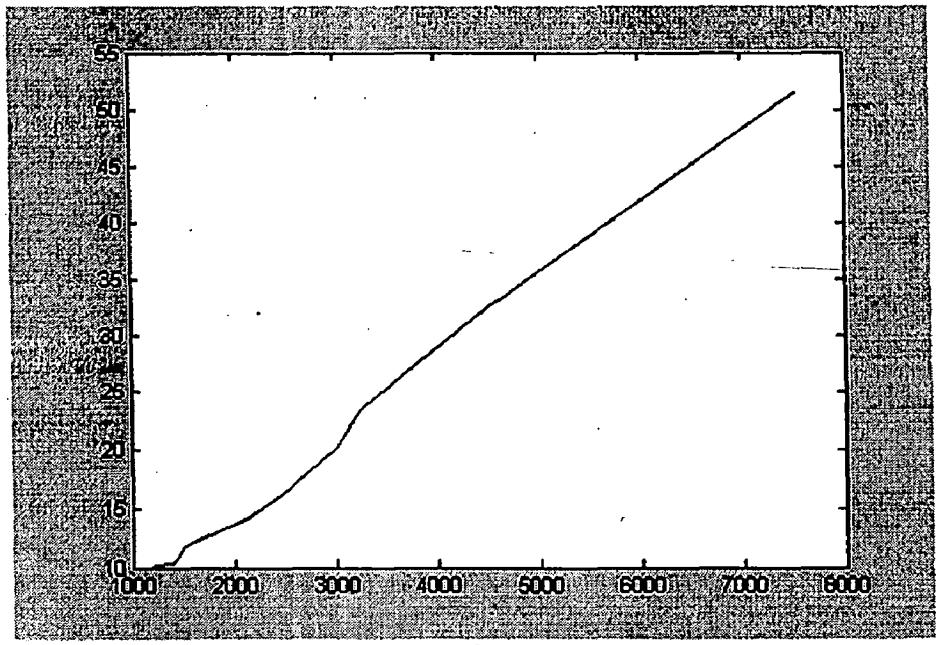

Fig 4.6 Output Power Vs Input Current for Single switch high power factor rectifier

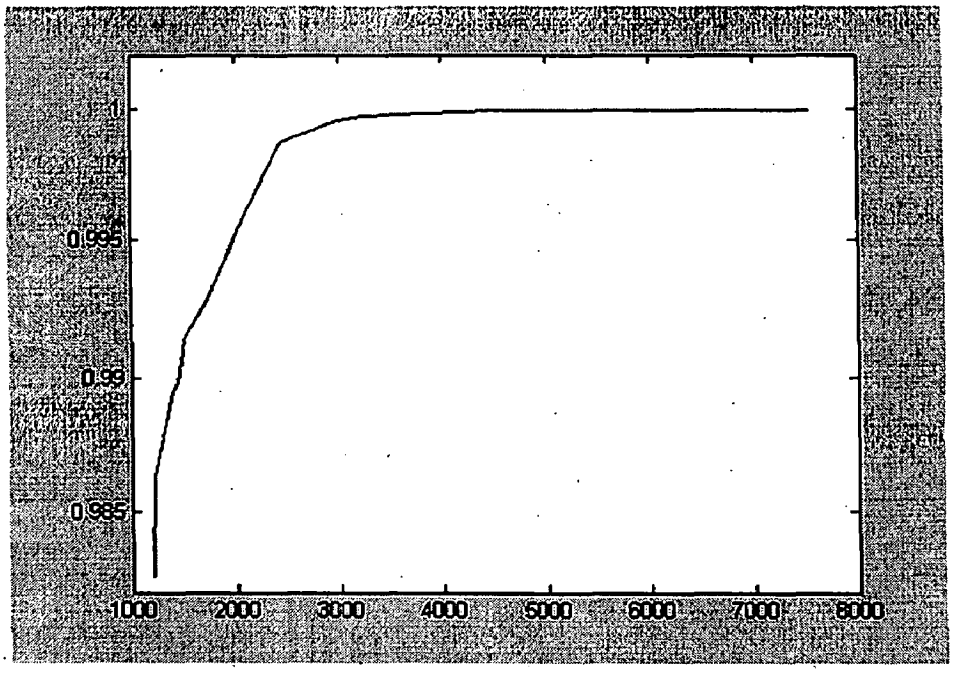

Fig 4.7 Output Power Vs Input Power Factor for Single switch high power factor rectifier

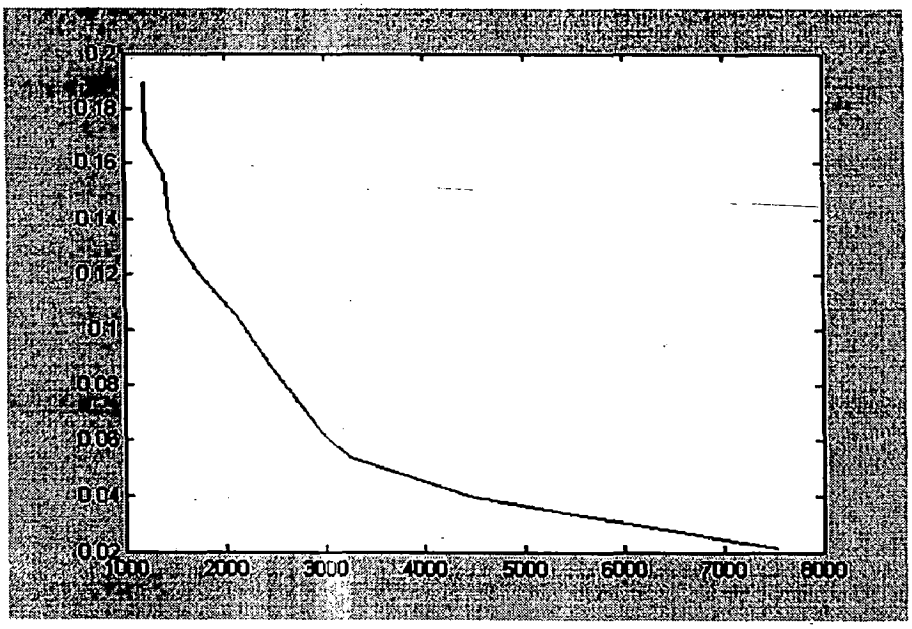

Fig 4.8 Output Power Vs Input Harmonic factor for Single switch high power factor rectifier

4.2 Sinusoidal Pulse Width Modulation

The SIMULINK model of the converter under sinusoidal PWM with instantaneous current control is as shown in the figure (4.5):

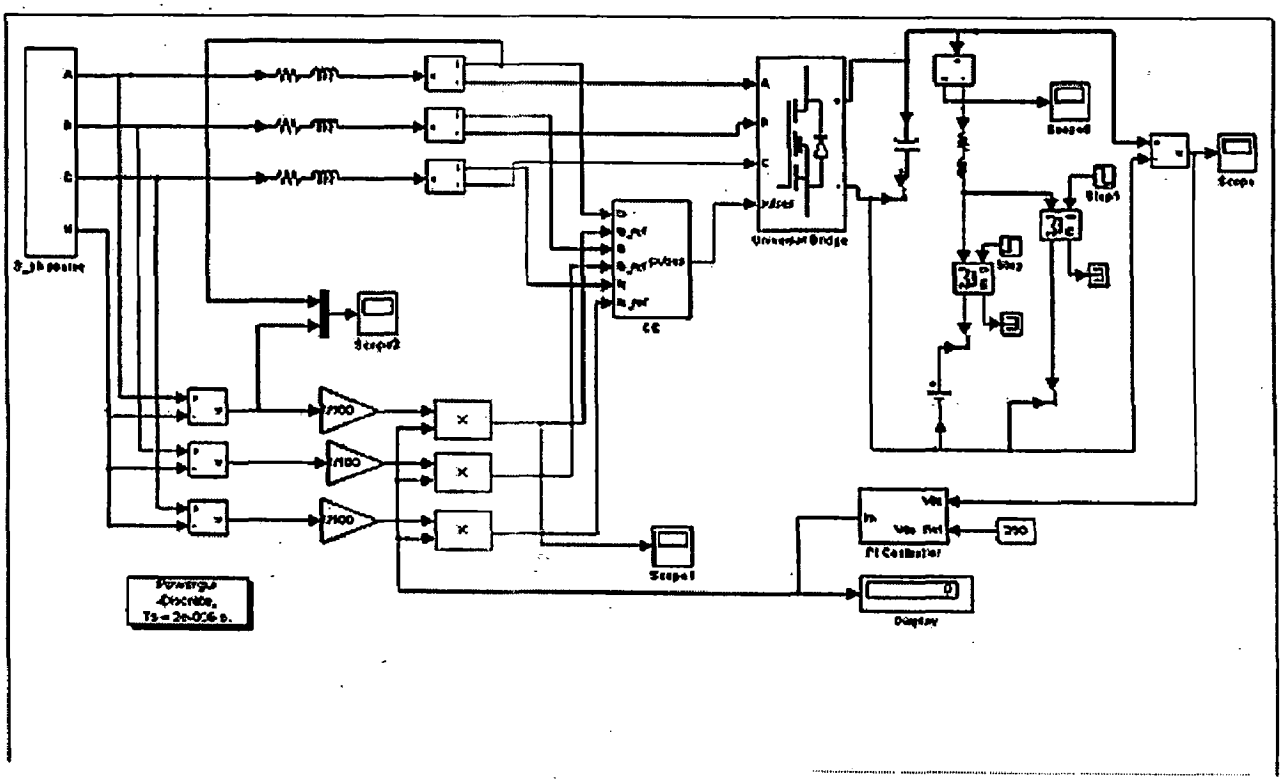

Fig 4.9 SIMULINK model of the converter under SPWM

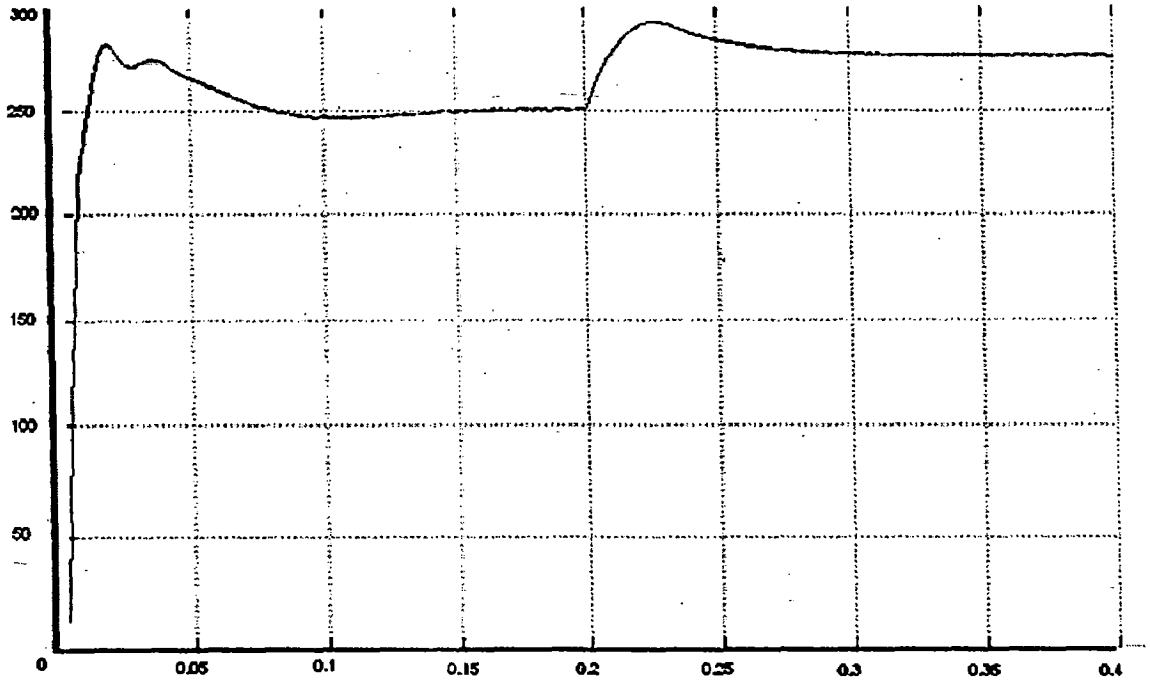

Fig 4.10 DC Output voltage for a switching frequency of 1 KHz

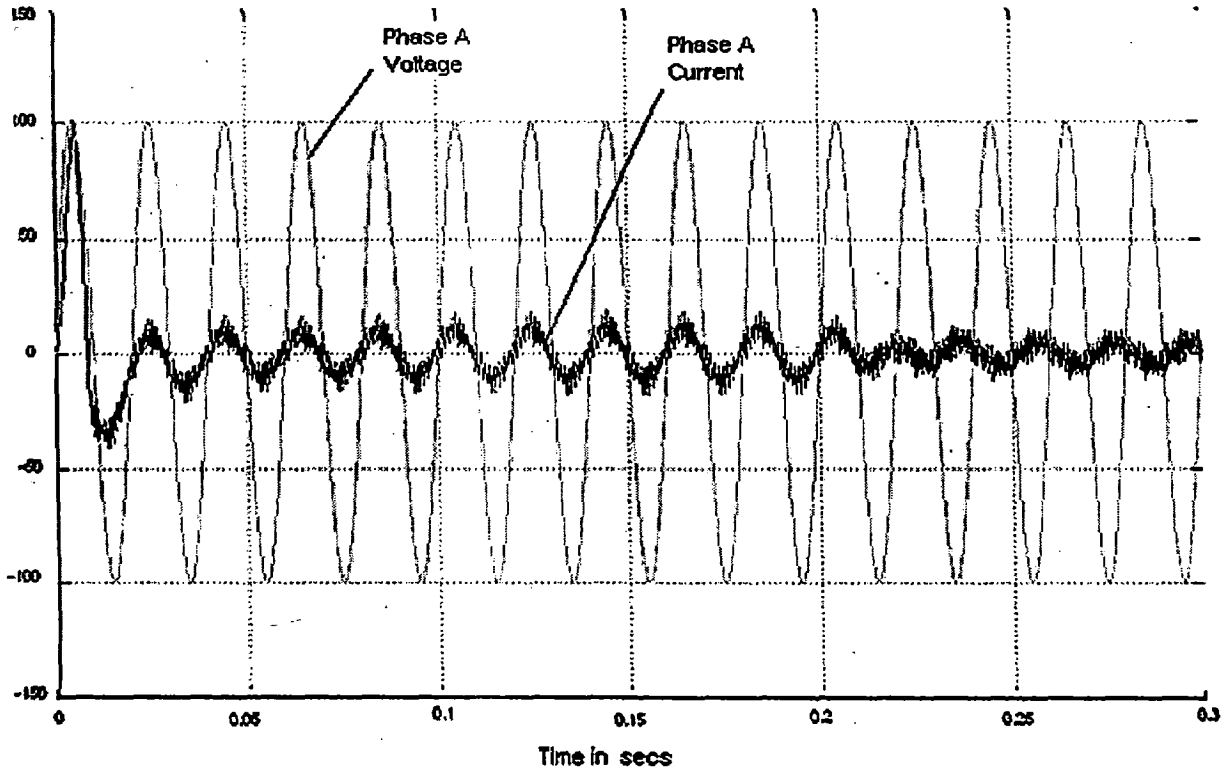

Fig 4.11 Phase A current for fs = 1KHz

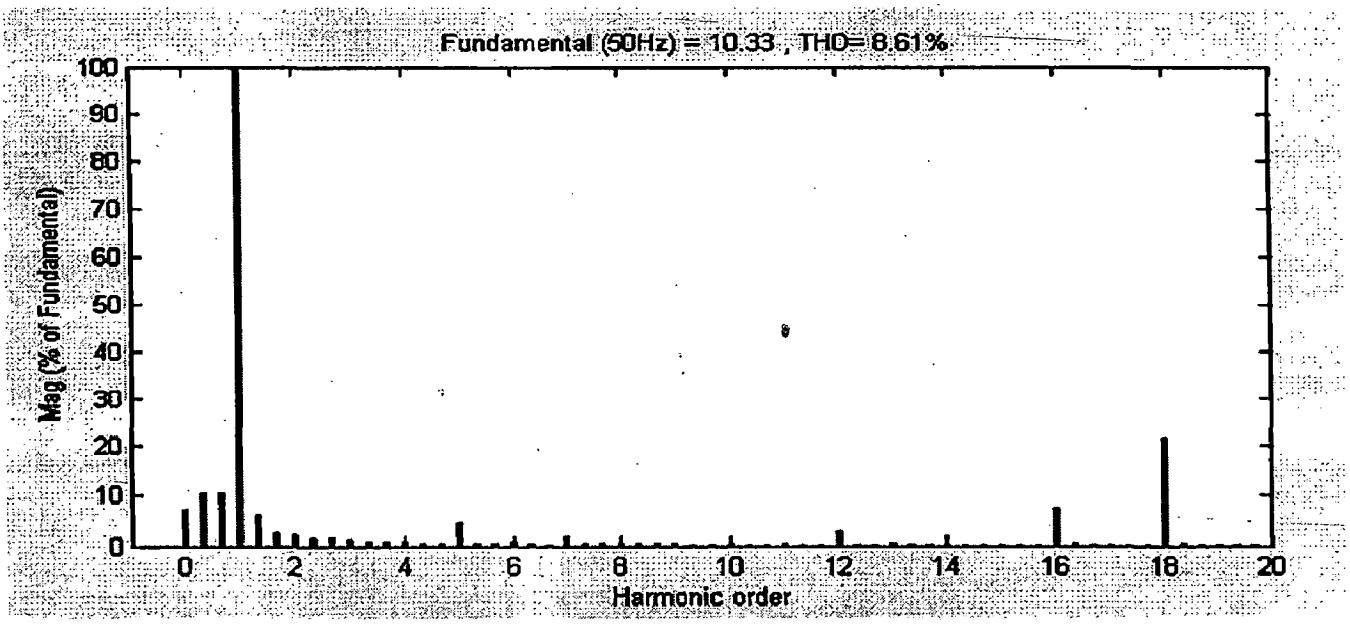

Fig 4.12 FFT Analysis of source current for fs = 1KHz

The DC output voltage of the converter under Sinusoidal Pulse Width Modulation (SPWM) is shown in Fig 4.6. The switching frequency is 1KHz. The source current waveform is shown in fig 4.7. It can be seen that the source current is exactly in phase with the source voltage and when the converter operates in the regenerative mode from 0.2 sec, the source current is 90° out of phase with the source voltage. The FFT analysis of the source current is shown in fig 4.8. The total harmonic distortion of the source current is 8.61% and the major component of the source current is the DC component and some higher order harmonics (16 and 18).

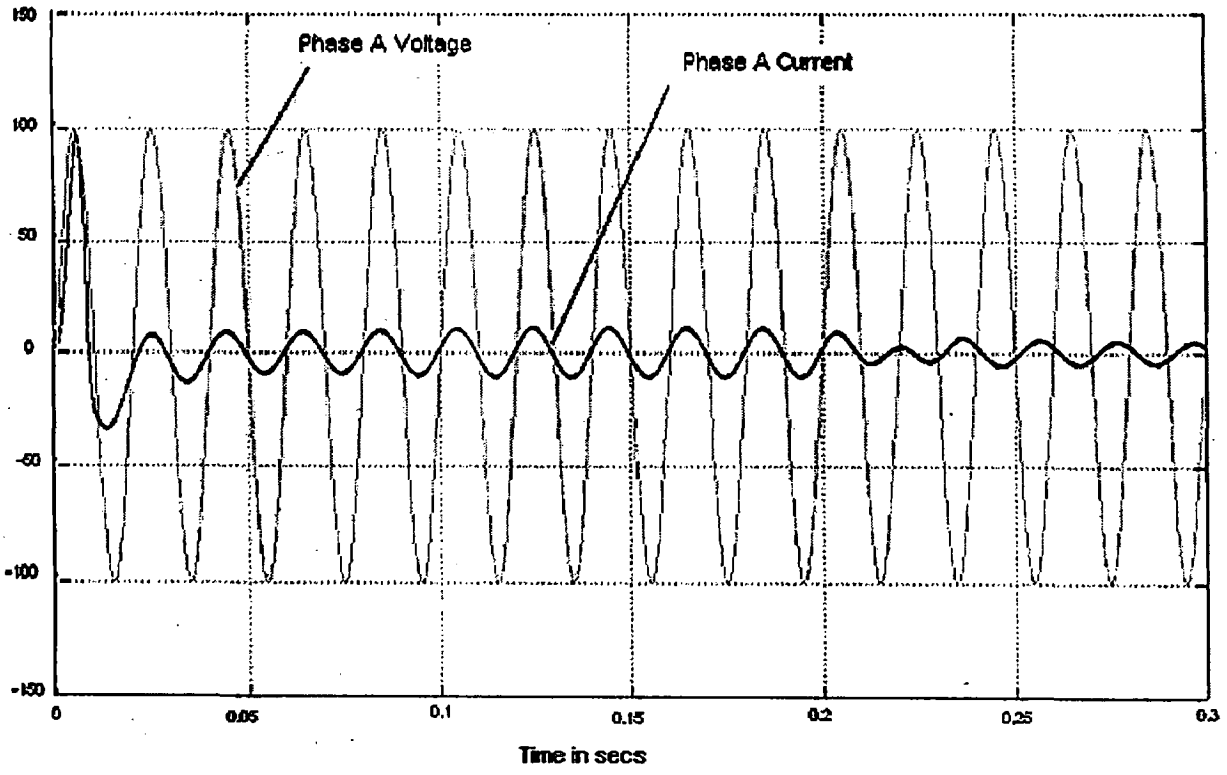

Fig 4.13 Phase A current for fs = 10 KHz

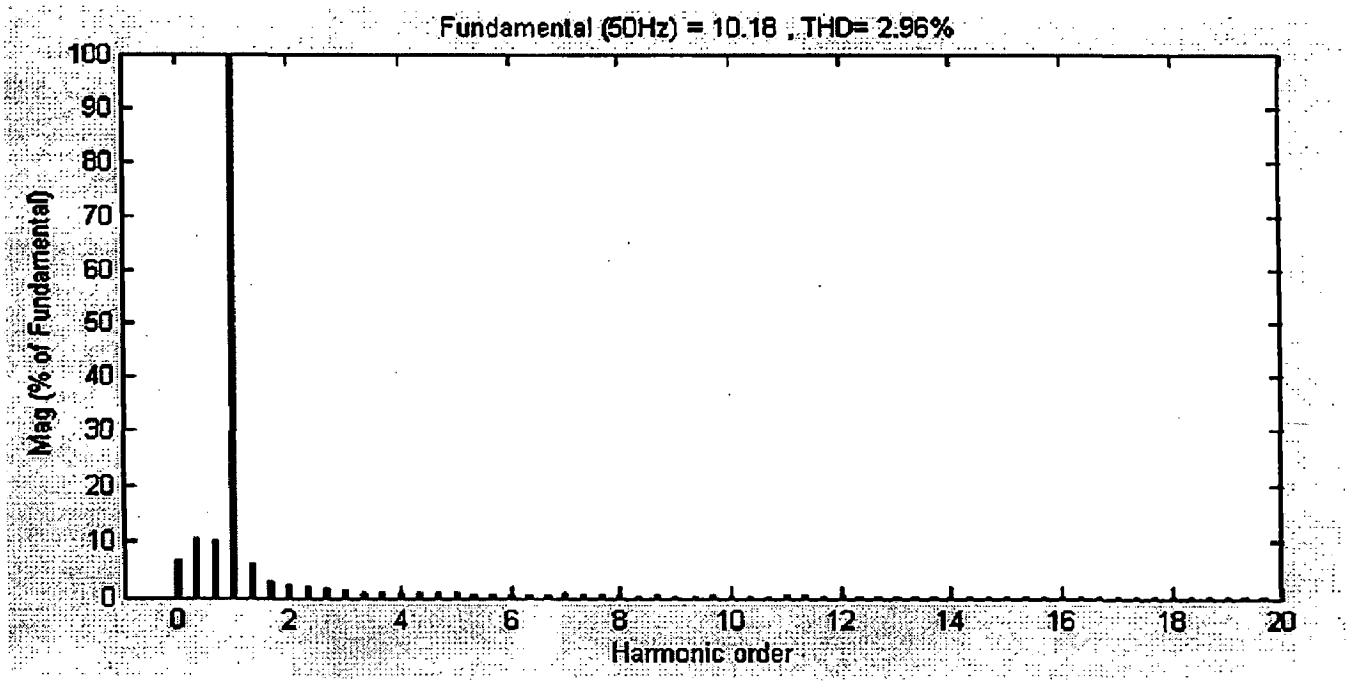

Fig 4.14 FFT Analysis of source current for fs = 10 KHz

The source current waveform for a switching frequency of 10 KHz is shown in fig 4.9. By increasing the switching frequency by ten times the wave shape of the source current is greatly improved. The FFT analysis of the source current for this switching frequency is shown in fig 4.10. The total harmonic distortion of the source current is 2.96% which satisfies the standards.

The plots of various parameters of the converter with a variation in the output power are shown below.

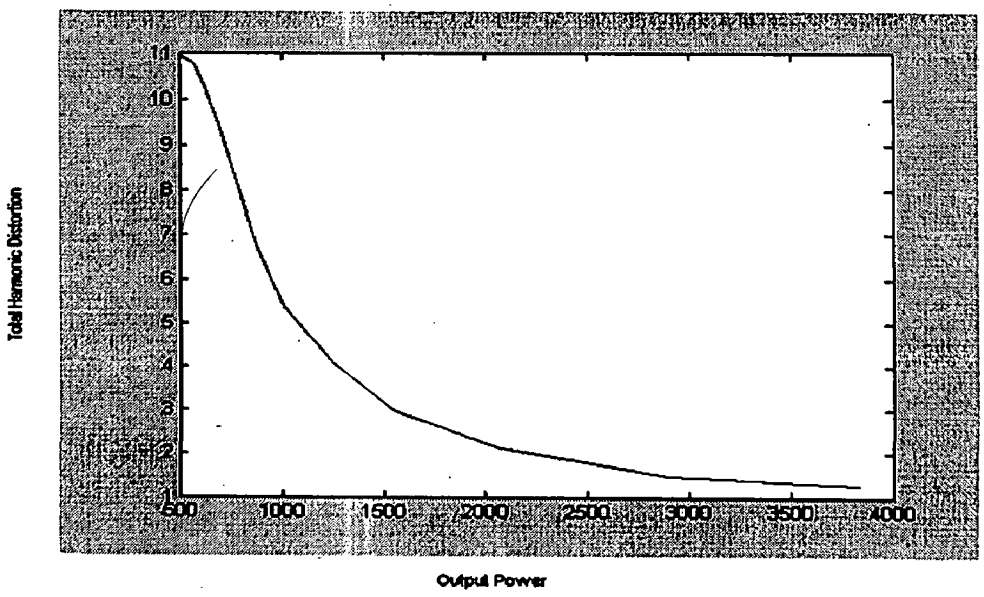

Fig 4.15 Output Power Vs THD for SPWM

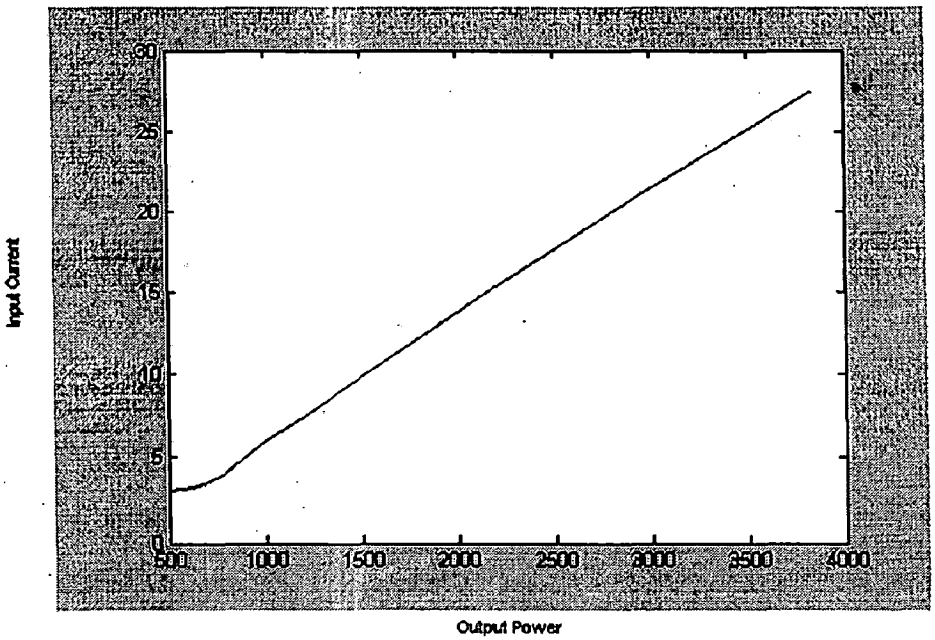

Fig 4.16 Output power Vs Input current for SPWM

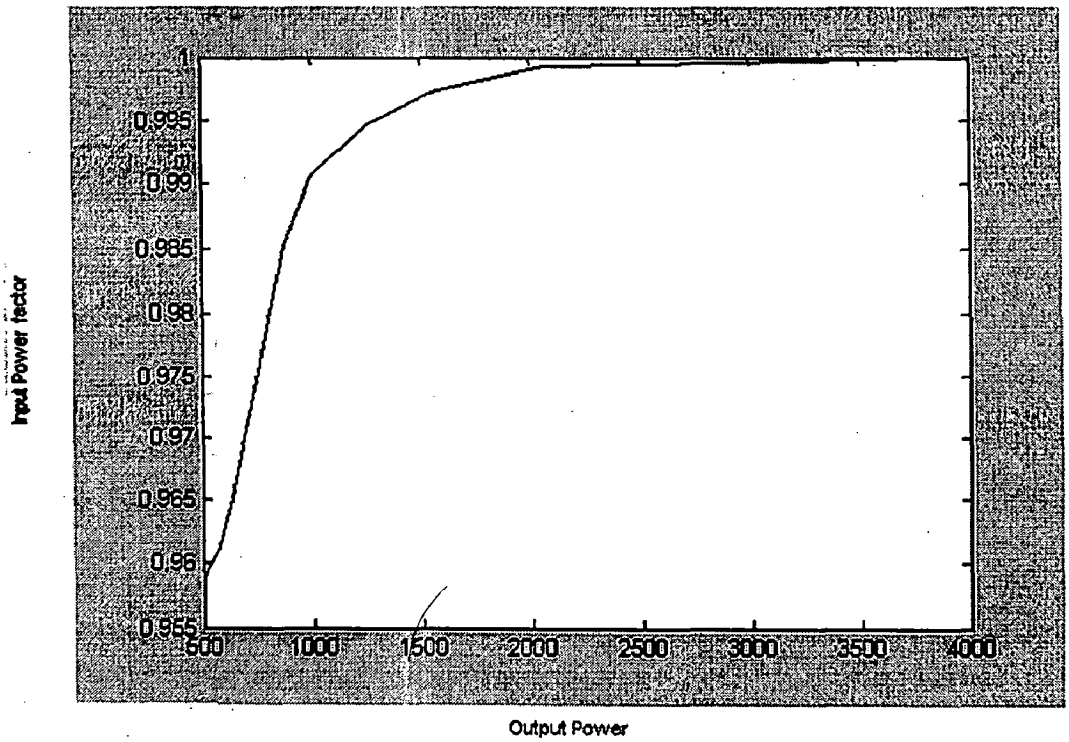

Fig 4.17 Output power Vs Input power factor for SPWM

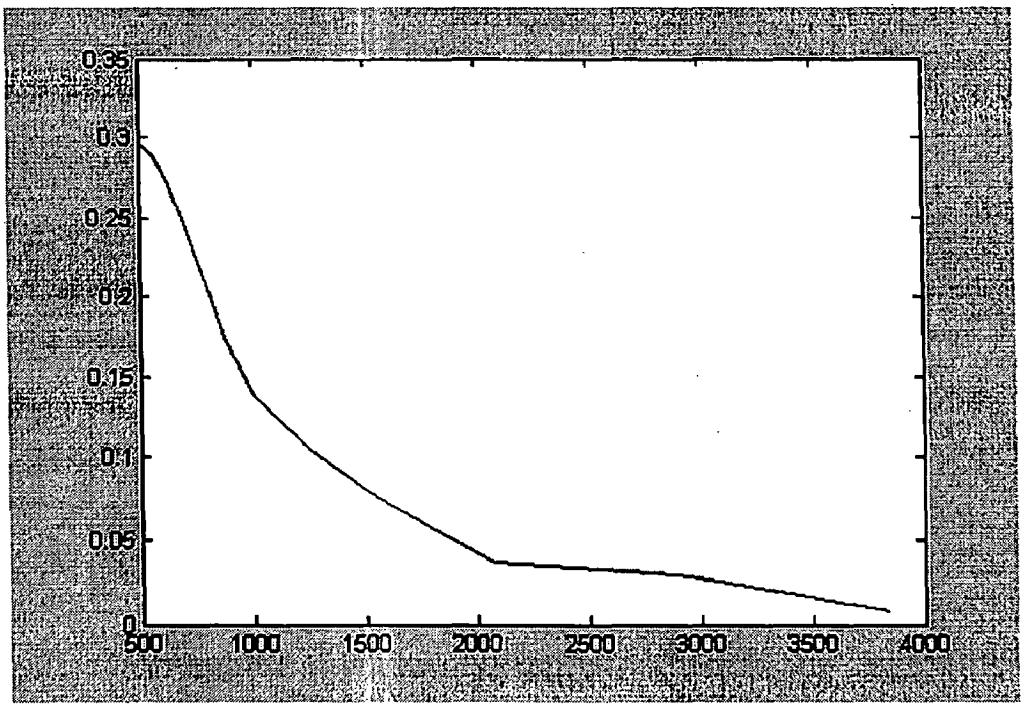

Fig 4.18 Output power Vs Input harmonic factor for SPWM

4.3 Hysteresis Current Control

The SIMULINK model of the converter under HCC is as shown in Fig 4.11. The converter is simulated with hysteresis bands of 5Amps and 0.5Amps

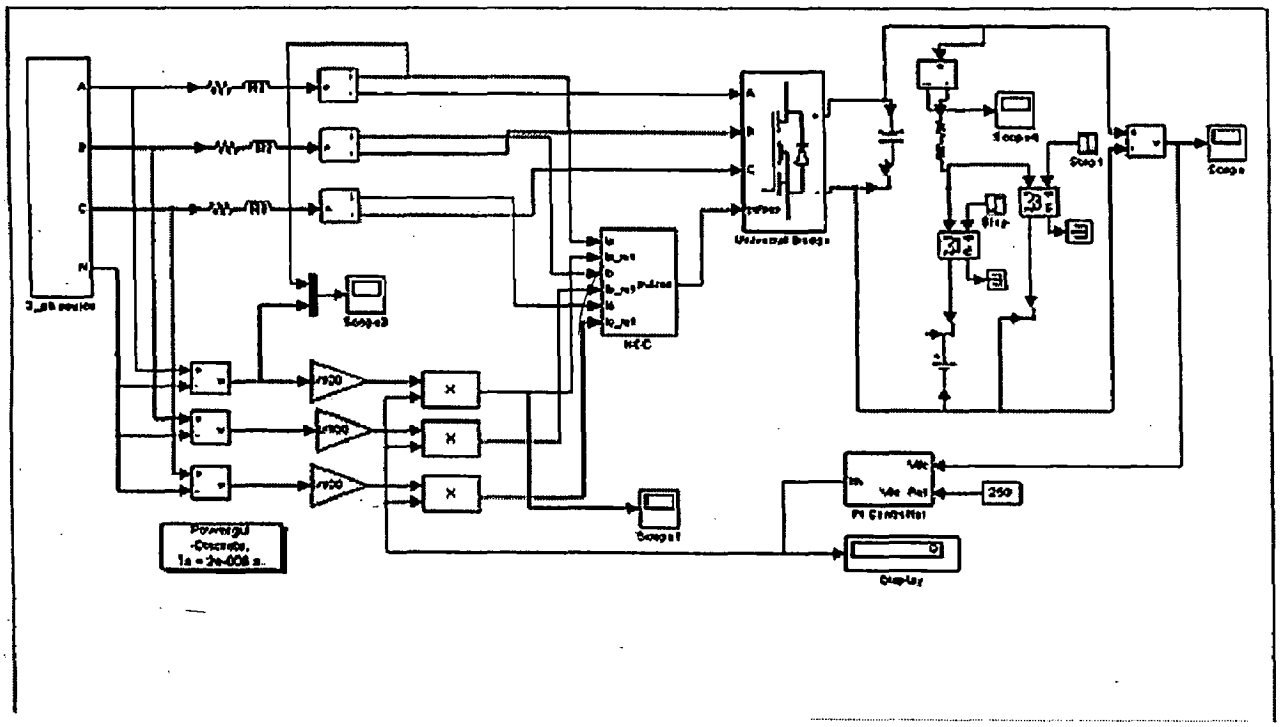

Fig 4.19 SIMULINK model of HCC controlled converter

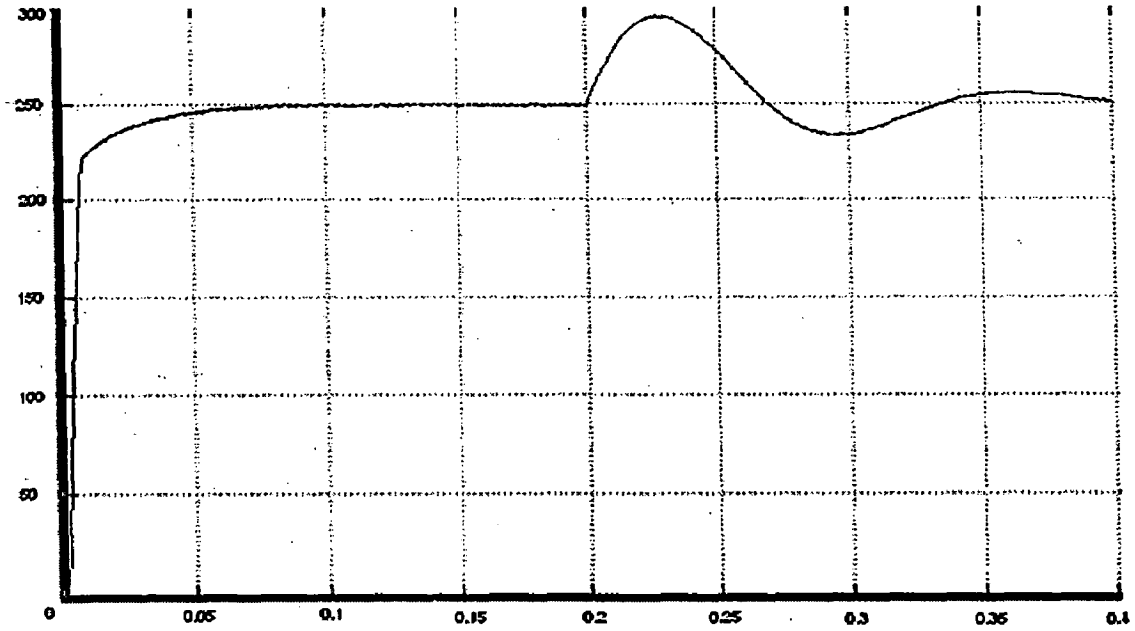

Fig 4.20 DC output voltage of HCC converter where HB=±5Amps

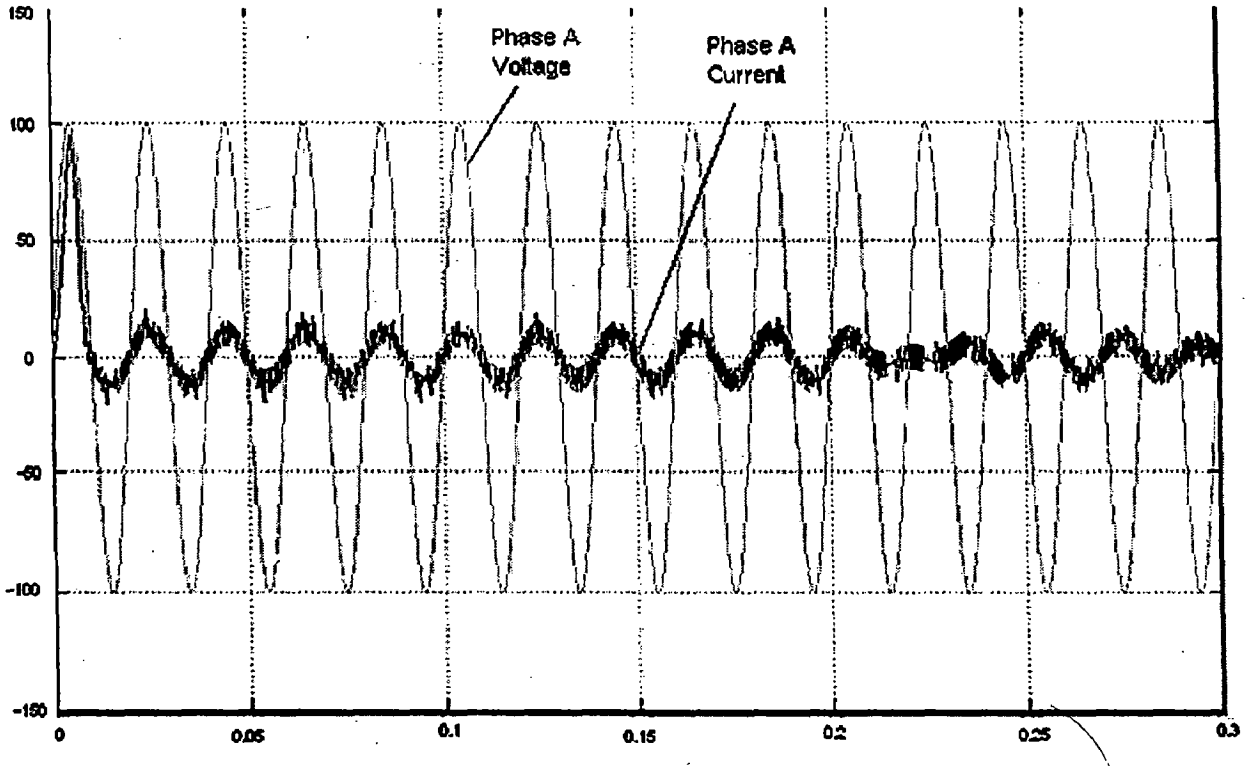

Fig 4.21 A Phase Current of the converter where HB=±5Amps

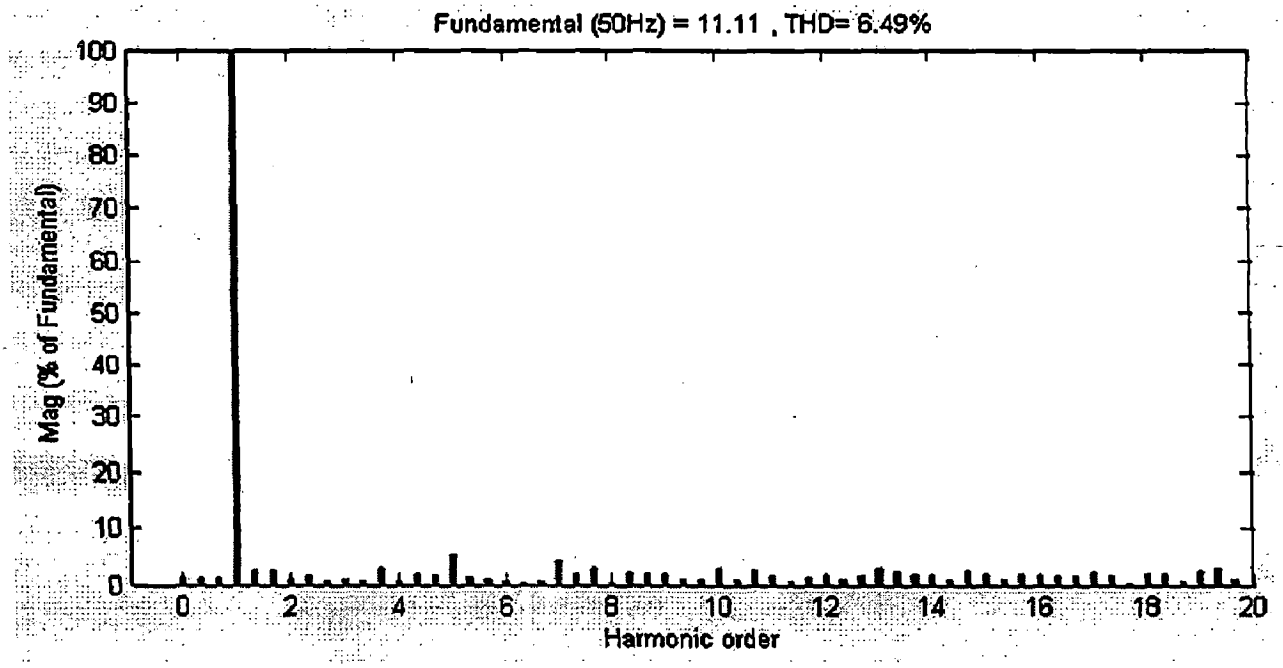

Fig 4.22 FFT Analysis of Source current where HB=±5Amps

The waveform of output DC voltage of the AC-to-DC converter under hysteresis current control strategy with a hysteresis band of 5Amps is as shown in the figure 4.12. It can be seen that the output voltage reaches the reference voltage in a time period less than 0.1 sec. The input current waveform of the converter is shown in Fig 4.13. It can be seen that the input current is exactly in phase with the input voltage. At 0.2 sec, a DC voltage source of 350V is introduced into the load. As a result the converter operates in the regenerative mode. So the source current is 90° out of phase with the input voltage. The FFT analysis of the source current is as shown in Fig 4.14. It can be seen that the total harmonic distortion in the source current is 6.49%. From the harmonic spectrum it can be observed that the major harmonics are the DC component, third, fifth and seventh.

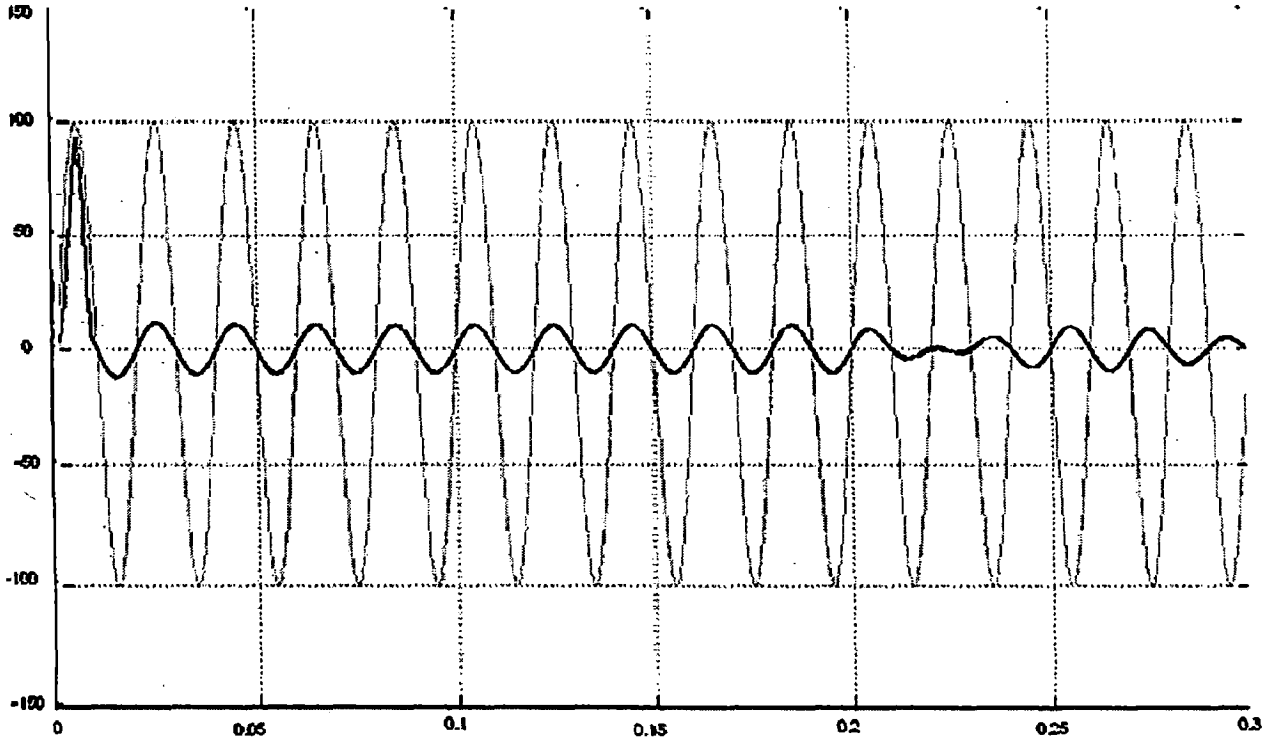

Fig 4.23 Phase A Current where HB=±0.5 Amps

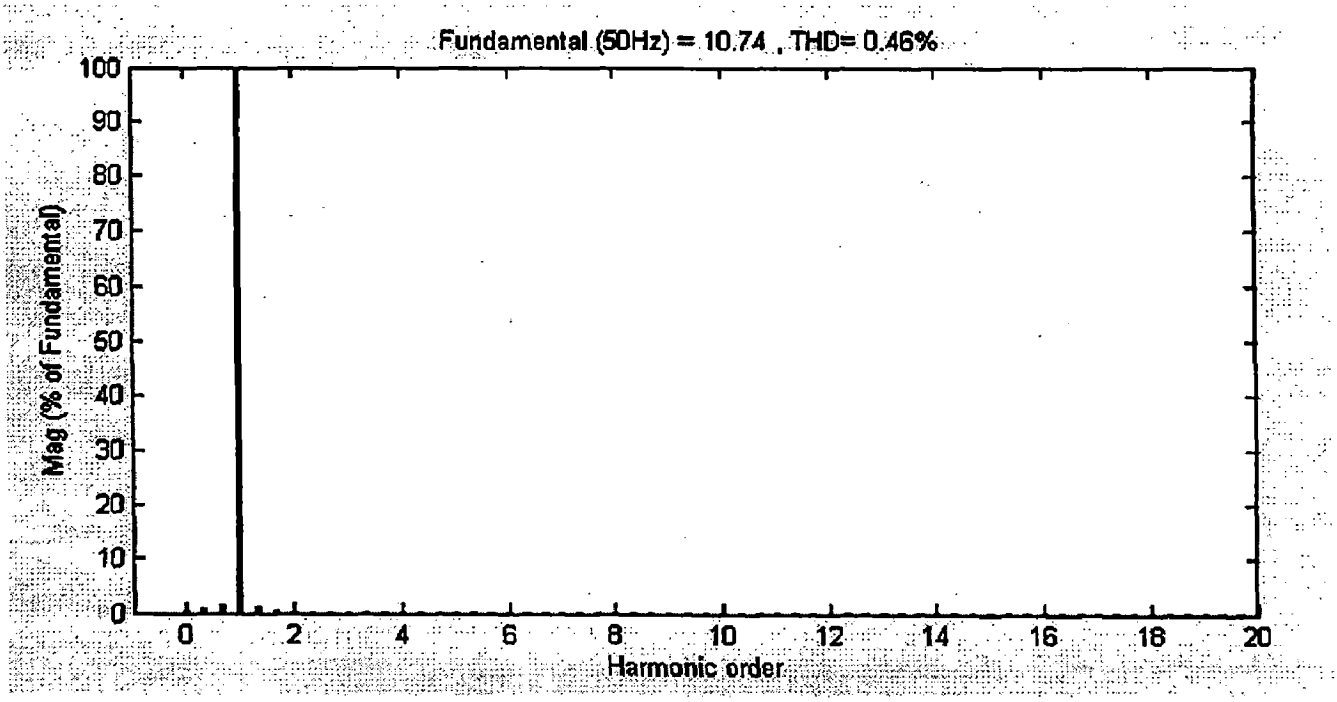

Fig 4.24 FFT Analysis of Source current

The source current waveform of the converter for a hysteresis band of 0.5amps is as shown in Fig 4.15. It can be seen that when the hysteresis band is reduced by ten times, the current waveform is greatly improved. The FFT analysis of the source current is depicted in fig 4.16. The total harmonic distortion of the input current is 0.46%. According to IEEE-519 standards, the total harmonic distortion must be less than 5%, where the individual harmonics should not be more than 3%. The above results thus satisfy these standards.

The output power of the converter is varied and various parameters are plotted against the output power. These plots are shown in the graphs below.

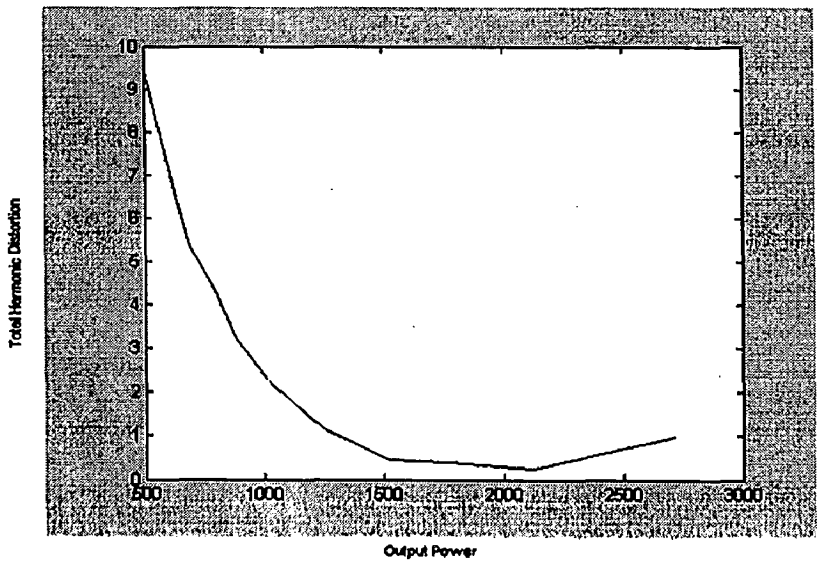

Fig 4.25 Output power Vs Total Harmonic Distortion for HCC

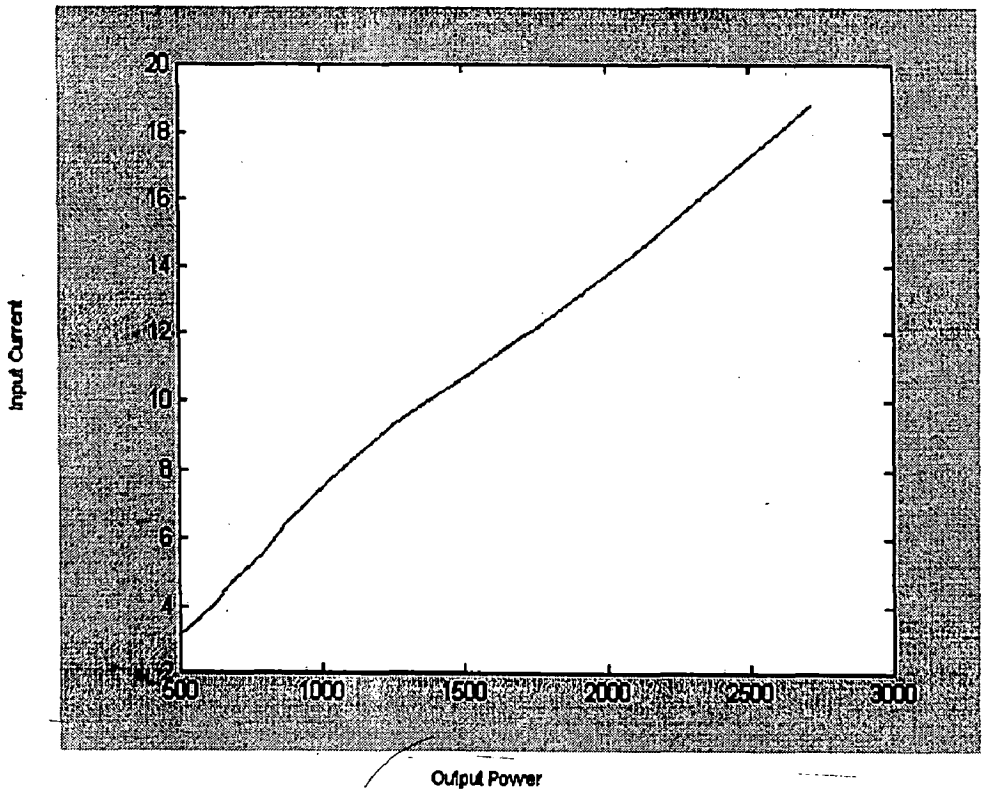

Fig 4.26 Output power Vs Input current for HCC

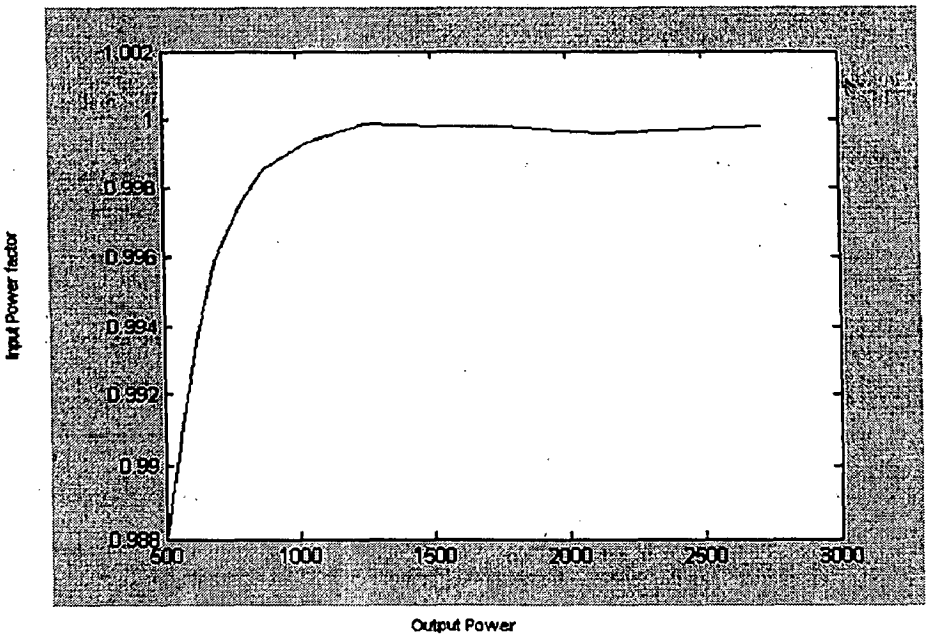

Fig 4.27 Output power Vs input power factor for HCC

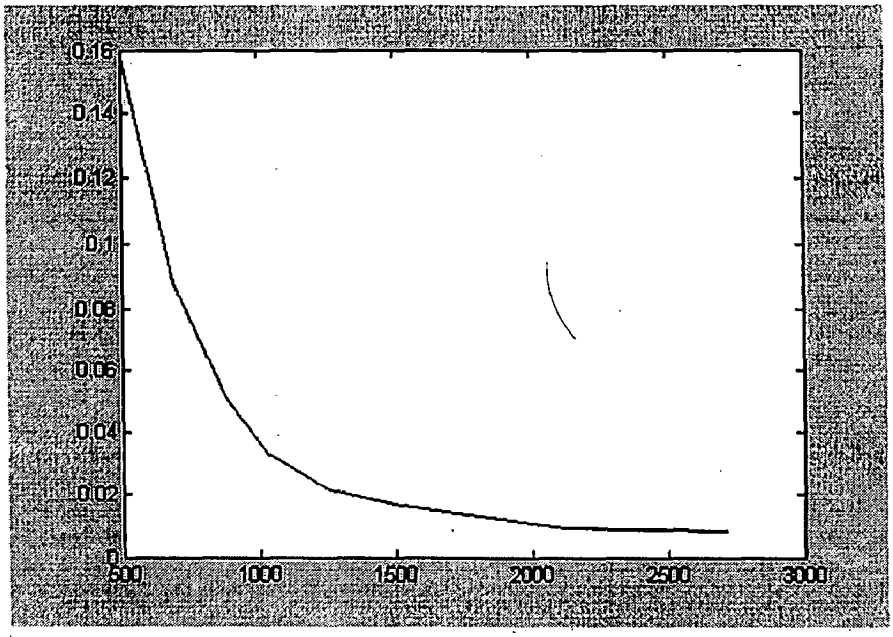

Fig 4.28 Output power Vs input harmonic factor for HCC

4.5 Indirect Current Control

The SIMULINK model of the PWM converter under indirect current control is shown in fig 4.17:

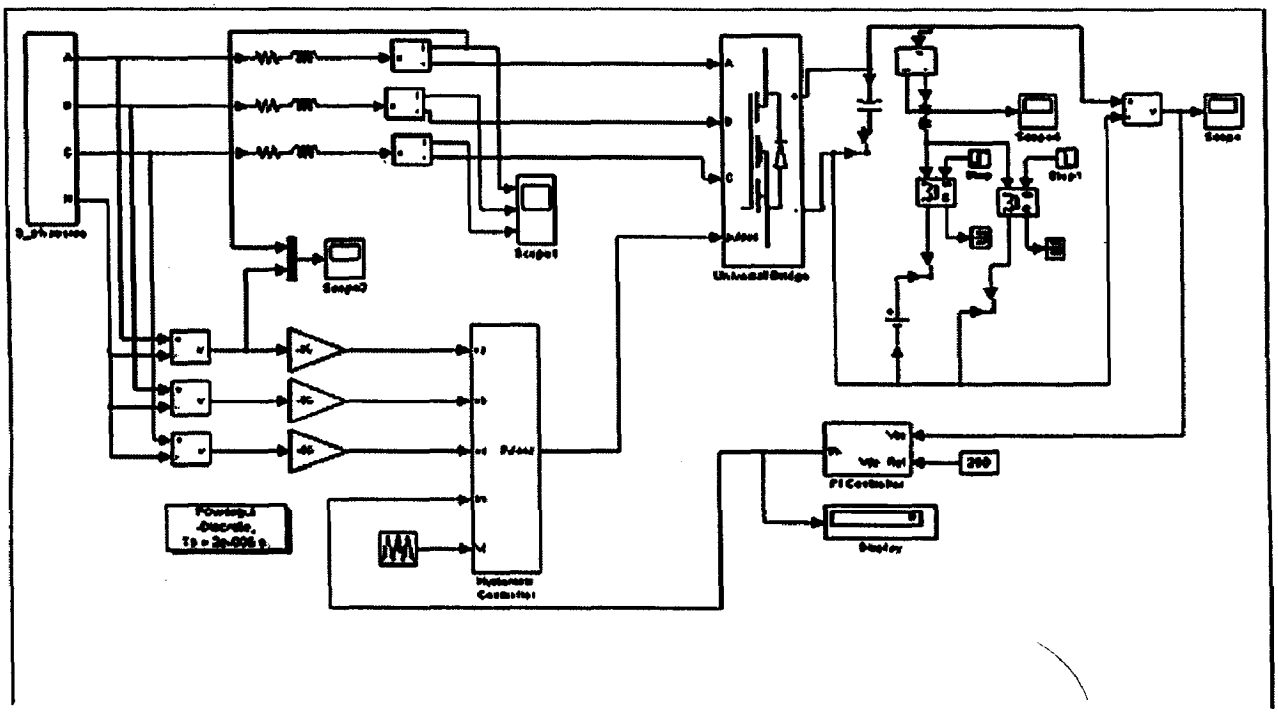

Fig 4.29 SIMULINK model of the converter under IDC

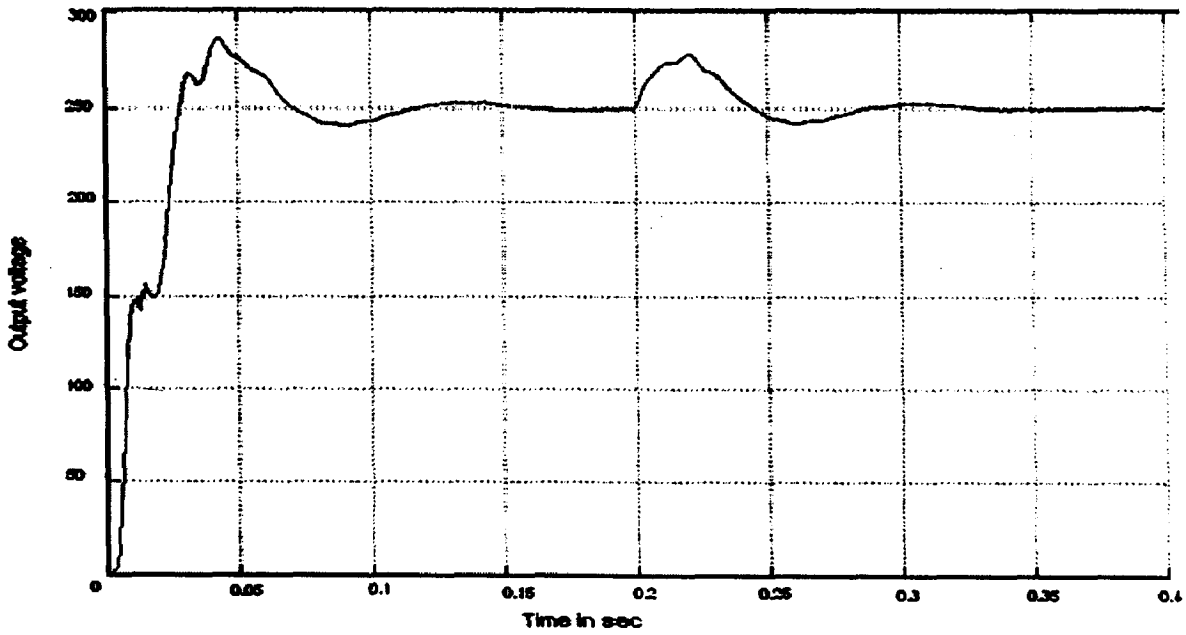

Fig 4.30 Output Voltage for fs = 1 KHz under IDC

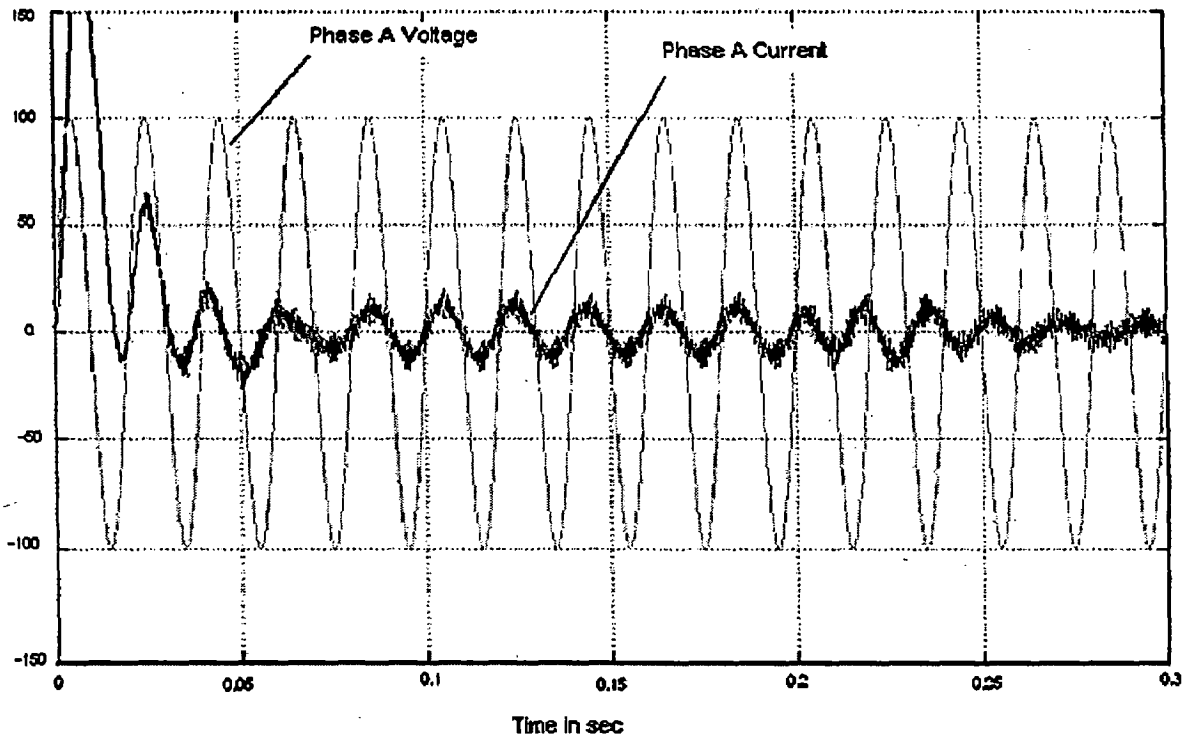

Fig 4.31 Phase A current for fs = 1KHz

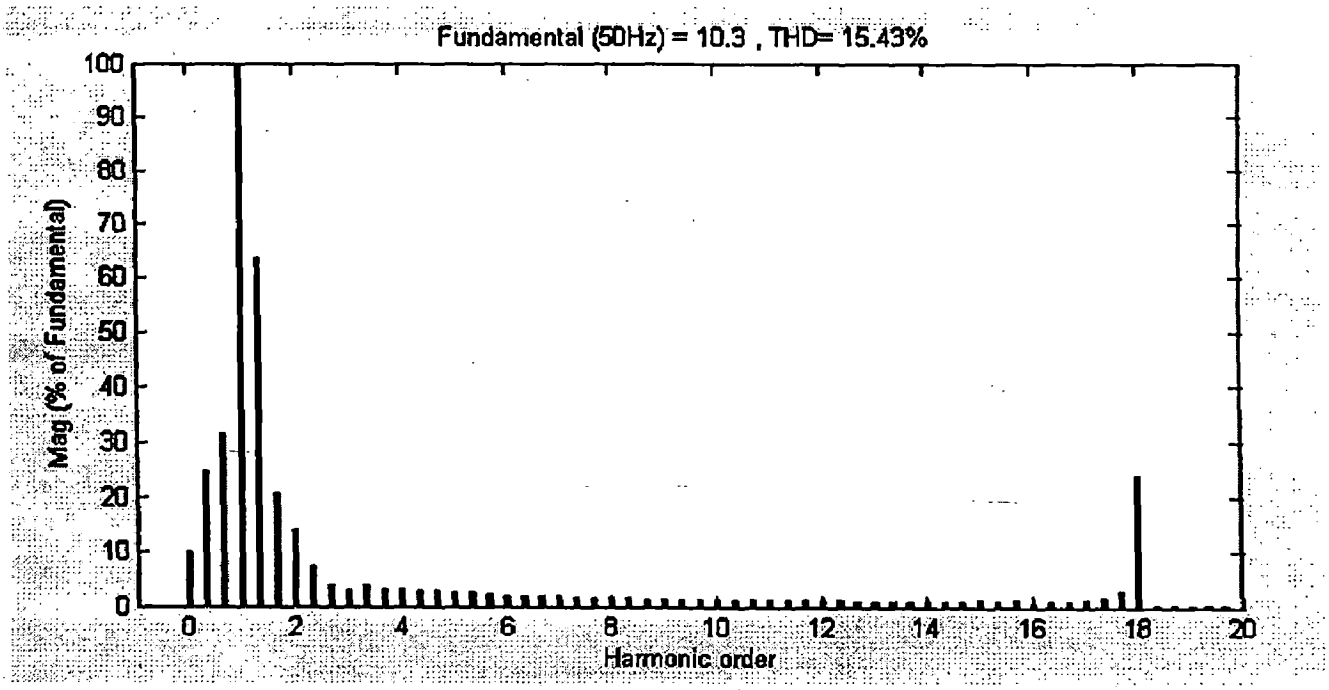

Fig 4.32 FFT analysis of source current for fs = 1KHz

The output voltage waveform of the converter under indirect current control for a switching frequency of 1 KHz is shown in fig 4.18. The source current is in phase with the source voltage when the converter operates in the generative mode. As soon as the converter changes to regenerative mode at 0.2 sec, the source is 90° out of phase with the source voltage. It can be observed from the source current waveform that the current takes longer

time to align with the source voltage as compared to HCC and SPWM. Also the FFT analysis reveals that the total harmonic distortion of the source current is high in this scheme and does not comply with the standards.

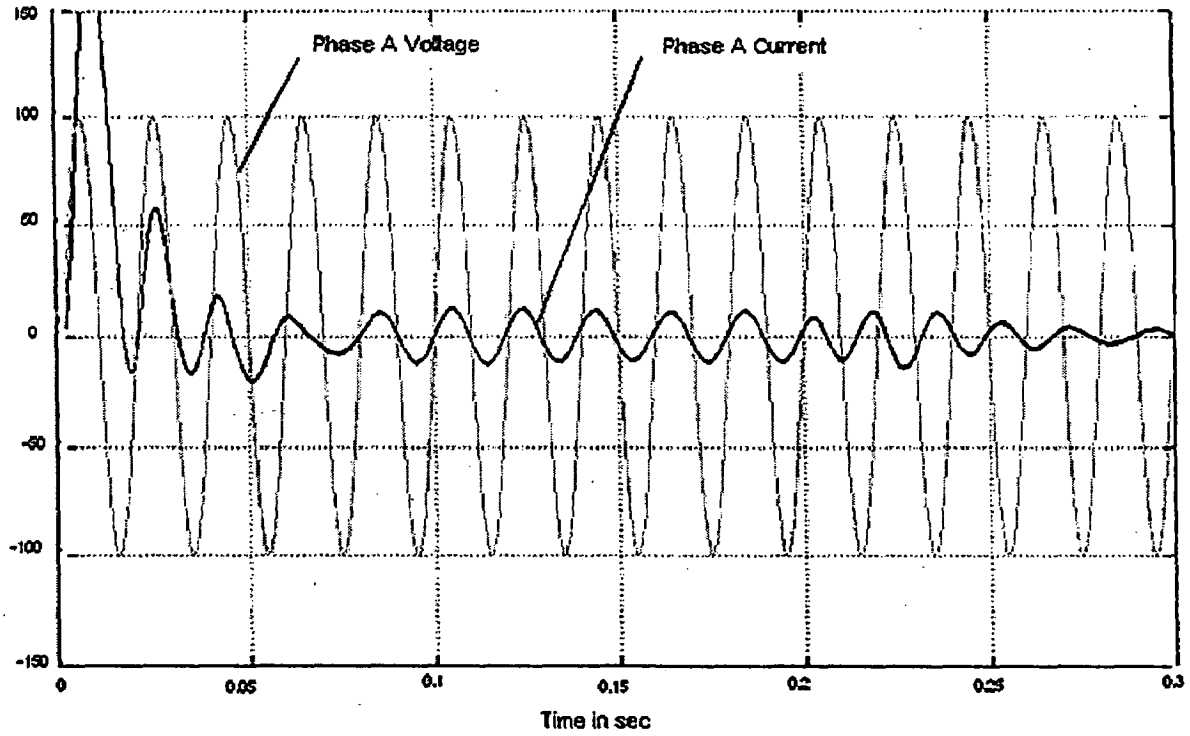

Fig 4.33 Phase A Current for fs = 10KHz

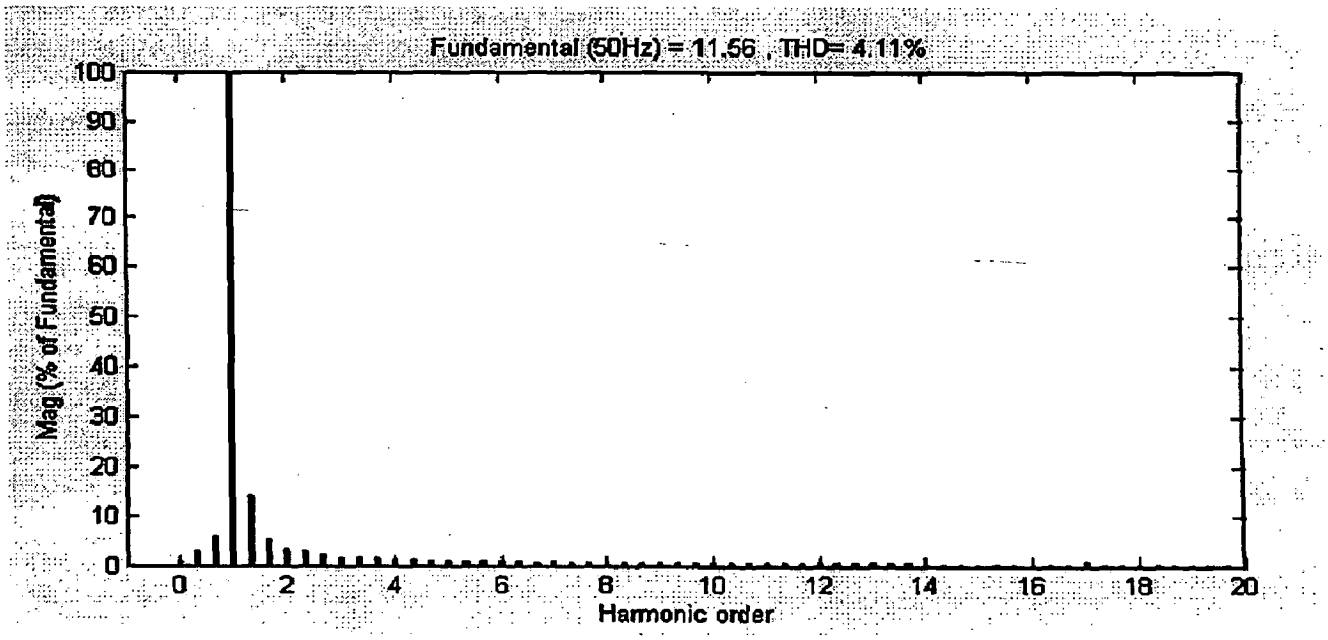

Fig 4.34 FFT analysis of source current for fs = 10 KHz

The source current waveform of the converter for a switching frequency of 10 KHz is shown in fig.4.21. The FFT analysis of the source current gives the total harmonic distortion to be 4.11% which is less than 5%. So the converter under indirect current control satisfies the IEEE standards for higher switching frequencies.

The graphs of various parameters of the converter as the output is varied are depicted below.

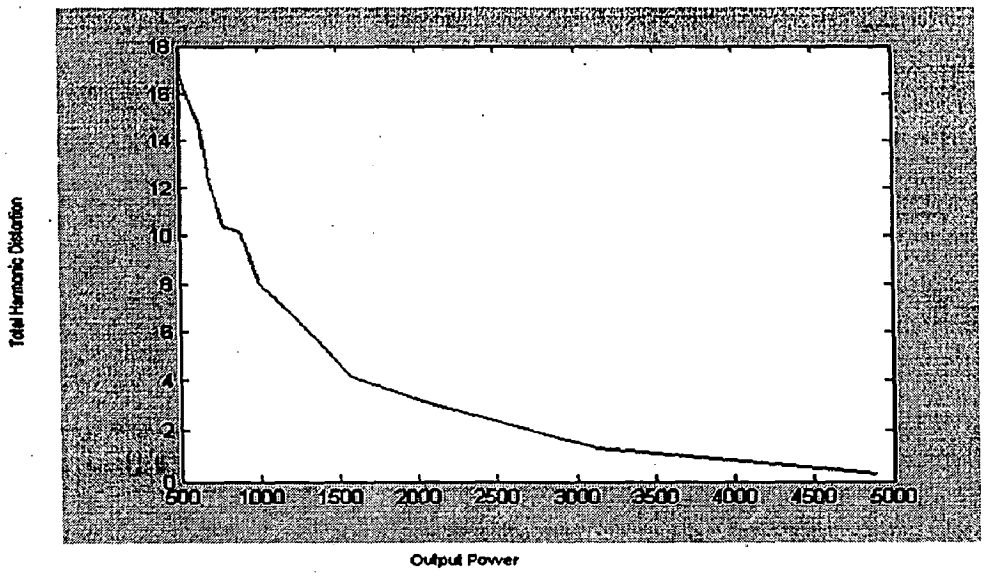

Fig 4.35 Output Power Vs THD for IDC

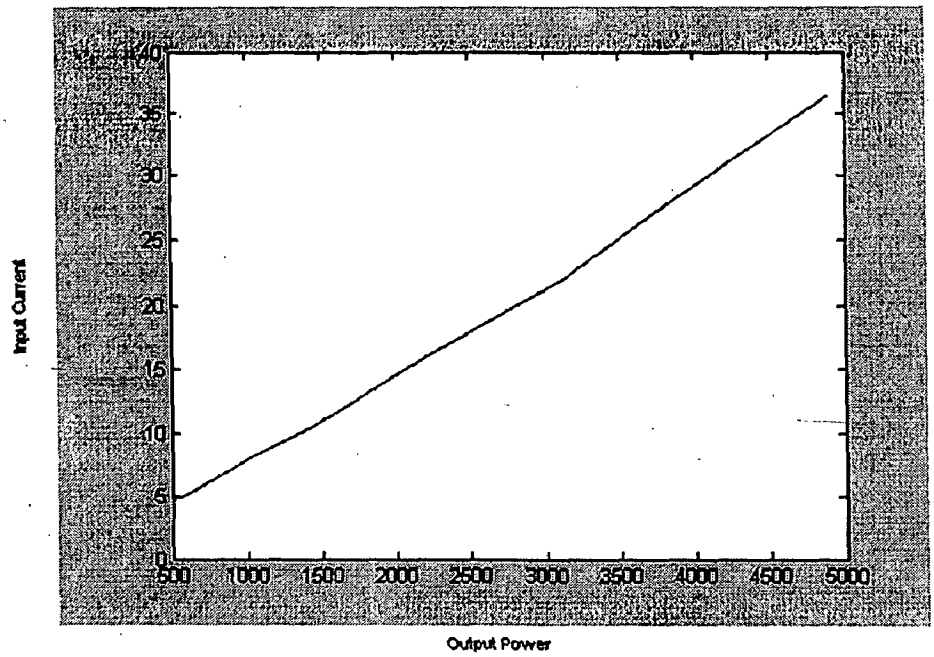

Fig 4.36 Output Power Vs Input Current for IDC

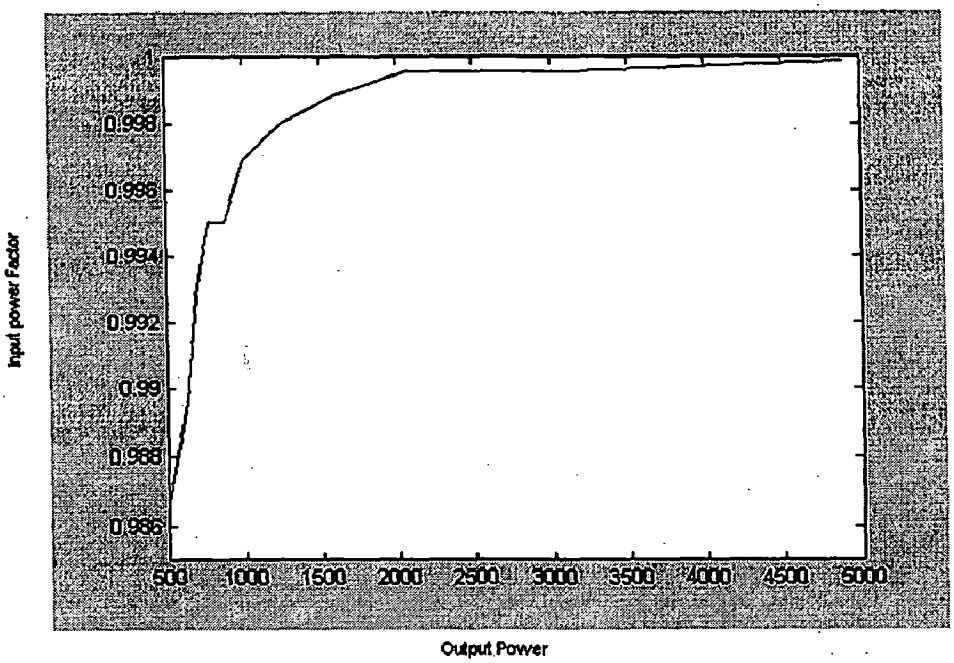

Fig 4.37 Output Power Vs Input Power Factor for IDC

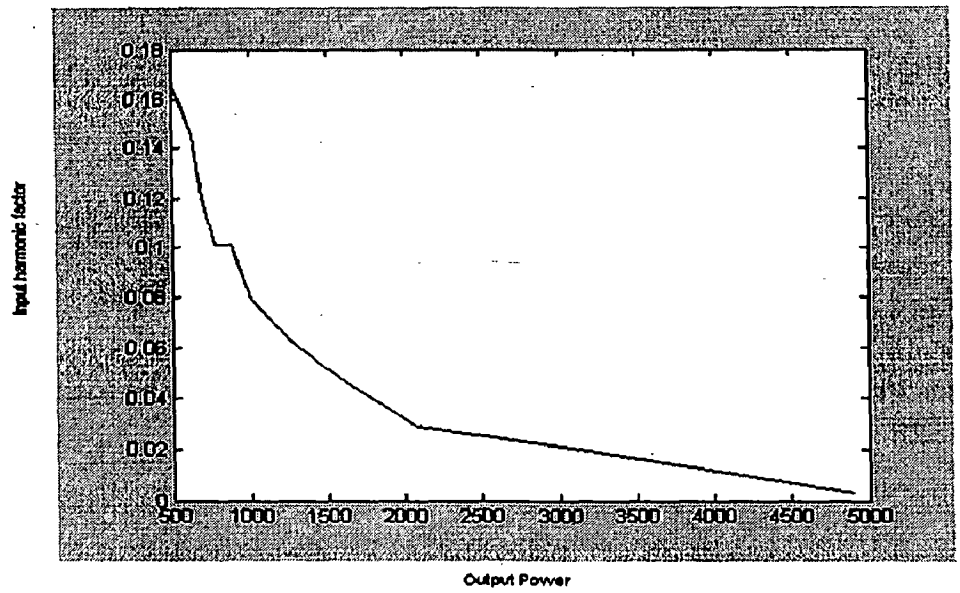

Fig 4.38 Output Power Vs Input Harmonic Factor for IDC

4.6 Space Vector Modulation

The SIMULINK model of the converter control by Space Vector modulation is as shown below (Fig 4.23):

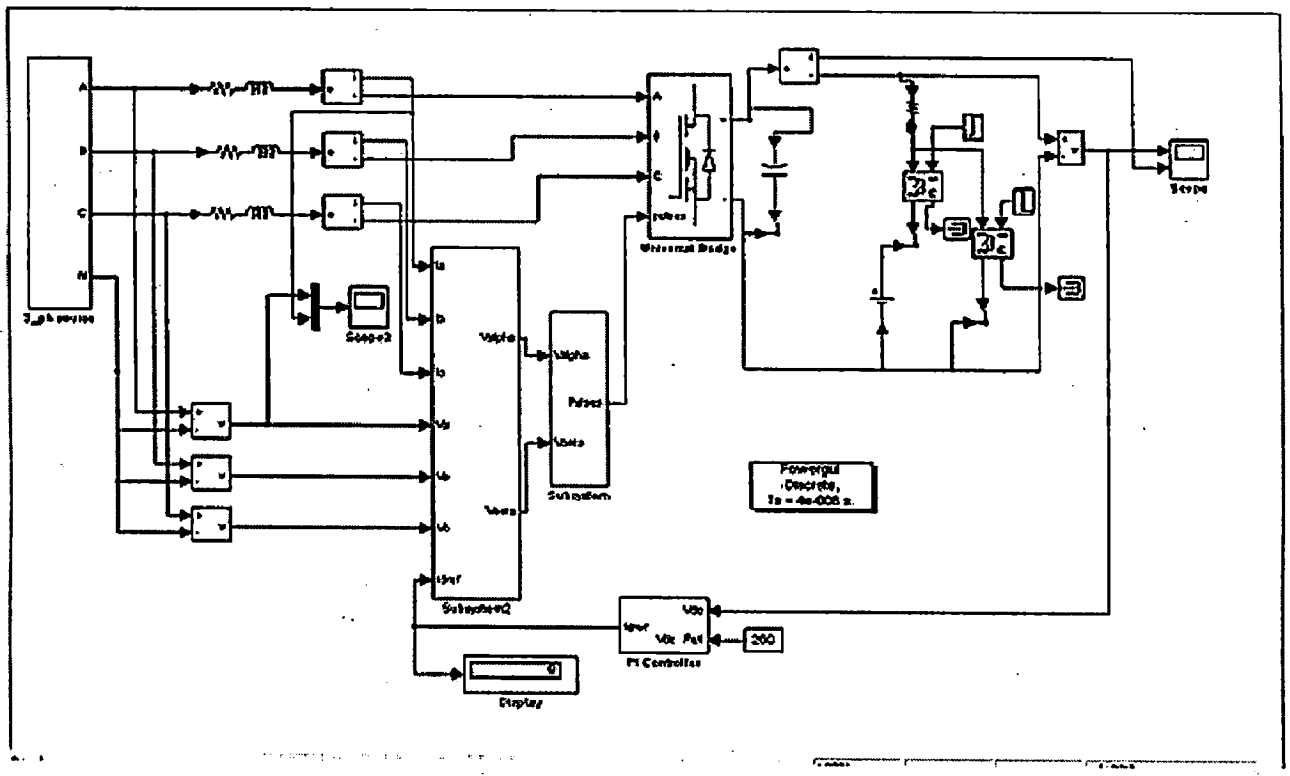

Fig 4.39 SIMULINK Model of the converter under SVM

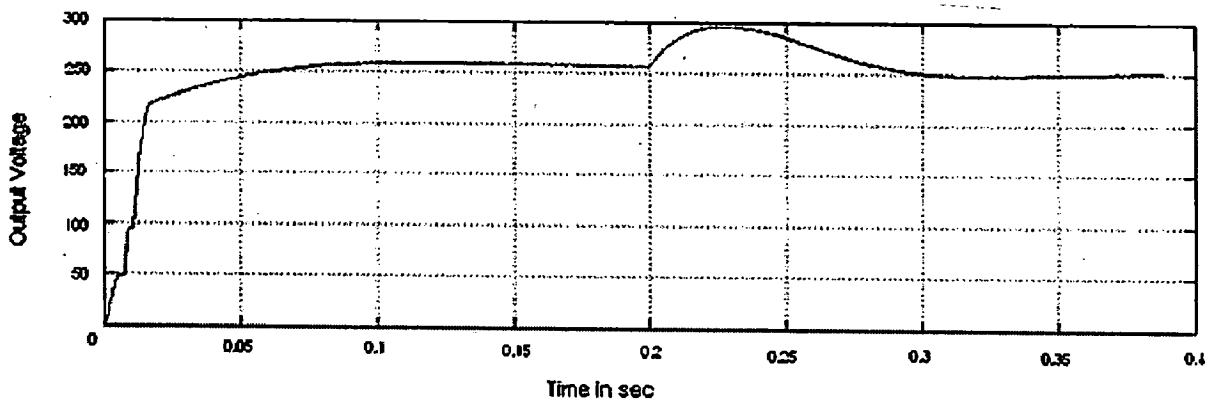

Fig 4.40 Output Voltage for fs = 1KHz for SVM

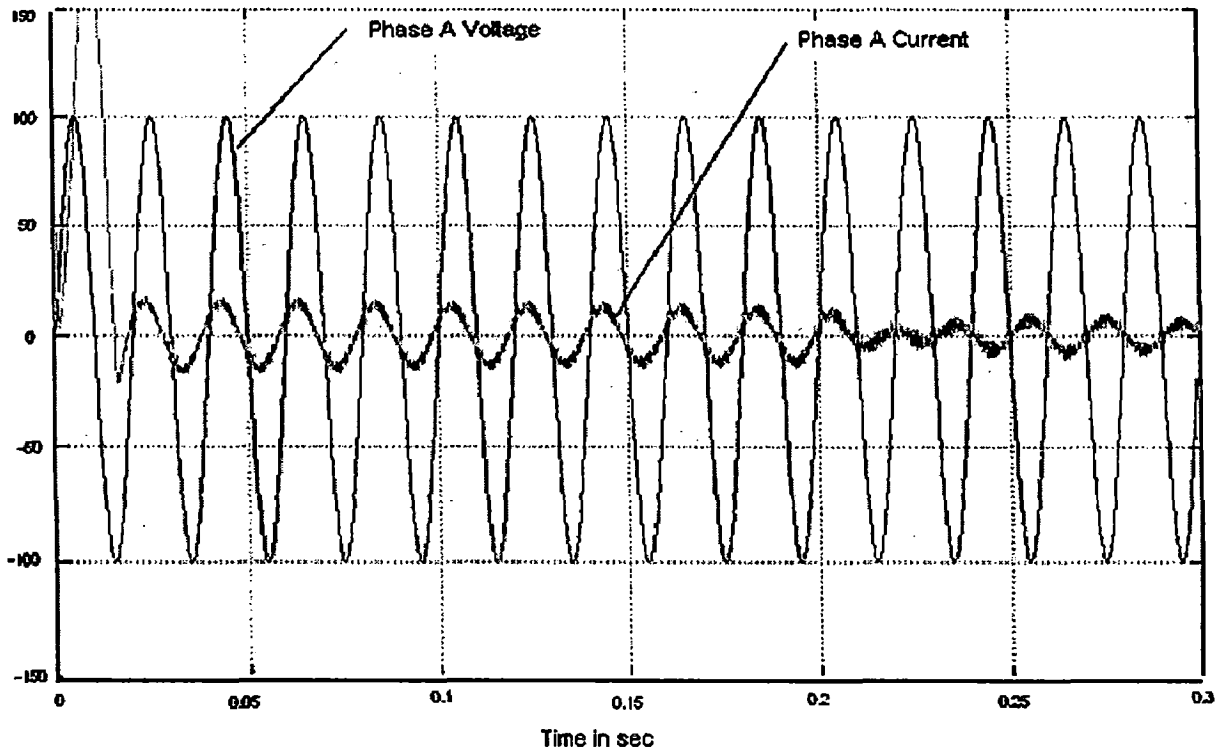

Fig 4.41 Phase A Voltage for fs = 1KHz under SVM

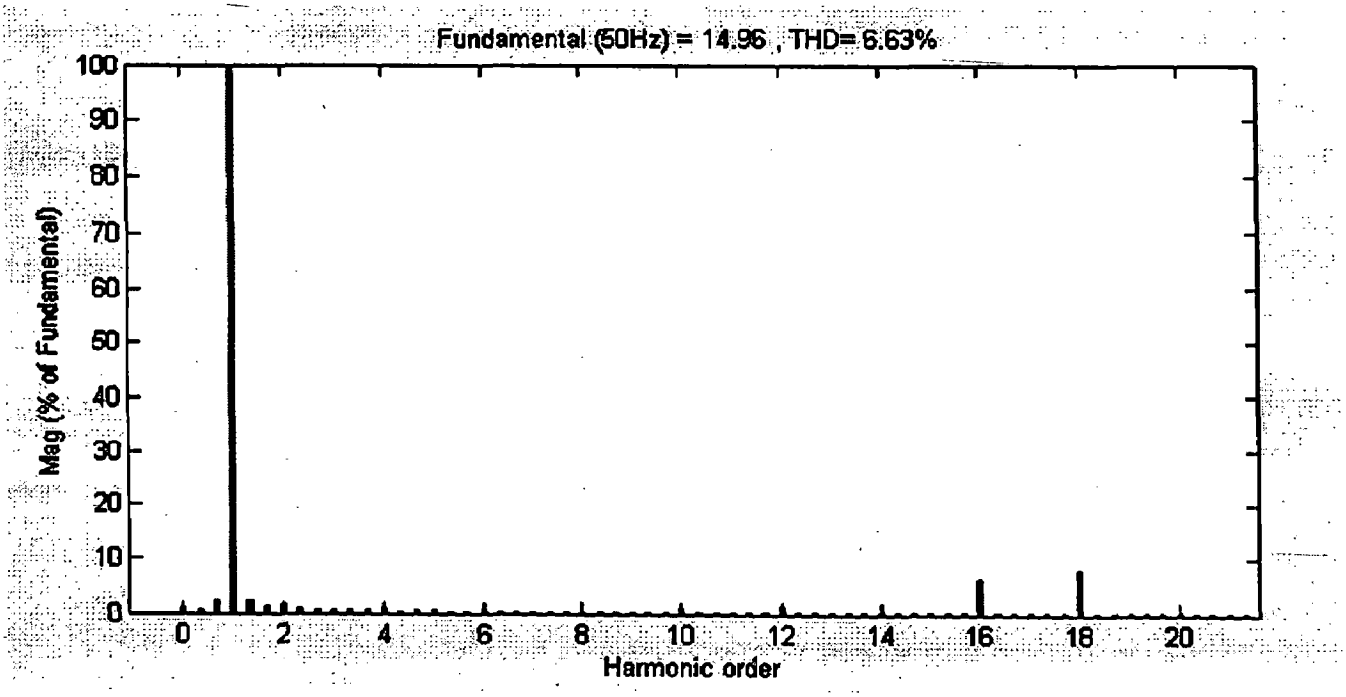

Fig 4.42 FFT Analysis of the source current for fs = 1KHz under SVM

The output voltage and source current waveforms of SVM controlled converter for a switching frequency of 1 KHz are shown in figs 2.34 and 2.35 respectively. The source current comes in phase with the source voltage only after the output voltage settles to its reference value (250V). The FFT analysis of the source current is depicted in fig 2.36. The total harmonic distortion of the source current is 6.63% which is better as compared to

SPWM for the same switching frequency. Also the magnitude of input current is higher in SVM. The FFT analysis reveals that the major order harmonics in the input current are of very high order viz. 10, 12, 16 and 18. The shape of the input current is improved when the converter is controlled by SVM.

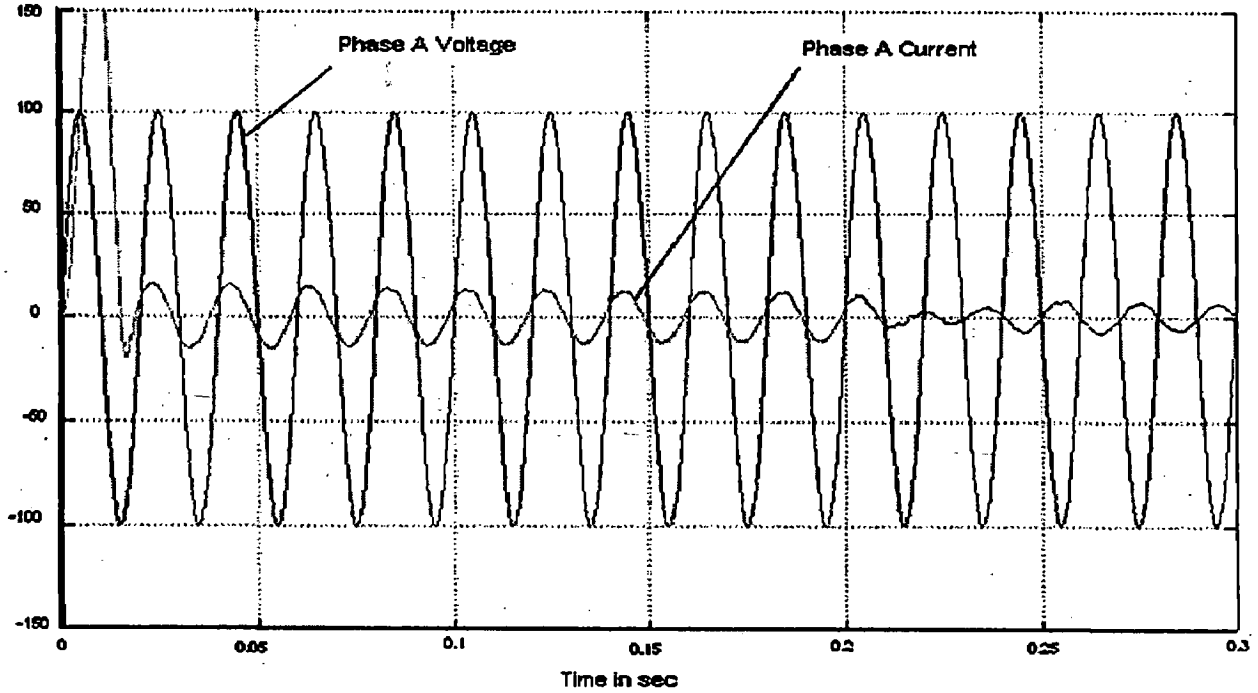

Fig 4.43 Phase A Current for fs = 10 KHz under SVM

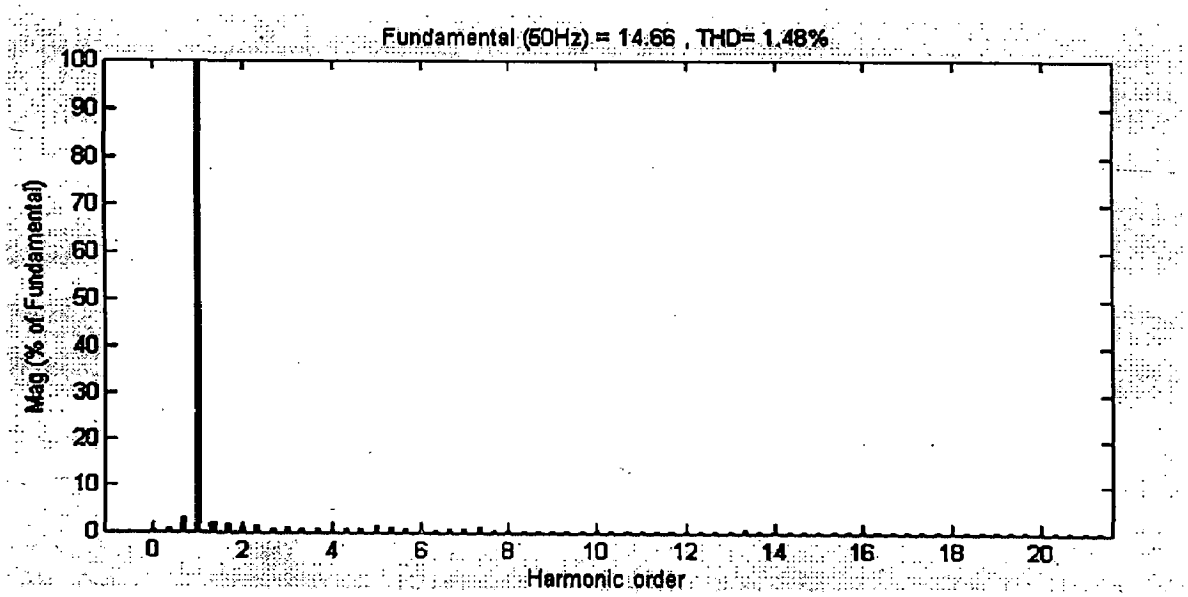

Fig 4.44 FFT Analysis of the source current for fs = 10KHz under SVM

The source current waveform of the converter under SVM for a switching frequency of 10 KHz is shown in fig 2.37. The current is in phase with the source voltage and when the converter changes to regenerative mode at 0.2 sec, the current is 90° out of phase with the voltage. The FFT analysis of the source current is depicted in fig 2.38. The total harmonic

distortion of the current comes out to be 1.48% as compared to 2.96% for SPWM for the same switching frequency. Hence SVM is a better control strategy when compared to SPWM. The THD results show that the converter satisfies the standards.

The various graphs of the converter for different values of output power are given below.

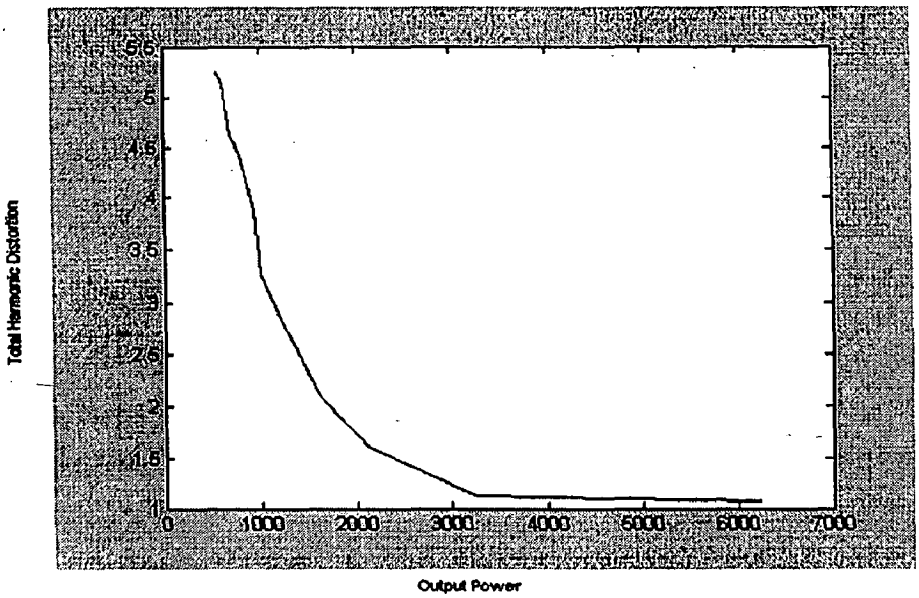

Fig 4.45 Output Power Vs Total Harmonic Distortion for SVM

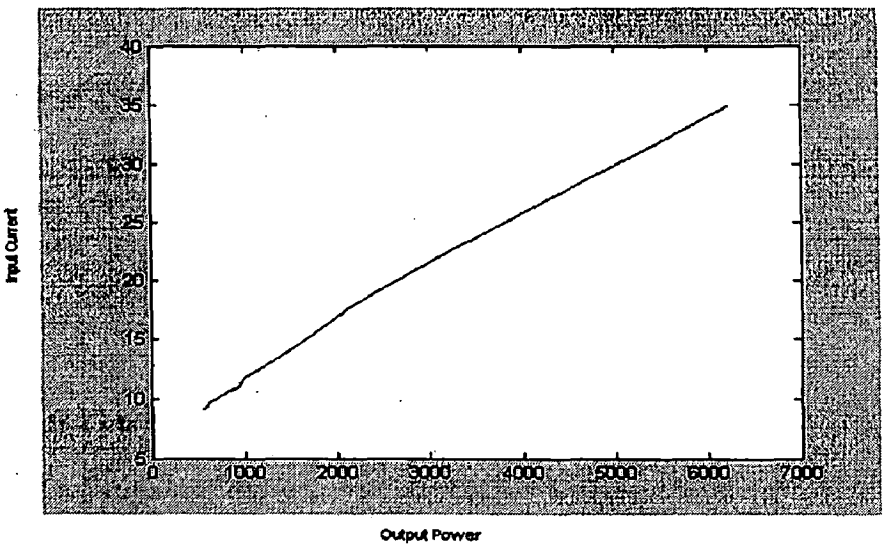

Fig 4.46 Output Power Vs Input Current for SVM

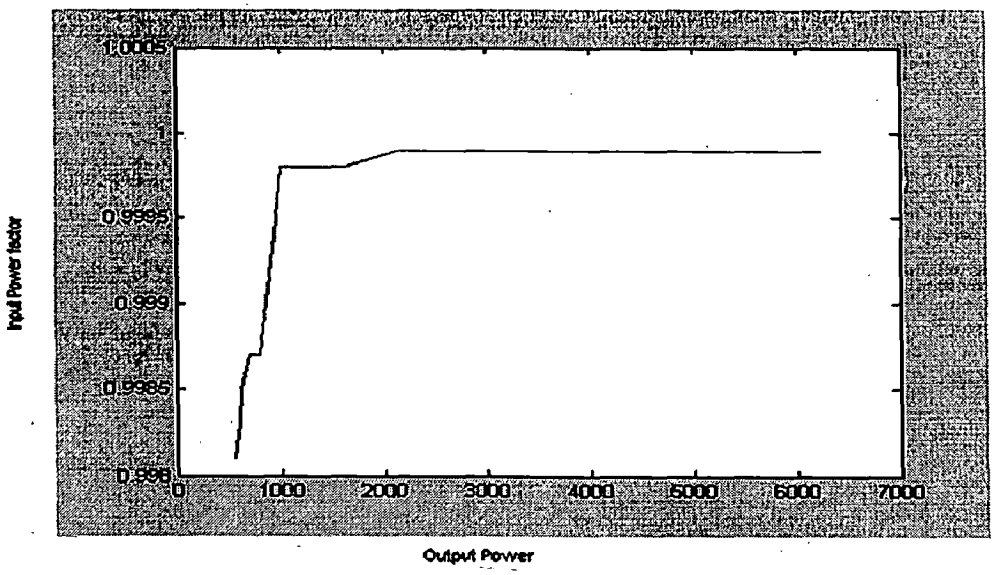

Fig 4.47 Output Power Vs Input power factor for SVM

4.7 Four Wire Rectifiers

Two schemes have been used in the simulation of four wire rectifiers. These are

1. Average Predictive Current Control
2. Hysteresis Current Control

4.7.1 Average Predictive Current Control

The SIMULINK model of the converter is shown in fig 4.29.

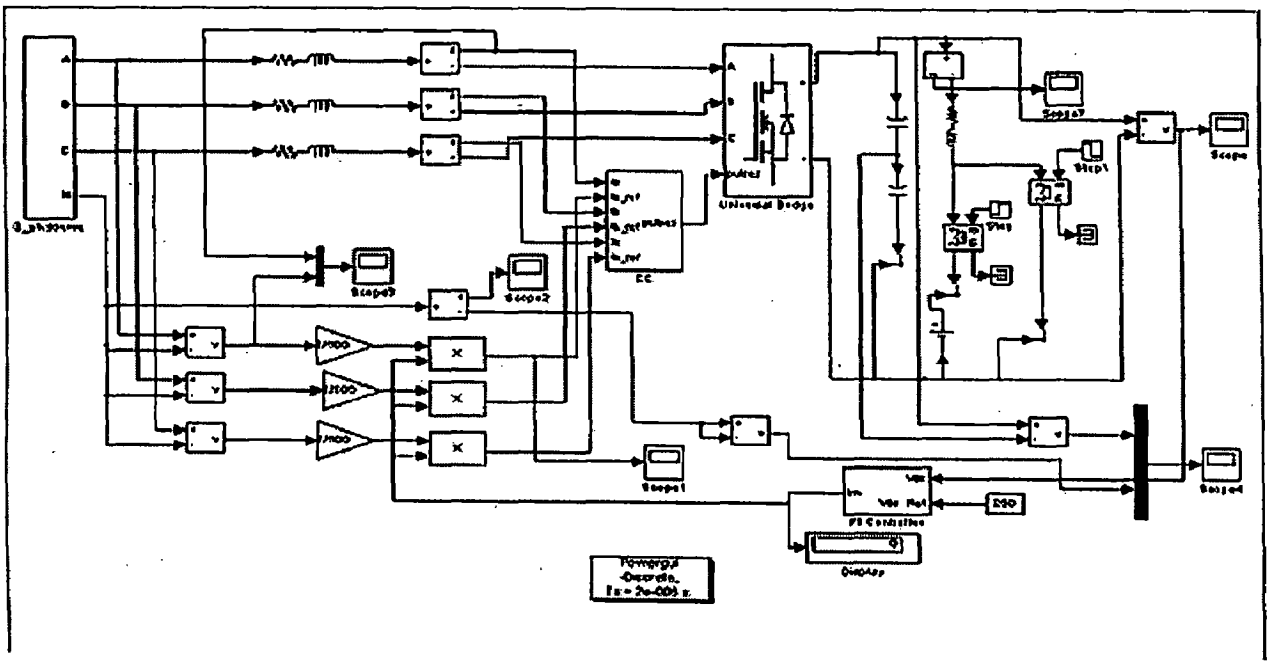

Fig 4.48 SIMULINK model of the converter under APCC

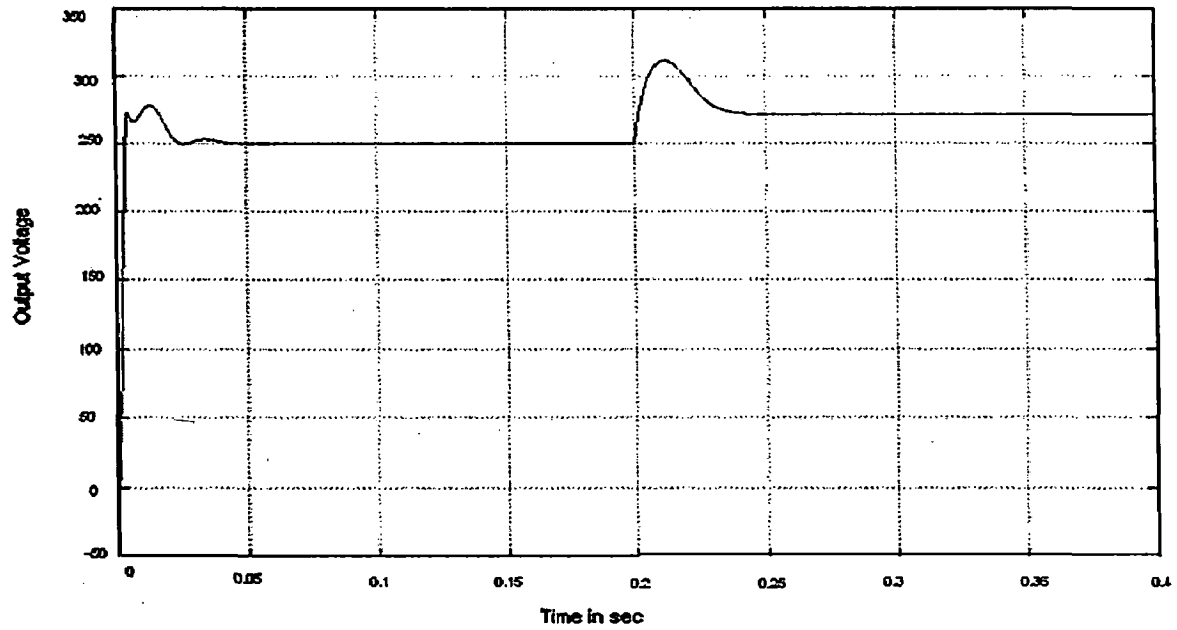

Fig 4.49 Output Voltage of the converter for fs = 10 KHz

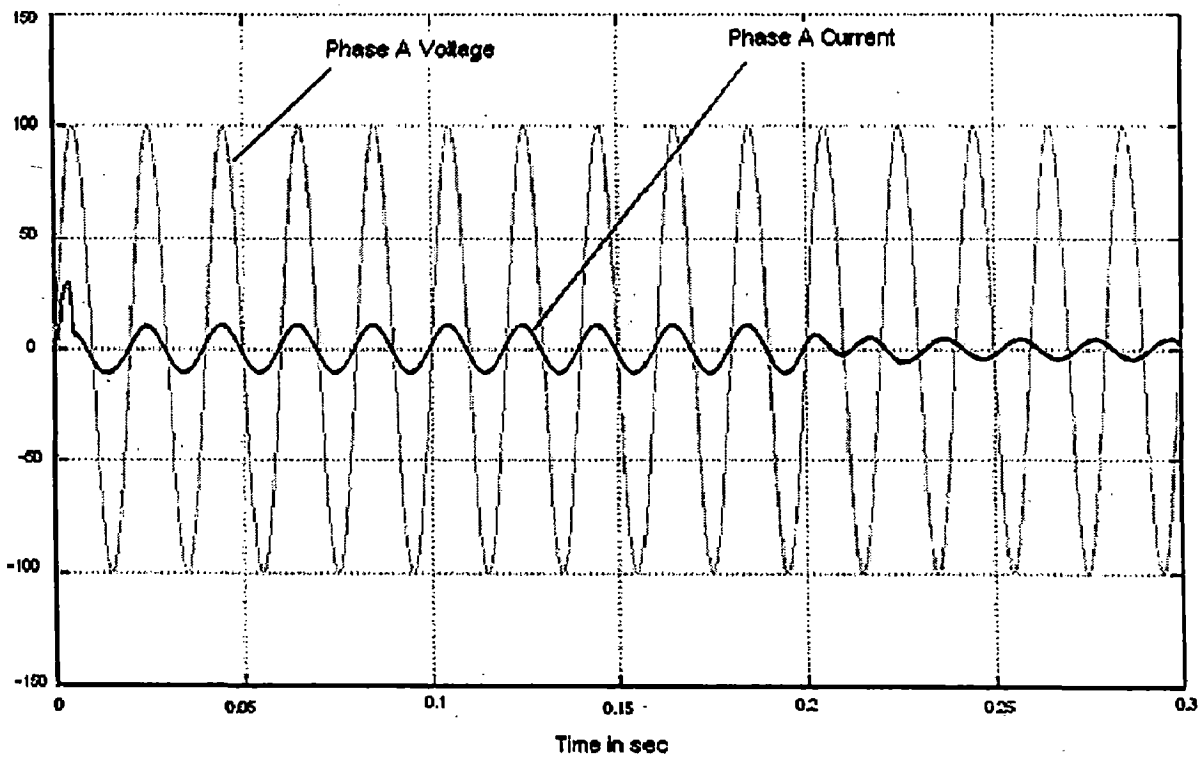

Fig 4.50 Phase A current for fs = 10 KHz

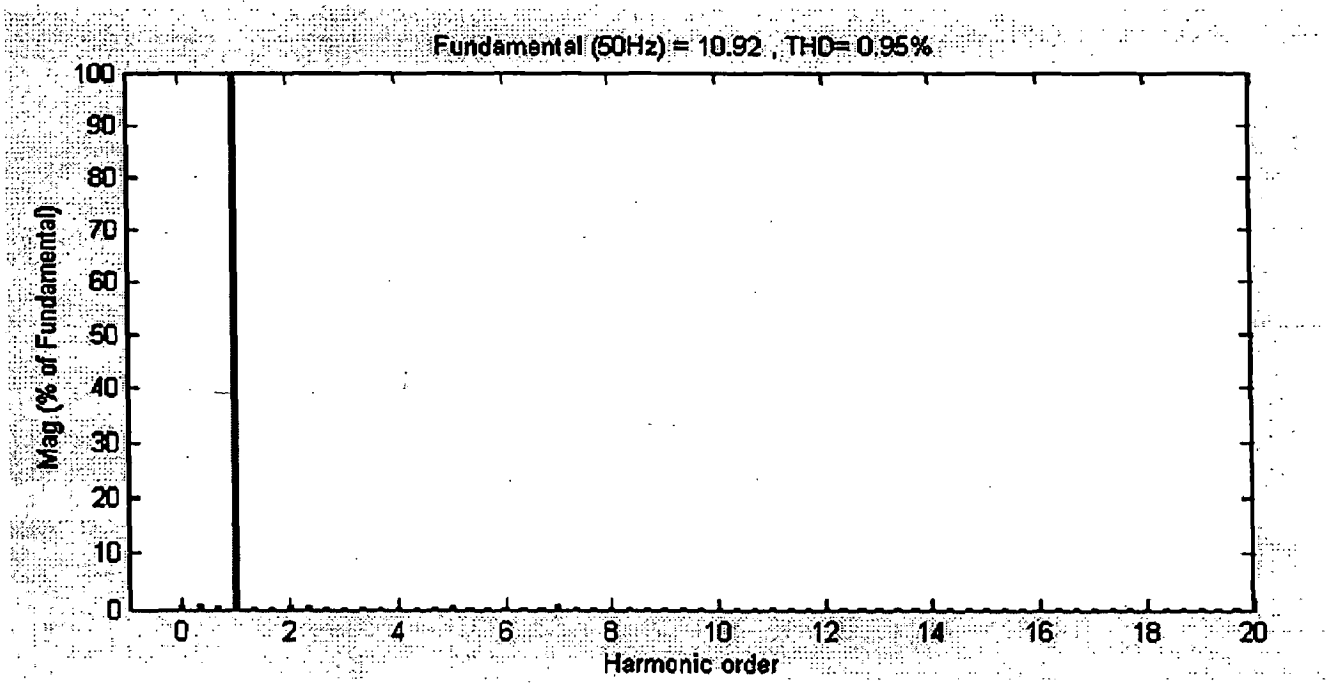

Fig 4.51 FFT Analysis of source current for fs = 10 KHz

The Output voltage of the four wire rectifier under APCC for a switching frequency of 10 KHz is shown in fig 2.42. The waveform reveals that the four wire rectifier responds quickly when the operating mode changes as compared to a three wire rectifier. The source current wave shape is also better when compared to three wire rectifiers. The FFT analysis gives the total harmonic distortion of the source current to be 0.95% whereas the THD of the source current for a three wire rectifier with the same control strategy and the switching frequency came out to be 2.96%. However the response time is more in four wire rectifier as compared to its three wire counter part.

The graphs of the converter are shown below.

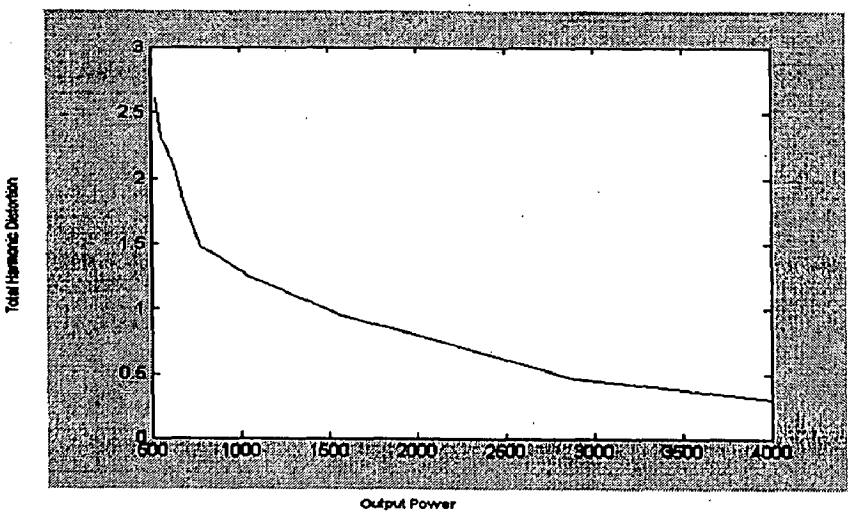

Fig 4.52 Output Power Vs THD for 4wire APCC

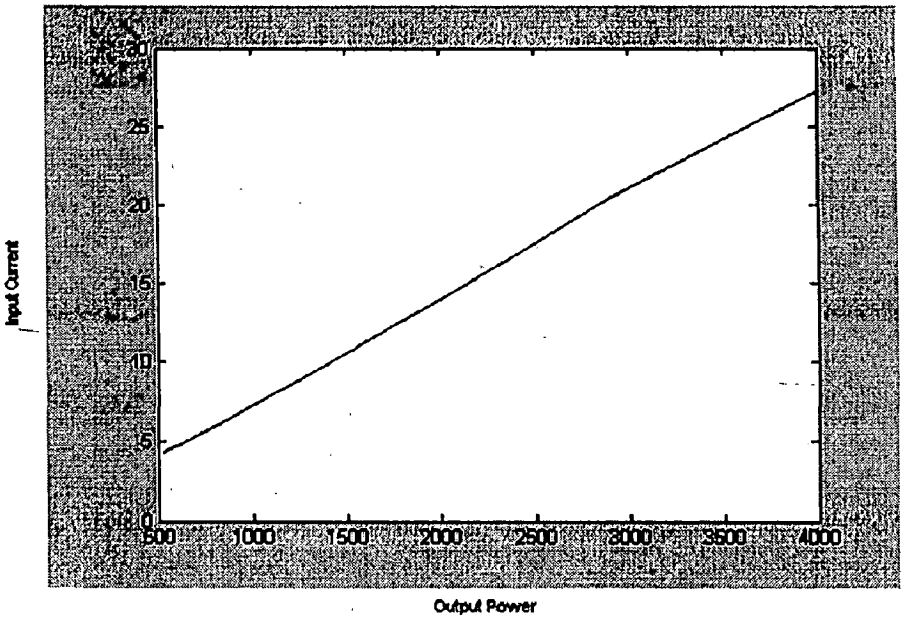

Fig 4.53 Output Power Vs Input Current for 4wire APCC

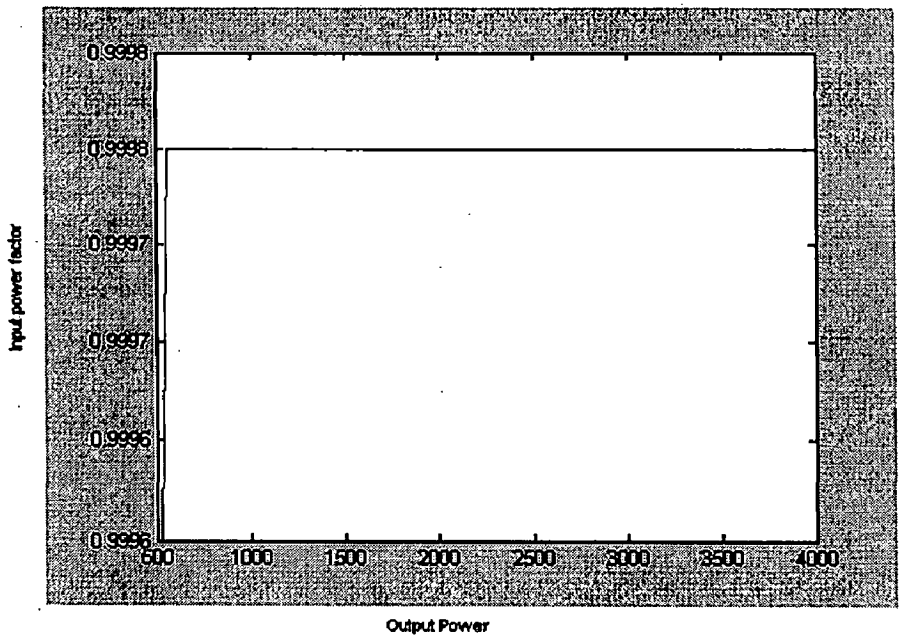

Fig 4.54 Output Power Vs Input Power Factor for 4wire APCC

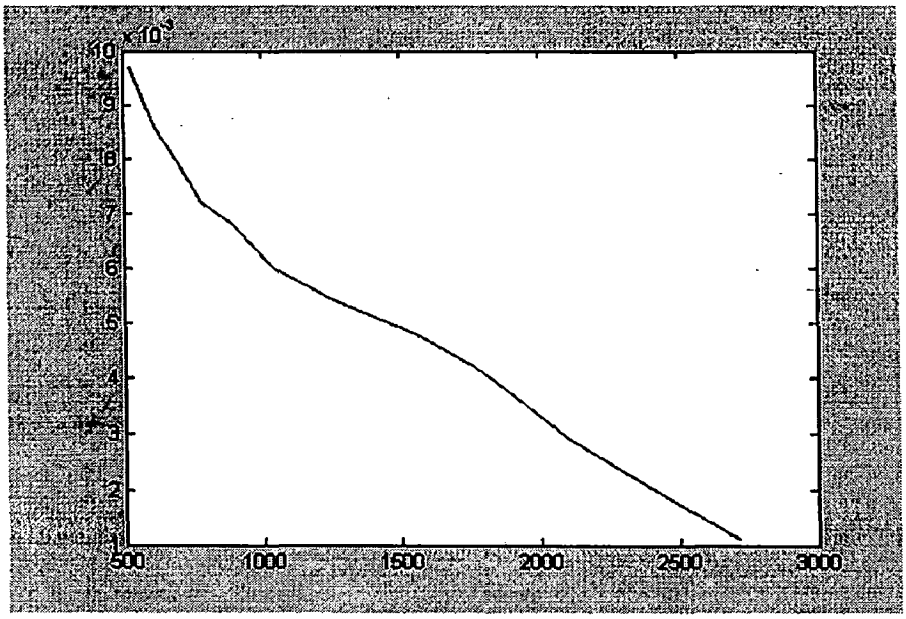

Fig 4.55 Output Power Vs Input Harmonic factor for 4wire APCC

4.6.2 Hysteresis Current Control

The SIMULINK model of the four wire rectifier is as shown in fig 4.33.

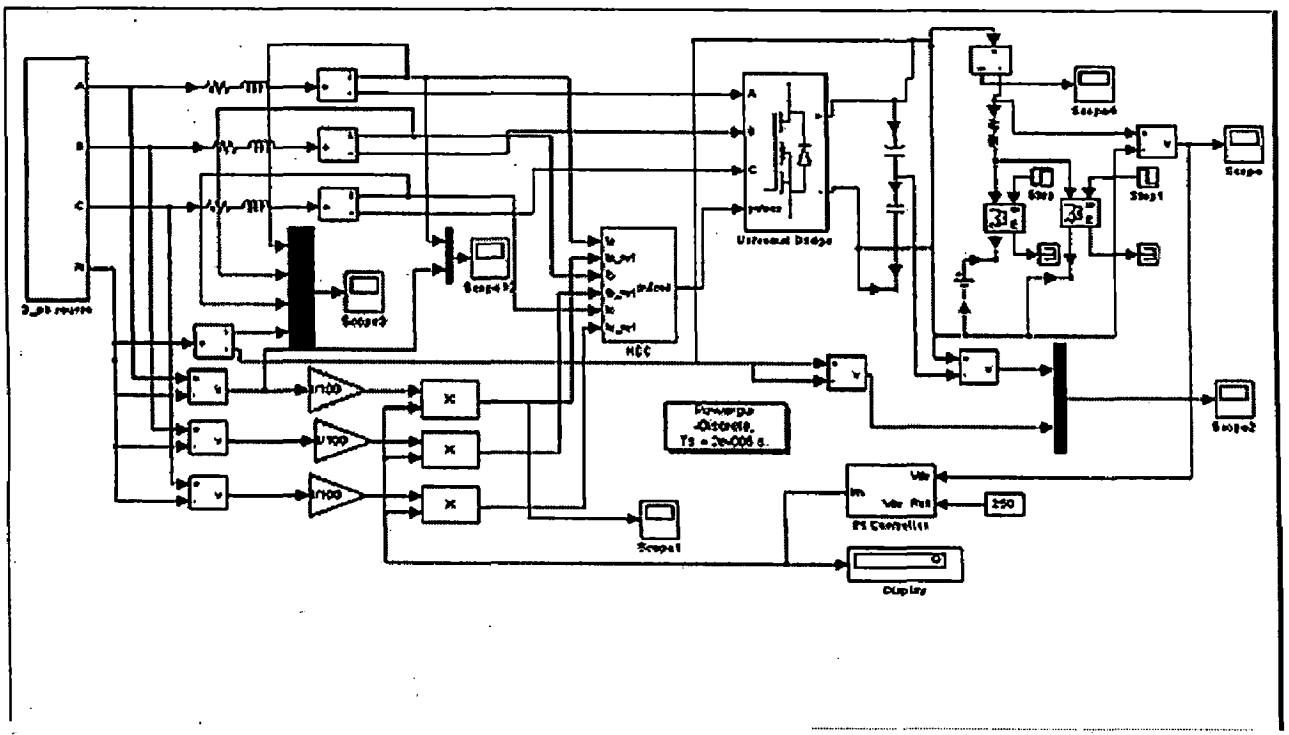

Fig 4.56 SIMULINK model of the 4 wire rectifier under HCC

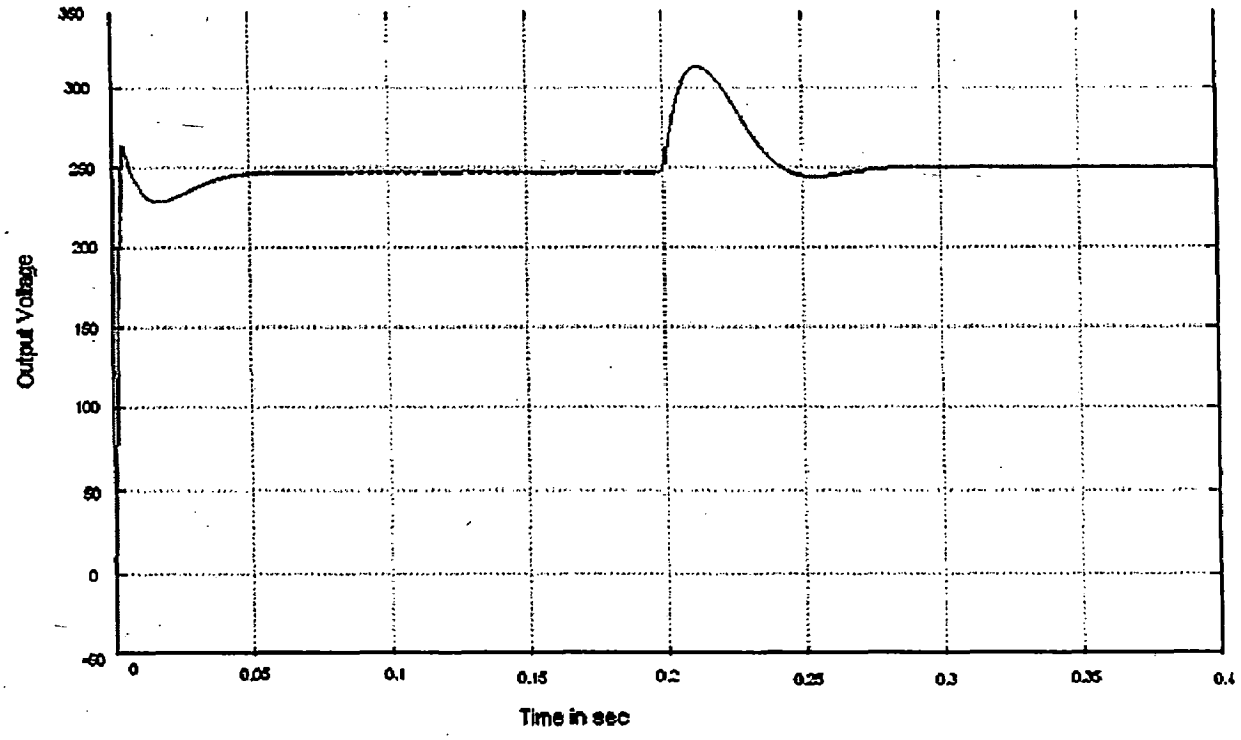

Fig 4.57 Output Voltage for fs = 10 KHz for 4wire rectifier under HCC

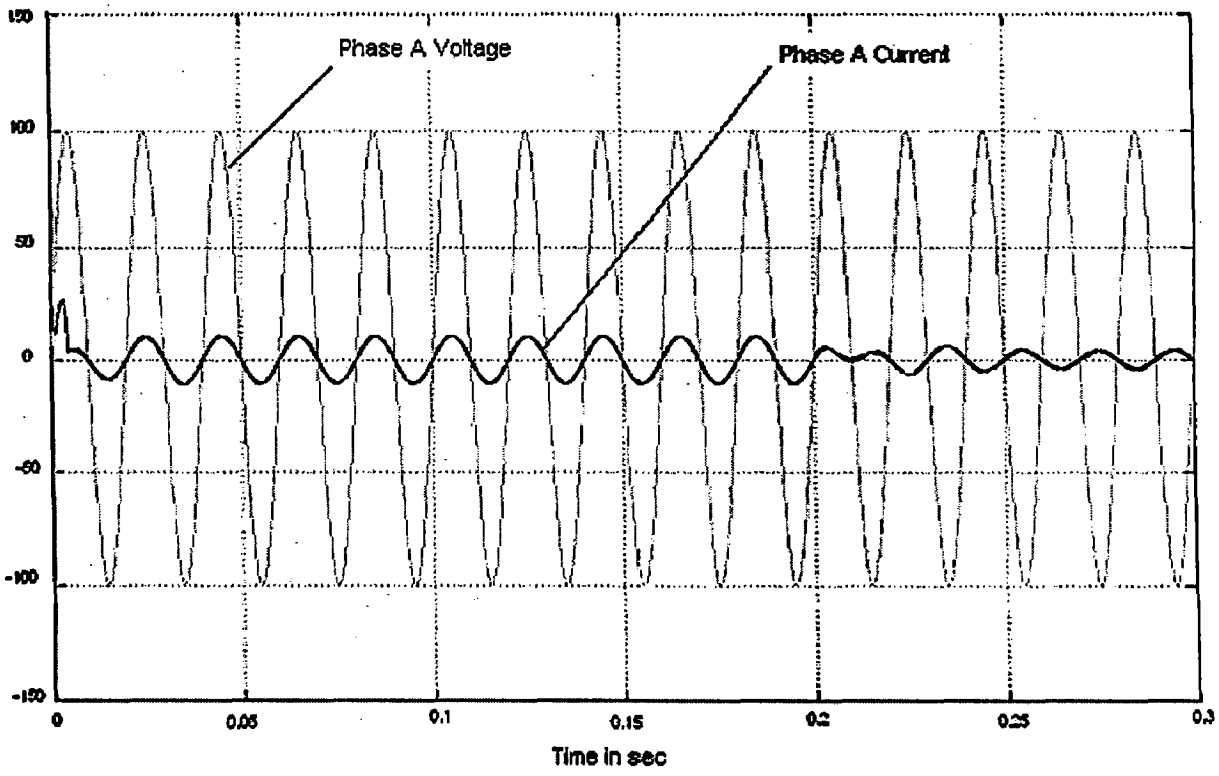

Fig 4.58 Phase A Current for fs = 10KHz for 4 wire rectifier under HCC

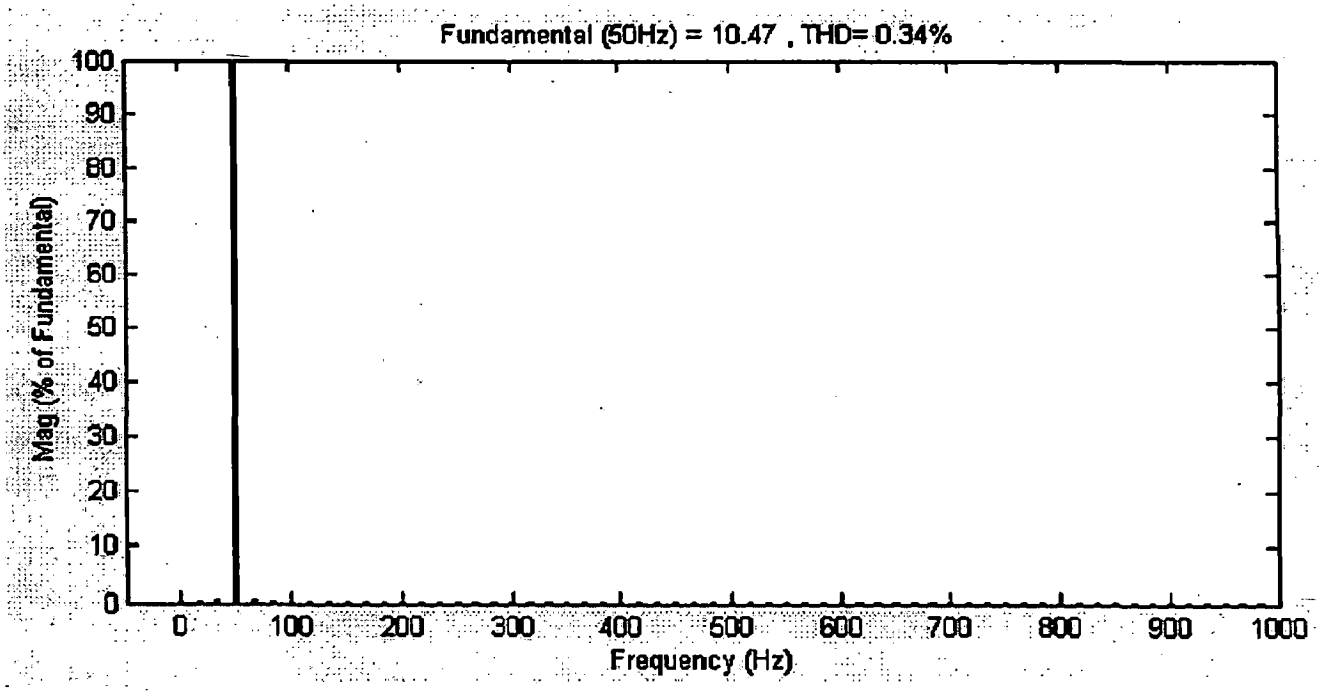

Fig 4.59 FFT Analysis of Source Current for fs = 10 KHz

The output voltage of the four wire rectifier under HCC with a hysteresis band of ±0.5 Amps is shown in fig 2.46. As compared to the three wire rectifier under the same conditions the output voltage recovers soon when the rectifier changes its operating mode from generative to regenerative. The source current waveform is shown in fig 2.47. The FFT analysis gives the total harmonic distortion of the source current to be 0.34% as compared to 0.46% for three wire rectifier.

The graphs of the converter for various parameters with a variation in the output power are given below.

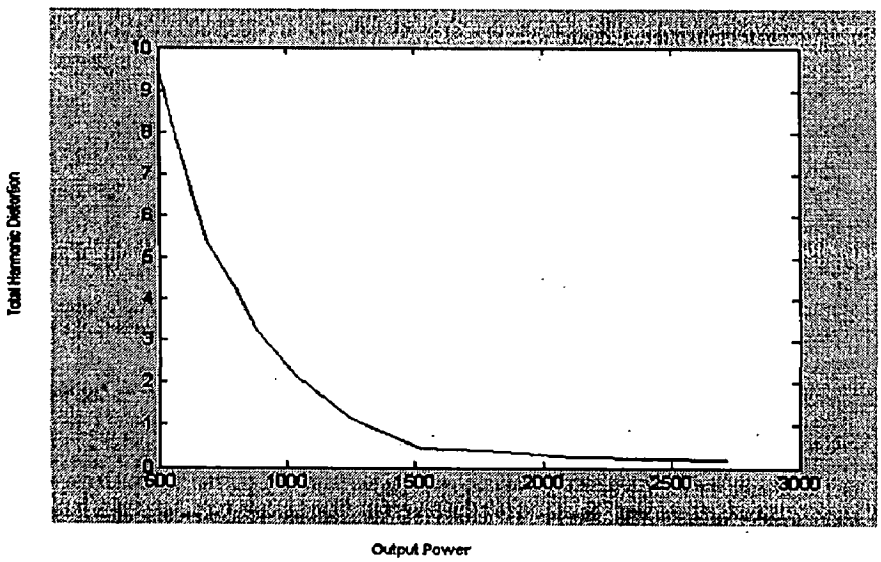

Fig 4.60 Output Power Vs THD for 4 wire rectifier under HCC

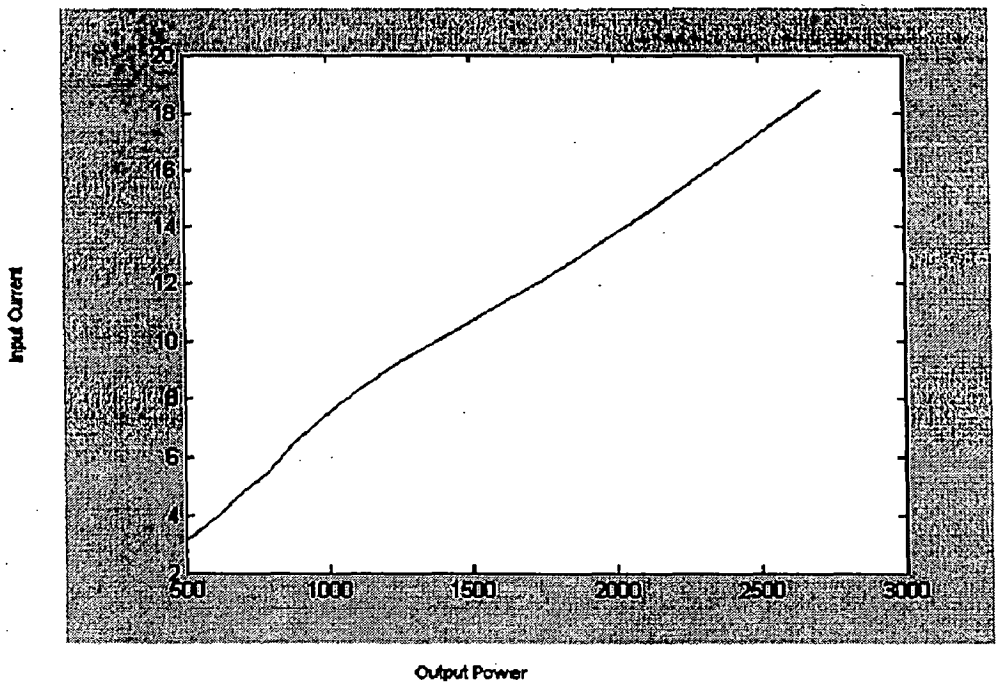

Fig 4.61 Output Power Vs Input Current for 4 wire rectifier under HCC

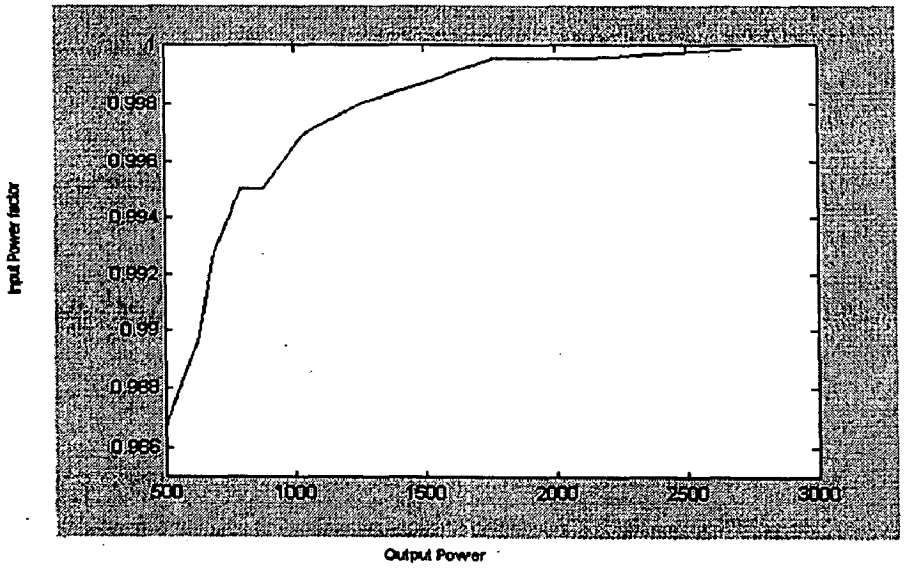

Fig 4.62 Output Power Vs Input Power Factor for 4 wire rectifier under HCC

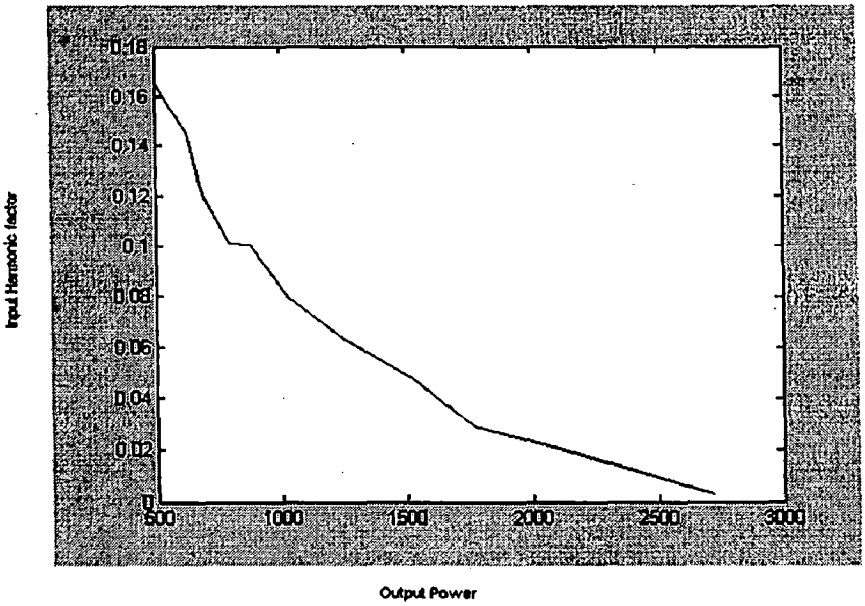

Fig 4.63 Output Power Vs Input Harmonic Factor for 4 wire rectifier under HCC

Hence from the above analysis of the four wire rectifiers, it can be concluded that four wire rectifiers are better than three wire rectifiers with respect to the output voltage wave shape and the THD of the source current.

The simulated results of all the control strategies discussed in the previous chapters are presented here. The results are taken for different switching frequencies, for different loads and for different operating modes. The output power is varied and some performance measures are plotted against it for each of these converters.

CHAPTER 5

Comparative Analysis of Control Strategies Studied

5.1 Introduction

This chapter mainly aims at the comparative analysis of control strategies whose performance evaluation has been done in the previous chapter. Some performance measures are specified and calculated for all the rectifiers and finally the results are tabulated.

The various control strategies of AC-to-DC converters that have been studied are:

1. Hysteresis Current Control
2. Sinusoidal PWM with Instantaneous Current Control
3. Indirect Current Control
4. Average Predictive current control
5. Control of Boost rectifier with single switch

Normally the input voltage to an AC-to-DC converter is sinusoidal but the input current is non-sinusoidal i.e. harmonic currents are present in the ac lines. This has two main adverse effects. These harmonic currents conduct through the ac lines and interfere with other equipment connected to the same lines. Furthermore they cause electromagnetic interference to nearby telephone and communication lines. However the input current can be made nearly sinusoidal with the above control strategies and unity power factor operation can also be achieved. Even though the input current is controlled there is a ripple in the output voltage which in turn generates ripple in the output current. This ripple current has several adverse effects. Therefore there are some external performance measures that are defined for these converters. These are:

- Total Harmonic Distortion of Output Voltage
- Total Harmonic distortion of Input Current
- Input Displacement Factor
- Input Power Factor
- Input Current Distortion Factor
- Input Harmonic Factor
- Voltage Ripple Factor
- Crossover time
- Response time

5.2 External Performance Measures [22]

Input Displacement factor (IDF): This is defined as the cosine of the input displacement angle φ which is the angular displacement between the fundamental component of the ac supply current and the associated line to neutral voltage. It is also known as the fundamental power factor (FPF).

Input Power Factor (IPF): This is defined as the ratio of the total mean input power to the total rms apparent power input to the converter. Since only the fundamental component contributes to the mean input power, the PF may be defined as

$$PF = V_1 I_1 \cos\varphi / V_{rms} I_{rms} = (I_1/I_{rms}) \cos\varphi$$

Where

$V_1 = V_{rms}$ = Phase Voltage

I_1 = Fundamental component of the supply current

Φ = Input displacement angle

I_{rms} = Supply rms current

Input current distortion factor: It is defined as the ratio of the rms amplitude of the fundamental component to the rms amplitude. It is a measure of the distortion present in the supply current.

Input Harmonic factor: It is the ratio of the total harmonic content to the fundamental component

$$I_H = (I_{rms}^2 - I_1^2)^{1/2}/I_1$$

Voltage Ripple factor: It is defined as the ratio of the net harmonic content of the output voltage to the average output voltage.

$$K_V = (V_{0rms}^2 - V_{0av}^2)^{1/2}/V_{0av}$$

Crossover time: This is defined as the time taken by the input current to reach a steady state value when the operating mode of the AC-to-DC converter changes from generating to regenerative.

Response time: It is defined as the time taken by the output DC voltage of the converter to reach a steady state value.

For a comparative analysis of the control strategies studied, all the above parameters have been calculated for each strategy under different load conditions and switching conditions. These are enlisted in the tables below.

Control Strategy	DC output Voltage(V)	THD of Output voltage (%)	THD of Input Current (%)	Response time (sec)	Crossover time (sec)	Input Current distortion factor	Input harmonic factor	Input power factor	Fundamental input current (A)	Voltage Ripple Factor
HCC	246.5	0.51	6.49	.08	.04	.9991	.0422	.999	11.11	.00895
SPWM	260.7	1.37	8.61	.15	.04	.9972	.07404	.997	10.33	.00632
IDC	261.1	1.21	15.43	.15	.03	.9839	.1784	.984	10.3	.0346
SVM	247.3	1.43	6.67	.06	.04	.9995	.0307	.999	14.98	.00623
Boost rectifier	313.8	7.01	13.15	.2	-	.9925	.1231	.993	15.54	.0767
Four wire rect. With HCC	247.8	0.46	7.15	.05	.03	.9981	.0609	.998	10.67	.01267
Four wire rect. With APCC	251.4	0.42	7.74	.045	.04	.9996	.0276	.999	11.1	.0089

Table 5.1 Various Parameters of the converters for load resistance=40ohms, load inductance=2mH and switching frequency of 1 KHz

Control Strategy	DC output Voltage(V)	THD of Output voltage (%)	THD of Input Current (%)	Response time (sec)	Crossover time (sec)	Input Current distortion factor	Input harmonic factor	Input power factor	Fundamental input current (A)	Voltage Ripple Factor
HCC	243.7	.49	.46	.07	.04	.9998	.0162	.999	10.74	.0013
SPWM	259.3	1.3	2.96	.15	.022	.9972	.0746	.997	10.18	.00894
IDC	261.1	1.19	6.28	.16	.04	.9965	.0837	.997	9.689	.0283
SVM	247.9	1.39	1.72	.06	.04	.9993	.03664	.999	14.97	.00623
Boost rectifier	310	4.62	6.58	.25	-	.9978	.0664	.998.	17.37	.05334
Four wire rect. With HCC	245.7	.56	.34	.05	.02	.9995	.0285	.999	10.47	.00201
Four wire rect. With APCC	250.5	.27	.95	.05	.03	.9996	.02788	.999	10.92	.002

Table 5.2 Various Parameters of the converters for load resistance=40ohms, load inductance=2mH and switching frequency of 10KHz

Control Strategy	DC output Voltage(V)	THD of Output voltage (%)	THD of Input Current (%)	Response time (sec)	Crossover time (sec)	Input Current distortion factor	Input harmonic factor	Input power factor	Fundamental input current (A)	Voltage Ripple Factor
HCC	246.5	.49	6.74	.08	.04	.9981	.0618	.998	11.12	.0063
SPWM	260.7	1.37	8.42	.14	.06	.9968	.0794	.997	10.34	.00894
IDC	261.1	1.21	15.44	.16	.04	.9835	.18405	.984	10.3	.0283
SVM	247.3	1.43	6.65	.06	.04	.9998	.01094	.999	14.99	.0088
Boost rectifier	304	7.95	10.07	.2	-	.9948	.10199	.995	14.73	.1184
Four wire rect. With HCC	247.8	.6	6.65	.05	.03	.9979	.06319	.998	10.64	.00895
Four wire rect. With APCC	251.4	.42	7.75	.05	.03	.9979	.0639	.998	11.09	.008945

Table 5.3 Various Parameters of the converters for load resistance=40ohms and switching frequency of 1 KHz

Control Strategy	DC output Voltage(V)	THD of Output voltage (%)	THD of Input Current (%)	Response time (sec)	Crossover time (sec)	Input Current distortion factor	Input harmonic factor	Input power factor	Fundamental input current (A)	Voltage Ripple Factor
HCC	243.7	.47	1.1	.08	.04	.9998	.01622	.999	10.74	.00089
SPWM	259.4	1.3	2.96	.15	.05	.9975	.0706	.998	10.2	.00632
IDC	261.1	1.22	15.46	.15	.08	.9865	.16346	.987	9.938	.02833
SVM	248	1.4	1.55	.06	.04	.9992	.0395	.999	14.52	.088
Boost rectifier	295	5.45	8.26	.25	-	.9967	.0804	.997	15.33	.03794
Four wire rect. With HCC	245.6	.56	1.03	.05	.02	.9999	.01376	.999	10.45	.0009
Four wire rect. With APCC	250.7	.28	.97	.05	.04	.9996	.0278	.999	10.94	.002

Table 5.4 Various Parameters of the converters for load resistance=40ohms and switching frequency of 5 KHz

The above tables give the various parameters of the converter for each control strategy for different load conditions. It can be observed from the table that the hysteresis current control strategy is the best one in all the respects. However in this scheme the switching frequency does not remain constant which increases the switching losses of the converter. The space vector modulation technique is definitely an improvement over the sinusoidal pulse width modulation technique as the THD of the source current is reduced and the magnitude of input current is very high in SVM as compared to SPWM. Though the indirect current control scheme has a higher THD in the source current, the output DC voltage is high. The boost rectifier with single switch has the highest magnitudes of both the input current and the output voltage when compared to all other schemes. However this converter suffers from the disadvantage of higher THD in the input current and more ripple in the output DC voltage. The four wire rectifiers have proven to be better than the three wire rectifiers with respect to the THD of the source current, THD of output voltage, response time and crossover time. However the ripple factor of the output voltage is high in these rectifiers as compared to their three wire counterparts.

These control schemes are also compared on the basis of some plots which give the variation of output power with various parameters like THD of input current, magnitude of input current, input power factor, input harmonic factor. These graphs are shown below.

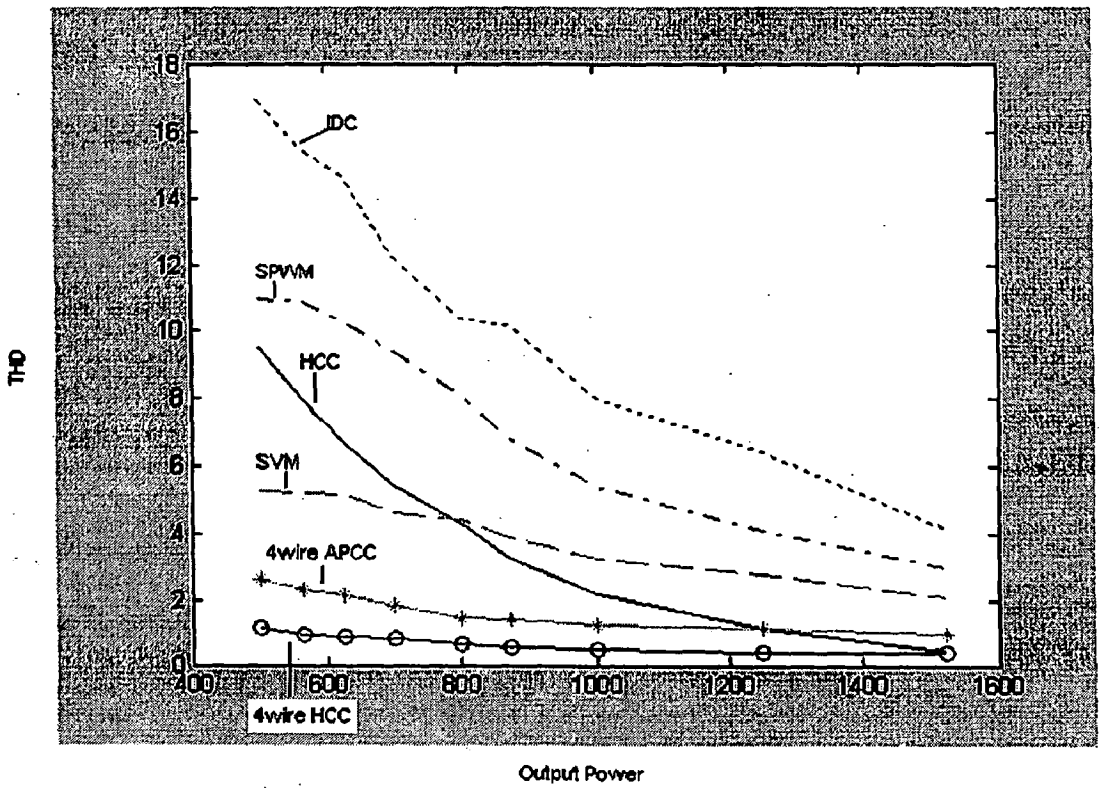

Fig 5.1 Output power Vs THD

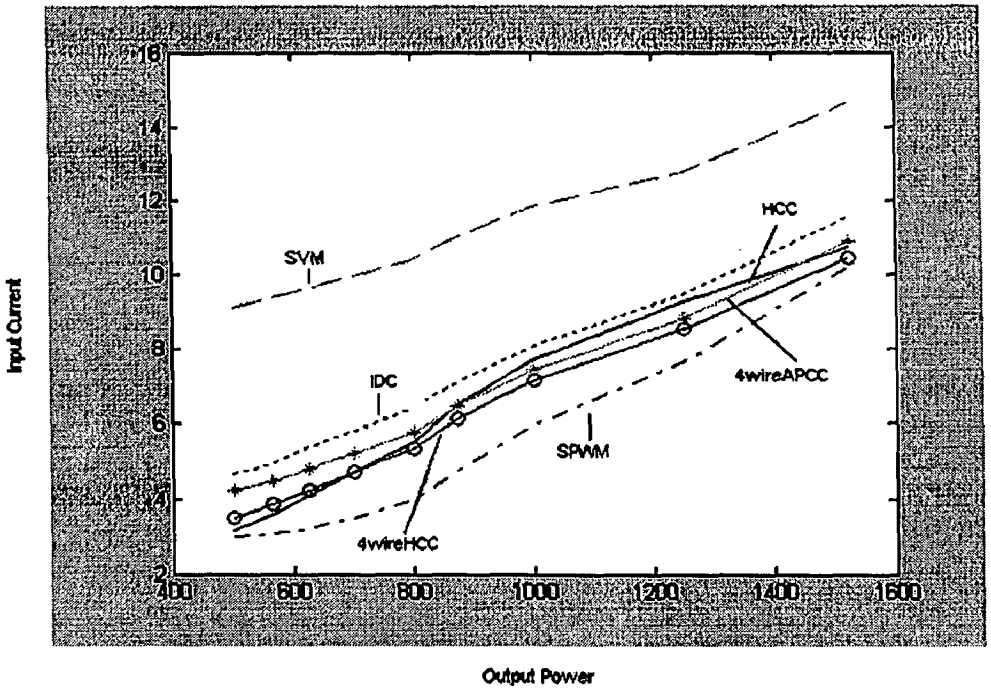

Fig 5.2 Output power Vs Input current

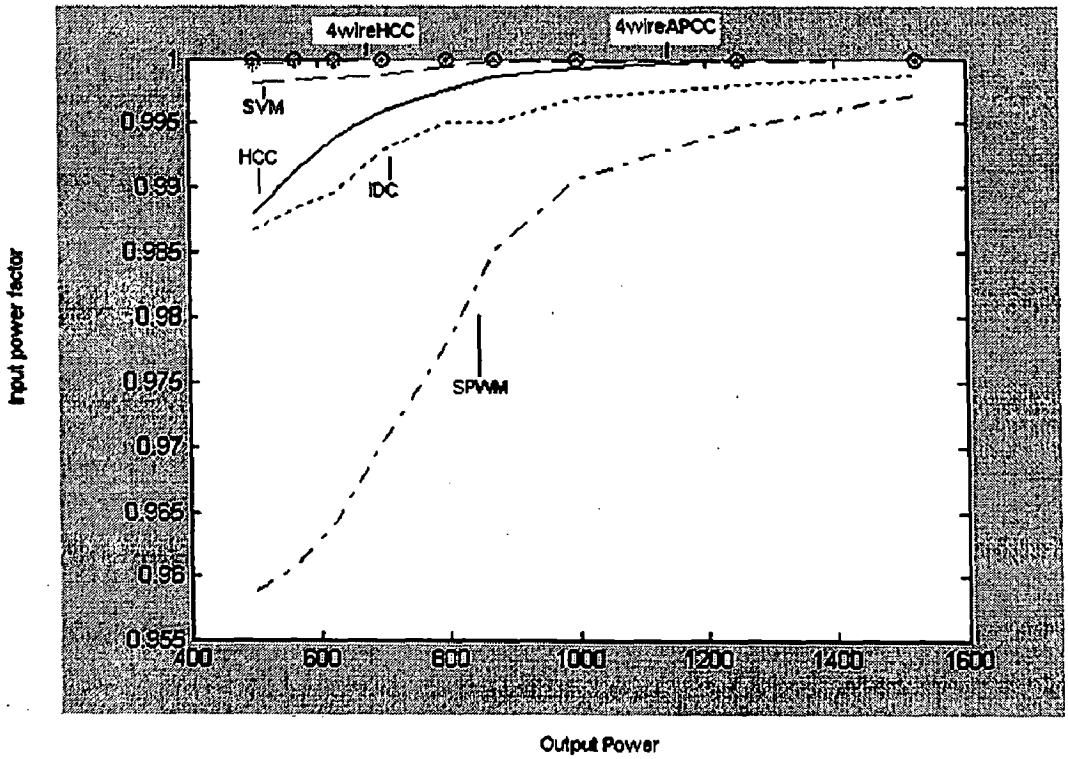

Fig 5.3 Output Power Vs Input power factor

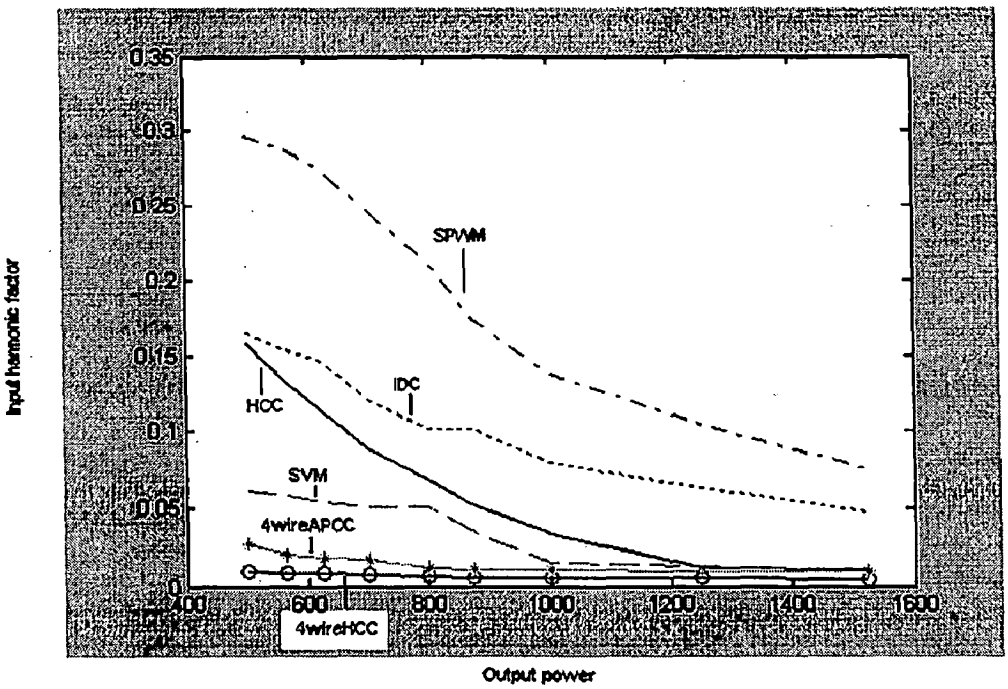

Fig 5.4 Output power Vs Input harmonic factor

From graph 5.1, it can be observed that the THD is the highest for indirect current control scheme whereas it is the lowest fro 4 wire rectifier under HCC. The magnitude of input current is the highest for SVM (Graph 5.2).

All the control schemes have been compared on the basis of a number of parameters. At the end graphs are plotted and compared to decide the best scheme. Each scheme has its own advantages and disadvantages. The selection of the control strategy to be used depends upon the application and requirements of the system.

Future Scope

Many new PWM control schemes are being developed which improve the performance of the converter. The predictive current control with fixed switching frequency is an improvement over the hysteresis current control scheme as the switching frequency remains constant and all the advantages of HCC are retained. Artificial Intelligence techniques are being developed for the implementation of control techniques in power electronics. Some of these are fuzzy logic control, artificial neural networks. Space vector modulation implementation is much easier using neural network training method as compared to the one that employs the d-q transformation.

REFERENCES

1. Clarissa Gatlan, Leonard Gatlan **"AC to DC PWM voltage source converter under hysteresis current control"** *Industrial Electronics, 1997. ISIE '97., Proceedings of the IEEE International Symposium on Volume 2*, 7-11 July 1997 Page(s):469 – 473.

2. Hirota A, Nagai S, Al. M.A, Rukonuzzaman M, Nakaoka M **"A novel hysteresis current control scheme for single switch type single phase PFC converter"** *Power Conversion Conference, 2002. Proceedings of the Volume 3*, 2-5 April 2002 Page(s):1223 – 1225.

3. A.W.Green, J.T.Boys, **"Hysteresis Current forced three phase voltage source reversible rectifier"** *IEEE Proceedings of Volume 136* May1989 Page(s): 113-120.

4. Wu R., Dewan S.B., Slemon G.R **"A PWM AC to DC converter with fixed switching frequency"** *Industry Applications Society Annual Meeting, 1988., Conference Record of the 1988 IEEE* 2-7 Oct. 1988 Page(s):706 - 711.

5. Dixon J.W., Boon-Teck Ooi **"Indirect current control of a unity power factor sinusoidal current boost type three-phase rectifier"** *Industrial Electronics, IEEE Transactions on Volume 35*, Issue 4, Nov. 1988 Page(s):508 – 515.

6. J.Choi, H.C.Kim, J.S.Kwak, **"Indirect Current Control Scheme in PWM Voltage-Sourced Converter"** *Power Conversion Conference 1997, IEEE Proceedings* Page(s):277-282.

7. Pan C.-T, Chen T.-C, **"Modeling and analysis of a three phase PWM AC-DC converter without current sensor"** *Electric Power Applications, IEE Proceedings B Volume 140,* Issue 3, May 1993 Page(s):201 – 208 .

8. Rathnakumar D, LakshmanaPerumal J., Srinivasan T, **"A new software implementation of space vector PWM"**, *SoutheastCon, 2005. Proceedings. IEEE* 8-10 April 2005 Page(s):131 – 136.

9. Ma Hao, Lang Yunping, Chen Huiming, "**A simplified algorithm for space vector modulation of three-phase voltage source PWM rectifier**", *Power Electronics Specialists Conference, 2004. PESC 04. 2004 IEEE 35th Annual Volume 5*, 20-25 June 2004 Page(s):3665 - 3670 Vol.5.

10. A.R. Prasad, 1P.D. Ziogas, S. Manias, "**An Active Power Factor Correction Technique for Three-phase Diode Rectifiers**," *IEEE Power Electronics Specialists Con. (PESC) Record,* 1989, pp. 58 - 66.

11. Yungtaek Jang, Milan M. Jovanovic, "**A Comparative Study of Single-Switch Three-Phase High-Power-Factor Rectifiers**", IEEE Transactions on Industry Applications, VOL. 34, NO. 6, November/December 1998, Page(s):1327-1334.

12. Fraser M.E., Manning C.D., Wells B.M., "**Transformer less Four-Wire PWM Rectifier and its Application in AC-DC-AC Converters**", *IEEE Proceedings.-Electrical Power Applications* Volume142.Page(s):410- 416.

13. M. E. Fraser and C.D. Manning, "**A Proposed Predictive Average Current Controller for four-wire boost rectifiers**" *IEEE Proceedings on Power Electronics and Variable Speed Drives',* 23-25 September 1996, Page(s):144-149.

14. Lin B.-R, Hung C.-H, Hung T.-L, Chiang H.-K, "**Unidirectional single-phase high power factor rectifier**" *Electric Power Applications, IEE Proceedings- Volume 150, Issue 4,* 8 July 2003 Page(s):380 – 388.

15. Borle L.J., Nayar C.V, "**Zero average current error controlled power flow for AC-DC power converters**", *IEEE Transactions on Power Electronics Volume 10, Issue 6*, Nov. 1995 Page(s):725 – 732.

16. Tarasantisuk C., Tunyasrirut S., Tipsuwanporn V, "**A Matlab/Simulink tool for enhancing efficient education of power electronics corresponding to the ETH power converter laboratory**" *Industrial Electronics Society, 2004. IECON 2004. 30th Annual Conference of IEEE Volume 2,* 2-6 Nov. 2004 Page(s):1629 - 1633 Vol. 2.

17. Ming-Tsung Tsai, W.I.Tsai, **"Analysis and Design of Three-Phase AC-to-DC Converters with high power factor and near optimum feed forward"** *IEEE Transactions on Industrial Electronics, Volume 46*,June1999.Page(s):535-543.

18. Vahe Caliskan, David J. Perreault, Thomas M. Jahns, John G. Kassakian, **"Analysis of Three-Phase rectifiers with constant-voltage loads".**

19. J.W.Kolar, F.C.Zach, **"A Novel Three-phase Three-switch Three-level unity power factor PWM rectifier"** *Proceedings of Power Conversion Conference* June 1994.Page(s):125-138.

20. M.H.Rashid, **"Power Electronics, Circuits, Devices, and Applications"** *2nd Ed. Prentice Hall* 1993.

21. Bimal K. Bose **"Modern Power Electronics and AC Drives"** *Pearson Education, Inc.* Third Indian Reprint 2003.

22. G.K. Dubey, S.R. Doradla, A. Joshi, R.M.K. Sinha, **"Thyristorised Power Controllers"** *New Age International (P) Limited, Publishers* Reprint 2003.

23. M.D. Singh, K.B. Khanchandani, **"Power Electronics"** *Tata McGraw-Hill Publishers Fourth* Reprint 2001.

24. Iuliano G., Lo Sciavo A., Marino P., Testa A., **"Voltage Quality Control in a Industrial System by means of a three-phase four wire rectifier"** *IEEE Proceedings on Harmonics and Quality of Power*, Oct 1998, Page(s)-107-114.

Papers Related to Sinusoidal PWM

1. Kaura,V. Blasko, V, "**A method to improve linearity of a sinusoidal PWM in the overmodulation region**", *IEEE Proceedings on Power Electronics, Drives and Energy Systems for Industrial Growth*, Vol. 1, June 1996, Page(s)-325-330.

2. Halasz, S., Csonka, G.; Hassan, A.A.M, "**Sinusoidal PWM techniques with additional zero-sequence harmonics**", *20th International Conference on Industrial Electronics, Control and Instrumentation*, Vol.1, Sept. 1994, Page(s):85 – 90.

3. Ohnishi, T., Hojo, M., "**Harmonics compensator by connecting sinusoidal voltage PWM converters**", *Proceedings of the Power Conversion Conference*, Vol.3, April 2002 Page(s):1399 – 1404.

4. Ando, I., Takahashi, I., Utsunomiya, K, "**Simple sensorless method for sinusoidal PWM converters**", *Proceedings of the Power Conversion Conference – Nagaoka*, Vol.1, Aug. 1997 Page(s):241 – 246.

5. Profumo, F., Boglietti, A., Griva, G., Pastorelli, M, "**Space vector and sinusoidal PWM techniques comparison keeping in account the secondary effects**", *AFRICON '92 Proceedings, 3rd AFRICON Conference*, Sept. 1992 Page(s):394 – 399.

6. Fukuda, S., Iwaji, Y., Aoyama, T, "**Modelling and control of sinusoidal PWM rectifiers**", *Fifth European Conference on Power Electronics and Applications*, Vol.4, Sep 1993 Page(s):115 – 120.

7. Khan, B.H., Doradla, S.R., Dubey, G.K, "**A three-phase AC-DC GTO thyristor converter employing equal pulse-width modulation (EPWM)**", *IEEE Transactions on Industry Applications*, Volume 27, March-April 1991 Page(s):370 – 379.

8. Rodrigues, M., Teixeira, E., Braga, H.A.C, "**A Family of High Power Factor Current Multilevel Rectifiers Employing a Sinusoidal PWM Technique**", *IEEE 36th Conference on Power Electronics Specialists*, June, 2005 Page(s):2547 – 2552.

Papers related to HCC

1. Xu Dianguo, Gu Jianjun, Liu Hankui, Gong Maozhong, "**Improved hysteresis current control for active power filter**", *IEEE International Symposium on Industrial Electronics*, vol. 2, June 2003 Page(s):836 – 840.

2. Maswood, A.I, Fangrui Liu, "**A unity power factor front-end rectifier with hysteresis current control**", *IEEE Transactions on Energy Conversion*, Volume 21, March 2006 Page(s):69 – 76.

3. Jiann-Jong Chen, Yuh-Shyan Hwang, Juing-Huei Su; Wei-Chung Shih, "**New Current Sensing Circuit for Hysteresis-Current-Controlled Buck Converters**", *International Conference on Power Electronics and Drives Systems*, Volume 1, Nov. 2005 Page(s):452 – 455.

4. Dawande, M.S., Kanetkar, V.R., Dubey, G.K, "**Three-phase switch mode rectifier with hysteresis current control**", *IEEE Transactions on Industry Applications*, Volume 25, July-Aug. 1989 Page(s):644 – 651.

5. Kang, B.J., Liaw, C.M, "**Robust hysteresis current-controlled PWM scheme with fixed switching frequency**", *IEEE Proceedings Electric Power Applications*, Volume 148, Nov. 2001 Page(s):503 – 512.

6. Dalessandro, L., Drofenik, U., Round, S.D., Kolar, J.W, "**A novel hysteresis current control for three-phase three-level PWM rectifiers**", *Twentieth Annual IEEE Applied Power Electronics Conference and Exposition*, Volume 1, March 2005 Page(s):501 – 507.

7. Maswood, A.I., Fangrui Liu, "**A unity power factor converter using the synchronous reference frame based hysteresis current control**", *Twentieth Annual IEEE Applied Power Electronics Conference and Exposition*, Volume 3, March 2005 Page(s):1667 – 1673.

8. Choudhury, M.A., Rahman, K.M., Rahman, M.A., Bhuiya, A.R, "**Hysteresis current controlled PWM converter for AC/AC voltage control**", *IEEE 1997 Canadian Conference on Electrical and Computer Engineering*, Volume 2, May 1997 Page(s):431 – 434.

9. Bor-Ren Lin, Hsin-Hung Lu, "**A novel PWM scheme for single-phase three-level power-factor-correction circuit**", *IEEE Transactions on Industrial Electronics*, Volume 47, April 2000 Page(s):245 – 252.

Papers Related to IDC

1. Rahmani, S., Al-Haddad, K., Kanaan, H.Y, "**Experimental design and simulation of a modified PWM with an indirect current control technique applied to a single-phase shunt active power filter**", *Proceedings of the IEEE International Symposium on Industrial Electronics*", Volume 2, June 2005 Page(s):519 – 524.

2. Farrokhi, M., Jamali, S., Mousavi, S.A, "**Fuzzy logic based indirect current control of the shunt active power filter**", *39th International Universities Power Engineering Conference*, Volume 1, Sept. 2004 Page(s):489 – 493.

3. Hamadi, A., Al-Haddad, K., Lagace, P.J., Chandra, A, **Indirect current control techniques of three phase APF using fuzzy logic and proportional integral controller: comparative analysis**", *11th International Conference on Harmonics and Quality of Power,* Sept. 2004 Page(s):362 – 367.

4. Kanetkar, V.R., Dawande, M.S., Dubey, G.K, "**Indirect current control with separate IZ drop compensation for voltage source converters**", *Proceedings of the 1996 International Conference on Power Electronics, Drives and Energy Systems for Industrial Growth*, Volume 2, Jan. 1996 Page(s):662 – 668.

5. Dixon, J.W., Ooi, B.T, "**Dynamically stabilized indirect current controlled SPWM boost type 3-phase rectifier**", *Conference Record of the 1988 IEEE Industry Applications Society Annual Meeting*, Vol.1, Oct. 1988 Page(s):700 – 705.

6. Sriram, V.B., SenGupta, S., Patra, A, "**Indirect current control of a single-phase voltage-sourced boost-type bridge converter operated in the rectifier mode**", *IEEE Transactions on Power Electronics,* Volume 18, Sept. 2003 Page(s):1130 – 1137.

7. Weiyang Wu, Yingnan Zheng, Liqiao Wang, Xiaofeng Sun, "**A novel indirect current controlled realization for the three phase voltage source reversible converter**", *The Third International Power Electronics and Motion Control Conference,* Volume 2, Aug. 2000 Page(s):985 – 989.

Papers Related to SVM

1. Shen, D., Lehn, P.W, "**Fixed-frequency space-vector-modulation control for three-phase four-leg active power filters**", *IEEE Proceedings Electric Power Applications*, Volume 149, July 2002 Page(s):268 – 274.

2. Holmes, D.G, "**The general relationship between regular-sampled pulse-width-modulation and space vector modulation for hard switched converters**", *IEEE Industry Applications Society Annual Meeting,* Vol.1, Oct. 1992 Page(s):1002 – 1009.

3. Wiechmann, E.P., Burgos, R.P., Rodriguez, J.R, "**Reduced switching frequency active front end converter for medium voltage current-source drives using space vector modulation**", *IEEE International Symposium on Industrial Electronics,* Volume 1, Dec. 2000 Page(s):288 – 293.

4. Marques, G.D, "**A PWM rectifier control system with DC current control based on the space vector modulation and AC stabilization**", *Seventh International Conference on Power Electronics and Variable Speed Drives*, Sept. 1998 Page(s):74 – 79.

5. Perales, M.A., Prats, M.M., Portillo, R., Mora, J.L., Leon, J.I., Franquelo, L.G, "**Three-dimensional space vector modulation in abc coordinates for four-leg voltage source converters**", *IEEE Power Electronics Letters*, Volume 1, Dec 2003 Page(s):104 – 109.

6. Malinowski, M., Jasinski, M., Kazmierkowski, M.P, "**Simple direct power control of three-phase PWM rectifier using space-vector modulation (DPC-SVM),** *IEEE Transactions on Industrial Electronics,* Volume 51, April 2004 Page(s):447 – 454.

7. Alberto, F., Batista, B., Barbi, I, "**Space vector modulation applied to three-phase three-switch two-level unidirectional PWM rectifier**", *Twenty-First Annual IEEE Applied Power Electronics Conference and Exposition*, March 2006.

8. Mazumder, S., Nayfeh, A.H., Borojevic, D, "New **sensorless control of three-phase bi-directional converter using space-vector modulation**", *30th Annual IEEE Power Electronics Specialists Conference,* Volume 2, 27 June-1 July 1999 Page(s):783 – 788.

9. Erfidan, T., Urgun, S., Karabag, Y., Cakir, B, **"New software implementation of the space vector modulation"**, *Proceedings of the 12th IEEE Mediterranean Electrotechnical Conference,* Volume 3, 12-15 May 2004 Page(s):1113 – 1115.

Papers Related to Single Switch Rectifiers

1. John C. Salmon, **"Techniques for Minimizing the Input Current Distortion of Current-Controlled Single-phase Boost Rectifiers"** *IEEE Transactions On Power Electronics,* Volume 8, Oct 1993, Page(s)-509-521.

2. Yungtaek Jang and Milan M. JovanoviC, **"A Comparative Study Of Single-Switch, Three-Phase, High-Power-Factor Rectifiers"**, *IEEE Transactions*, **1998, Page(s)-1093-1110.**

3. Yungtaek Jang and Milan M. JovanoviC, **"A Comparative Study Of Single-Switch, Three-Phase, High-Power-Factor Rectifiers"**, *IEEE Transactions on Industry Applications,* Volume 34, Nov 1998, Page(s)-1327-1335.

4. Souvik Chattopadhyay, V. Ramanarayanan, and V. Jayashankar, **"A Predictive Switching Modulator for Current Mode Control of High Power Factor Boost Rectifier"**, *IEEE Transactions On Power Electronics,* Vol. 18, January 2003, Page(s):114-124.

APPENDIX A

Parameters used for Simulation

AC input voltage = 100V

Supply frequency = 50Hz

Source resistance = 0.2 ohms

Source inductance = 2mH

Output filter capacitance = 2500μF

Load resistance = 40 ohms

Load inductance = 2 mH

DC reference voltage = 250V